

Copyright
by
David Stewart McIlrath
1999

**Improving Bridge Rating and Truck Permitting Procedures
through Finite Element Analysis**

by

David Stewart McIlrath, B.S.C.E.

Thesis

Presented to the Faculty of the Graduate School of

The University of Texas at Austin

in Partial Fulfillment

of the Requirements

for the Degree of

Master of Science In Engineering

The University of Texas at Austin

May, 1999

**Improving Bridge Rating and Truck Permitting Procedures
through Finite Element Analysis**

**Approved by
Supervising Committee:**

Supervisor: Karl H. Frank

Sharon L. Wood

Dedication

This work is dedicated with love and thanks to my family and friends, especially my parents and my late sister, Michelle. Their support and guidance were monumental in making me realize the importance of setting lofty goals and striving to achieve them.

Acknowledgements

This research was made possible through funding provided by the Texas Department of Transportation. I would like to thank everyone involved at TxDOT for their assistance and for enabling this research to be conducted. I would like to thank Dr. Karl H. Frank for the guidance he has offered throughout my time at The University of Texas, and Dr. Sharon L. Wood for being my second reader.

I would like to thank my bowling team members, Dr. Michael E. Kreger, Dr. Richard W. Furlong, Dr. James O. Jirsa, and Dr. Joseph A. Yura, for offering me the chance to get to know them as friends and engineers. I would like to say a special thank you to my colleagues at UT for exposing me to the many diverse talents we all have to offer and for making my time here most enjoyable. Thank you to my good friends Jon Richter, Parry Berkowitz, Matt Thiel, and Russell Kehl, for helping me keep my focus. Special thanks to Charles Bowen, David Jauregui, Norm Grady, Karl Pennings, Photis Matsis, and Blanca Velázquez, for help with bridge testing, rating, and analysis.

A special thank you goes out to Ramesh K. Pujara and Dr. Chris M. Foley in Milwaukee, for emphasizing the importance of an advanced degree in one's development as a professional engineer.

I would like to thank my late sister, Michelle, for reminding me to enjoy all of what life has to offer while I can. Most of all, I thank my parents for their love, guidance, and financial support. They have always stressed the importance of an education and I feel lucky to have them as parents. Mom, Dad, and Michelle, I love you.

May 7, 1999

Abstract

Improving Bridge Rating and Truck Permitting Procedures through Finite Element Analysis

David Stewart McIlrath, M. S. E.

The University of Texas at Austin, 1999

Supervisor: Karl H. Frank

Annually, state DOT's are confronted with thousands of overweight truck permit applications and must determine the ability of bridges along these routes to carry the permit loads. This research shows the benefits of performing more detailed analyses using SAP2000 and BRUFEM, rather than using the AASHTO empirical equations, which were developed based upon bridge behavior under design loads. Using these programs, Lateral Load Distribution Factors are more accurately calculated, giving better estimates of the actual stress levels in bridge elements. Procedures are discussed, and research results shown, to help an analyst determine which types of trucks will be likely to cause damage to various bridge designs. Implementation suggestions for the efficient office use of these computer programs are also discussed. Use of these programs will allow state DOT's to model the response and stress levels within bridge structures more accurately, allowing for longer bridge service lives in most cases.

Table of Contents

List of Tables.....	xi
List of Figures	xii
CHAPTER 1 INTRODUCTION	1
1.1. Importance of Load Rating of Bridges.....	2
1.2. Objectives of Research.....	4
1.2.1. Study of Two TxDOT Steel Bridge Designs from 1955.....	5
1.2.2. Study of Modern Bridge Design using AASHTO LRFD Edition 1.....	9
1.3. Overweight and Oversized Trucks in Texas	11
1.3.1. Related TxDOT Research Projects	12
1.4. Benefits of Finite Element Analysis.....	13
1.5. Overview of Tasks Completed during Research Program	15
CHAPTER 2 TEXAS PERMIT TRUCK DATABASE	18
2.1. Features of the Permit Truck Database	20
2.3. Trends Present in the Typical Permit Truck Database	23
2.3. Trends Present in the Superheavy Truck Database	27
CHAPTER 3 LINE-GIRDER ANALYSIS TECHNIQUES	34
3.1. Development of the EXCEL Spreadsheet Program	35
3.2. Selection of SAP2000 for Bridge Analysis Purposes	39
3.2.1. Using Line-Girder Analyses to Identify Critical Bridges	40
3.2.2. Simple Span Bridge Line-Girder Analyses	45
3.2.3. Continuous Span Bridge Line-Girder Analyses.....	59
3.2.3.1. Symmetric Two-Span Continuous Bridge Structures with Constant Cross-Sections	61

3.2.3.2. Symmetric Two-Span Continuous Bridge Structures with Modified Stiffness in the Negative Moment Region	67
3.2.4. Truck Characteristics that Affect Maximum Moment Ratios ...	69
CHAPTER 4 AASHTO APPROACH TO LATERAL LOAD DISTRIBUTION FACTORS... 74	
4.1. Using AASHTO Design Procedures for LLDF Calculation	76
4.1.1. Working Stress Design Empirical Equations	76
4.1.2. Interior Girder –LRFD Strength Limit State	79
4.1.2.1. Negative Moment Region Interior Girder LLDF	80
4.1.3. Exterior Girder – LRFD Strength Limit State	81
4.1.3.1. Exterior Girder LRFD Moment Distribution Factor – Lever Rule	82
4.1.3.2. Exterior Girder LRFD Moment Distribution Factor – Rigid Body Analysis	83
4.1.4. Summary of Single Vehicle AASHTO LLDF’s	85
4.1.4.1. TxDOT Reduction of AASHTO Design LLDF’s for Overloads	88
CHAPTER 5 BRUFEM LATERAL LOAD DISTRIBUTION FACTOR STUDY	91
5.1. Development of BRUFEM Input Files	91
5.1.1. Summary of BRUFEM Input Cases	92
5.1.1.1. BRUFEM Truck Wheel Layout Input	94
5.1.1.2. BRUFEM Transverse Truck Position Input	98
5.1.1.3. BRUFEM Longitudinal Truck Position Input	103
5.1.2. Determination of Critical Longitudinal Truck Positions	111
5.1.3. Running the BRUFEM Pre-Processor	118
5.1.3.1. BRUFEM Modeling of Example Bridge 1	118
5.1.3.2. BRUFEM Modeling of Example Bridge 2	121
5.1.3.3. BRUFEM Modeling of Example Bridge 3	122
5.2. Summary of BRUFEM Output Files	125

5.3. Differences between SIMPAL Output and POSTNT Output	127
5.4. User Modifications Required for POSTNT Results.....	129
5.4.1. Modifications Required for Non-Composite Girder Models ..	129
5.4.2. Modifications Required for BRUFEM EGM Composite Girder Models	131
CHAPTER 6 SUMMARY AND COMPARISON OF BRUFEM LLDF’S	135
6.1. LLDF and Slab Moment Results for Example Bridge 1 (Runs 1 through 5)	136
6.2. LLDF and Slab Moment Results for Example Bridge 2 (Runs 6 through 10)	140
6.3. LLDF and Slab Moment Results for Example Bridge 3 (Runs 11 through 15)	143
6.4. Comparison of BRUFEM Results with AASHTO and TxDOT LLDF Values.....	147
6.5 Using SAP2000 Output and BRUFEM Results to Calculate a Bridge Rating	152
CHAPTER 7 CONCLUSIONS AND RECOMMENDATIONS	156
7.1. Trends in LLDF Comparisons.....	157
7.2. Recommendations for Using SAP2000 and BRUFEM for Bridge Rating	159
7.3: Texas Permit Truck Database	160
APPENDIX A PERFORMING A LINE-GIRDER ANALYSIS USING SAP2000	162
APPENDIX B BRUFEM INPUT FILES	173
B.1. “History.pre” Files for all BRUFEM Runs	173
B.1.1. “History.pre” File for BRUFEM Run #1:	173
B.1.2. “History.pre” File for BRUFEM Run #2:	175
B.1.3. “History.pre” File for BRUFEM Run #3:	176
B.1.4. “History.pre” File for BRUFEM Run #4:	178
B.1.5. “History.pre” File for BRUFEM Run #5:	179

B.1.6. “History.pre” File for BRUFEM Run #6:	181
B.1.7. “History.pre” File for BRUFEM Run #7:	182
B.1.8. “History.pre” File for BRUFEM Run #8:	184
B.1.9. “History.pre” File for BRUFEM Run #9:	185
B.1.10. “History.pre” File for BRUFEM Run #10:	187
B.1.11. “History.pre” File for BRUFEM Run #11:	188
B.1.12. “History.pre” File for BRUFEM Run #12:	190
B.1.13. “History.pre” File for BRUFEM Run #13:	191
B.1.14. “History.pre” File for BRUFEM Run #14:	192
B.1.15. “History.pre” File for BRUFEM Run #15:	194
B.2. “Bar.dat” Files for Example Bridges 2 and 3	195
B.2.1. “Bar.dat” File for BRUFEM Runs 6 through 10 – Ex. Bridge 2.....	195
B.2.2. “Bar.dat” File for BRUFEM Runs 11 through 15 – Ex. Bridge 3.....	196
B.3. “Veh.dat” Files for all Non-Standard Vehicles	196
B.3.1. “Veh.dat” File for Vehicle #18 – BRUFEM Run #4.....	196
B.3.2. “Veh.dat” File for Vehicle #213 – BRUFEM Run #5.....	197
B.3.3. “Veh.dat” File for Vehicle #87 – BRUFEM Run #8.....	197
B.3.4. “Veh.dat” File for Vehicle #203 – BRUFEM Run #9.....	197
B.3.5. “Veh.dat” File for Vehicle #203 – BRUFEM Run #10.....	198
B.3.6. “Veh.dat” File for Vehicle #87 – BRUFEM Run #13.....	198
B.3.7. “Veh.dat” File for Vehicle #203 – BRUFEM Run #14.....	198
B.3.8. “Veh.dat” File for Vehicle #203 – BRUFEM Run #15.....	199
References	200
Vita	201

List of Tables

Table 1.1: Characteristics for Example Bridges 1, 2, and 3.....	7
Table 2.1: Permit Vehicle Database Summary	32
Table 3.1: Vehicle Record #21 Moment Values and Moment Ratios	54
Table 3.2: Simple Span Moment Ratio Summary.....	58
Table 3.3: Simple and Two-Span Continuous Moment Ratio Comparison.....	64
Table 3.4: Effects of Modified Negative Moment Region Girder Stiffness	68
Table 4.1: Positive Flexure Region Single Vehicle AASHTO Truck LLDF's (Ex. Bridge 3).....	86
Table 4.2: Negative Flexure Region Single Vehicle AASHTO Truck LLDF's (Ex. Bridge 3).....	87
Table 4.3: Single Vehicle LLDF Summary for Example Bridges 1, 2, & 3	88
Table 4.4: Vehicle Gage Values and TxDOT Reduction Factors	90
Table 5.1: Breakdown of 15 BRUFEM Runs on Example Bridges 1, 2, & 3	94
Table 6.1: Example Bridge 1 Analysis Results (Non-Composite).....	137
Table 6.2: Example Bridge 2 Analysis Results (Non-Composite).....	142
Table 6.3: Example Bridge 3 Analysis Results (Composite).....	146
Table 6.4: Interior and Exterior Girder LLDF Comparison.....	149

List of Figures

Figure 1.2: Example Bridge 2 Transverse Section and Half Elevation.....	8
Figure 1.3: Diaphragm Layouts for Example Bridges 1 and 2	9
Figure 1.4: Example Bridge 3 Section and Half Elevation	10
Figure 2.1: AASHTO H and HS Series Design Truck Layouts.....	19
Figure 2.2: Histogram of Permit Fees (excluding Superheavy Vehicles).....	21
Figure 2.3: Permitted Truck Length versus Total Truck Gross Weight.....	22
Figure 2.4: Maximum Axle Spacing Histogram of Permitted Vehicles (excluding Superheavy)	25
Figure 2.5: Minimum Axle Weight Histogram of Permitted Vehicles (excluding Superheavy)	25
Figure 2.6: Maximum Axle Weight Histogram of Permitted Vehicles (excluding Superheavy)	26
Figure 2.7: Total Length Histogram of Permitted Vehicles (excluding Superheavy)	26
Figure 2.8: Total Weight Histogram of Permitted Vehicles (excluding Superheavy)	27
Figure 2.9: Total Weight Histogram for Superheavy Vehicles Only.....	29
Figure 2.10: Total Length Histogram for Superheavy Vehicles Only	29
Figure 2.11: Maximum Axle Weight Histogram for Superheavy Vehicles Only.....	30

Figure 2.12: Maximum Axle Spacing Histogram for Superheavy Vehicles	
Only	30
Figure 2.13: Number of Axles on Superheavy Vehicles Histogram.....	31
Figure 3.1: Loading, Shear, and Moment Diagrams for HS-20 Truck at	
Critical Moment Location on a 100-Foot Simple Span	37
Figure 3.2: Example for Calculating a Truck’s Center of Gravity.....	38
Figure 3.3: Maximum Simple Span H15-44 Truck Moment Ratio vs. Total	
Vehicle Weight Excluding Superheavy Vehicles	48
Figure 3.4: Maximum Simple Span HS20-44 Truck Moment Ratio vs. Total	
Vehicle Weight Excluding Superheavy Vehicles	48
Figure 3.5: Maximum Simple Span H15-44 Truck Moment Ratio vs. Total	
Vehicle Weight – Superheavy Vehicles Only.....	49
Figure 3.6: Maximum Simple Span HS20-44 Truck Moment Ratio vs. Total	
Vehicle Weight – Superheavy Vehicles Only.....	49
Figure 3.7: TxDOT Database Vehicle Record #21 – “Mobile Crane”	50
Figure 3.8: AASHTO H-Series and HS-Series Moment Ratio Conversion	
Chart on Simple Spans of Varied Length	52
Figure 3.9: Three Continuous Girder Bridge Models with Constant Cross-	
Section.....	61
Figure 3.10: Maximum Continuous Span Positive H15 Truck Moment Ratio	
vs. Total Vehicle Weight – Superheavy Vehicles Only.....	62
Figure 3.11: Maximum Continuous Span Negative H15 Truck Moment Ratio	
vs. Total Vehicle Weight – Superheavy Vehicles Only.....	62

Figure 3.12: Maximum Continuous Span Positive HS20 Truck Moment Ratio vs. Total Vehicle Weight – Superheavy Vehicles Only.....	63
Figure 3.13: Maximum Continuous Span Negative HS20 Truck Moment Ratio vs. Total Vehicle Weight – Superheavy Vehicles Only.....	63
Figure 3.14: Three Continuous Girder Bridge Models with Modified Negative Moment Region Cross-Section	67
Figure 3.15: Maximum Continuous Span Positive HS20 Moment Ratio vs. Max. Axle Weight – Superheavy Vehicles Only	70
Figure 3.16: Maximum Continuous Span Negative HS20 Moment Ratio vs. Max. Axle Spacing – Superheavy Vehicles Only	71
Figure 3.17: Superheavy Truck Record #213 Producing Max. Positive Moment Ratio	72
Figure 3.18: Superheavy Truck Record #205 Producing Max. Negative Moment Ratio	72
Figure 4.1: Exterior Girder LRFD LLDF – Lever Rule.....	83
Figure 4.2: Exterior Girder Moment Distribution Factor – Rigid Body	84
Figure 4.3: TxDOT Reduction Factor Gage Definition	89
Figure 5.1: BRUFEM Standard H20-44 Wheel Configuration.....	95
Figure 5.2: BRUFEM Standard HS20-44 Wheel Configuration	96
Figure 5.3: BRUFEM Vehicle #18 Wheel Configuration.....	96
Figure 5.4: BRUFEM Vehicle #213 Wheel Configuration.....	97
Figure 5.5: BRUFEM Vehicle #87 Wheel Configuration.....	97
Figure 5.6: BRUFEM Vehicle #203 Wheel Configuration.....	97

Figure 5.7: H20 and HS20 Rear Axle Travel Lane Position on Ex. Bridge 1	99
Figure 5.8: HS20 Rear Axle Design Lane Position on Ex. Bridges 1 and 2.....	99
Figure 5.9: Vehicle #18 Rear Axle Travel Lane Position on Ex. Bridge 1.....	100
Figure 5.10: Vehicle #213 Rear Axle Travel Lane Position on Ex. Bridge 1.....	100
Figure 5.11: Vehicle #87 Rear Axle Travel Lane Position on Ex. Bridge 2.....	101
Figure 5.12: Vehicle #203 Rear Axle Travel Lane Position on Ex. Bridge 2.....	101
Figure 5.13: HS20 Rear Axle Design Lane Position on Ex. Bridge 3	102
Figure 5.14: Vehicle #87 Rear Axle Travel Lane Position on Ex. Bridge 3.....	102
Figure 5.15: Vehicle #203 Rear Axle Travel Lane Position on Ex. Bridge 3.....	103
Figure 5.16: H20-44 Max. Positive Moment Location on Ex. Bridge 1	104
Figure 5.17: HS20-44 Max. Positive Moment Location on Ex. Bridge 1.....	105
Figure 5.18: Vehicle #18 Max. Positive Moment Location on Ex. Bridge 1.....	105
Figure 5.19: Vehicle #213 Max. Positive Moment Location on Ex. Bridge 1....	106
Figure 5.20: HS20-44 Max. Negative Moment Location on Ex. Bridge 2.....	106
Figure 5.21: HS20-44 Max. Positive Moment in End Span Location on Ex. Bridge 2.....	107
Figure 5.22: Vehicle #87 Max. Positive Moment in Interior Span Location on Ex. Bridge 2	107
Figure 5.23: Vehicle #203 Max. Positive Moment in End Span Location on Ex. Bridge 2	108
Figure 5.24: Vehicle #203 Max. Negative Moment Location on Ex. Bridge 2..	108
Figure 5.25: HS20-44 Max. Positive Moment Location on Ex. Bridge 3.....	109
Figure 5.26: HS20-44 Max. Negative Moment Location on Ex. Bridge 3	109

Figure 5.27: Vehicle #87 Max. Positive Moment Location on Ex. Bridge 3.....	110
Figure 5.28: Vehicle #203 Max. Positive Moment Location on Ex. Bridge 3....	110
Figure 5.29: Vehicle #203 Max. Negative Moment Location on Ex. Bridge 3..	111
Figure 5.30: Maximum Positive Moment Influence Line in End Span of Ex. Bridge 2.....	115
Figure 5.31: Maximum Negative Moment Influence Line at Interior Support for Ex. Bridge 2.....	115
Figure 5.32: Maximum Positive Moment Influence Line in Interior Span of Ex. Bridge 2	116
Figure 5.33: Maximum Positive Moment Influence Line for Ex. Bridge 3	116
Figure 5.34: Maximum Negative Moment Influence Line for Ex. Bridge 3	117
Figure 5.35: BRUFEM Model of Non-Composite Slab-Girder Interaction	123
Figure 5.36: BRUFEM Models of Composite Slab-Girder Interaction	124
Figure 5.37: Total Moment on EGM Steel Girder Section	133
Figure A.1: Three Non-Curved Bridge Layout Classifications	164
Figure A.2: Loading and Shear Diagrams for HS-20 Truck at Critical Shear Location on a 100-Foot Simple Span.....	172

CHAPTER 1

INTRODUCTION

As traffic volumes and vehicle weights increase on the highway systems in the United States, the demand placed on our bridge structures increases accordingly. At this time, it is estimated that about 18,000 bridges located in Texas alone do not meet the design specifications mandated by the American Association of State Highway and Transportation Officials (AASHTO). The Texas Department of Transportation (TxDOT) is faced with the problem of evaluating the structural adequacy of the state's inventory of bridges for the passage of routine traffic, typical overloaded or oversized vehicles, and special "Superheavy" vehicles. This process, known as bridge rating, is commonly done to calculate the live load capacity of a bridge structure using empirical equations and other simplified design procedures. The AASHTO bridge design procedures are formulated to allow an engineer to complete a bridge design in a timely manner. However, using this method and its simplifying assumptions has drawbacks when an engineer needs to analyze existing structures for load rating purposes. This AASHTO approach to load rating is a useful first step in determining the live load capacity of an existing bridge, however, some reserve capacity often exists within a bridge structure that is not considered when using the AASHTO procedure.

1.1. IMPORTANCE OF LOAD RATING OF BRIDGES

Load rating can be done using non-destructive field tests on existing bridges, but that approach is a time-consuming process most often carried out in a research setting or on bridges with an extremely high importance factor or with very unusual field conditions. The most common approach to bridge rating is through the standards described within the AASHTO Manual for Condition Evaluation of Bridges (AASHTO Manual).^[3] These guidelines describe the processes for calculating both an inventory and operating rating for a bridge structure. The inventory rating represents the live load the bridge can safely carry for an indefinite amount of time. The operating rating represents the maximum live load permitted to cross the bridge.

If a bridge is not capable of handling the loads it sees on a daily basis due to the results of the AASHTO bridge rating, TxDOT, or the governing state DOT, must decide to either post the bridge or close it based on the severity of its predicted under-strength. Every bridge that is posted, however, is also required to be annually inspected, which is a financial burden and a time-consuming effort. Some problems occur when an engineer uses the AASHTO approach for bridge rating. The AASHTO general bridge rating methods are not valid for all possible bridge geometries. Special bridge layouts are best rated using structural analysis software rather than AASHTO empirical equations for this reason. It is important to realize that the AASHTO method of calculating Lateral Load Distribution Factors (LLDF's) was generated based on bridge behavior due to loads from

design trucks only. No provisions are made to account for the wide variation of axle weights and spacings common to overloaded or Superheavy vehicles. It is also important to note that the AASHTO bridge rating procedure neglects some possible sources of bridge capacity in order to simplify and reduce the time required for analysis. One of these sources neglected by the AASHTO procedure is the capability of the deck slab to carry a significant portion of the total moment in a bridge structure. This deck slab component may become quite significant in bridges with short span lengths. If a rating could be done that reflected the true bridge capacity without costing the engineer undue time, it would prevent some bridges from being posted, and would allow for more efficient traffic routes for heavy trucks. This would also prevent the premature closing or posting of adequate bridge structures that failed an AASHTO bridge rating.

Three example bridge designs are analyzed during this research program and used for completing a LLDF comparison. The LLDF's calculated from analysis are compared with both the old AASHTO Standard Specification LLDF's and the LLDF's calculated using the newest AASHTO Load and Resistance Factor Design Specification (LRFD). The old AASHTO LLDF values are based on equations using bridge girder spacing only, whereas the new LRFD LLDF equations are formulated as a function of girder spacing, girder span length, deck slab thickness, and the longitudinal girder stiffness.

1.2. OBJECTIVES OF RESEARCH

The main objectives of this research were to determine if other tools were available to the design engineer to supplement the AASHTO Manual and account for a bridge's reserve capacities, while minimizing the amount of extra time required to complete this process. The objectives of this project also include the determination of actual force effects in critical Texas bridges resulting from passage of both typical overweight or oversized vehicles and special Superheavy vehicles. The bridges deemed most critical by TxDOT are steel I-beam bridges, simple and continuous spans. Comparisons of force effects resulting from current analysis procedures and finite element analyses are also addressed. Finally, this project aims at determining if current TxDOT overweight vehicle regulations are adequate to protect or possibly extend the expected service lives of Texas bridges using the results of code procedures and analytical procedures.

This study will provide the information needed to assess current permitting regulations and their effect on the State's bridges. The results will allow TxDOT to modify their current methods of analyzing bridges for overloads, when necessary. The benefits to the State of Texas are reduction of damage to bridges due to overloads, extension of the service lives of bridges, and development of rational procedures to evaluate implications of overweight vehicles on the State's inventory of bridges.

A procedure using the program Bridge Rating Using Finite Element Methods, (BRUFEM) developed by the Florida Department of Transportation,

(FDOT) is presented and evaluated, along with a commercial finite element program entitled SAP2000, developed by Computers and Structures, Incorporated. BRUFEM was developed to help the bridge designer carry out bridge ratings in a timely manner. This thesis looks at the BRUFEM package and SAP2000 from the standpoint of the design engineer in an office setting and makes suggestions on how to use these packages without wasting inordinate amounts of time in the process. SAP2000 is used to carry out line girder analyses of bridge structures as the first step in analyzing maximum moment and shear effects produced by typical oversized and overweight vehicles as well as the Superheavy vehicles. AASHTO design trucks and the oversized or overweight trucks are analyzed using both program packages with results shown for three actual bridge designs.

1.2.1. Study of Two TxDOT Steel Bridge Designs from 1955

Two Texas non-composite steel girder bridge designs from the 1950's are studied. One example design (Example Bridge 1), is a 50-foot, simply supported span with right-girders (no skew). Example Bridge 1 is a non-composite bridge design using four W33x141 A7 steel stringers ($f_y = 33$ ksi), spaced 8 feet apart to support a 6- $\frac{1}{2}$ inch concrete deck that forms a 28 foot wide roadway. The concrete specified is Class A ($f'_c = 3,000$ psi) with reinforcing steel allowable stresses set at 20,000 psi. The slab overhangs the outer girders by 3'-7". The design truck used was the AASHTO H20-44 designation.

The second example design (Example Bridge 2), is taken from the same bridge structure as Example Bridge 1, but consists of a 195-foot continuous span portion of the bridge. Example Bridge 2 is a non-composite, three-span continuous right-girder steel bridge consisting of spans of 60-feet, 75-feet, and 60-feet, respectively. Example Bridge 2 uses four W33x130 A7 steel stringers with 10"x7/16"x11'-0" cover plates top and bottom at each interior pier. These stringers are spaced at 8 feet and carry the same 6-1/2 inch Class A concrete slab. Both Example Bridges 1 and 2 are taken from TxDOT record drawings for the Texas State Highway 71 bridge structure crossing Onion Creek in Travis County, Texas. Both of these bridges were designed using the AASHTO 1953 Standards and were selected to show the "typical" older simple span and continuous span steel stringer bridge designs existing in Texas today. Transverse cross sections, span layouts, diaphragm locations, and member sizes are shown for Example Bridge 1 in Figure 1.1 and for Example Bridge 2 in Figure 1.2. The diaphragm layouts and sizes for Example Bridges 1 and 2 are shown in Figure 1.3. Table 1.1 summarizes the relevant design data for both Example Bridges 1 and 2.

Table 1.1: Characteristics for Example Bridges 1, 2, and 3

	Example Bridge 1	Example Bridge 2	Example Bridge 3
Girder/Slab Design	Non-Composite	Non-Composite	Composite
Concrete f^c	3,000 psi	3,000 psi	4,000 psi
Steel Girder Yield Stress	33 ksi	33 ksi	50 ksi
Design Truck	H20-44	H20-44	LRFD
AASHTO Code Version	1953 Standard	1953 Standard	1994 LRFD, Ed. 1
Roadway Width	28'-0"	28'-0"	34'-0"
Girder Spacing	8'-0"	8'-0"	10'-0"
Minimum Slab Thickness	6 ½"	6 ½"	8"
Deck Overhang	3'-7"	3'-7"	3'-6"
Span Length	50'-0" Simple Span	195'-0" Contin. Span (60'-75'-60')	180'-0" Contin. Span (90'-90')

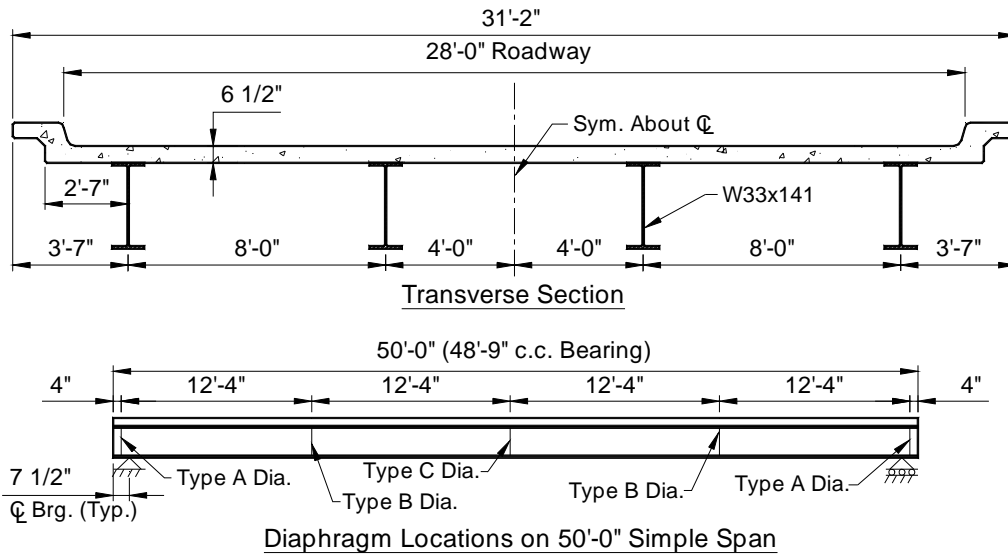


Figure 1.1: Example Bridge 1 Transverse Section and Elevation

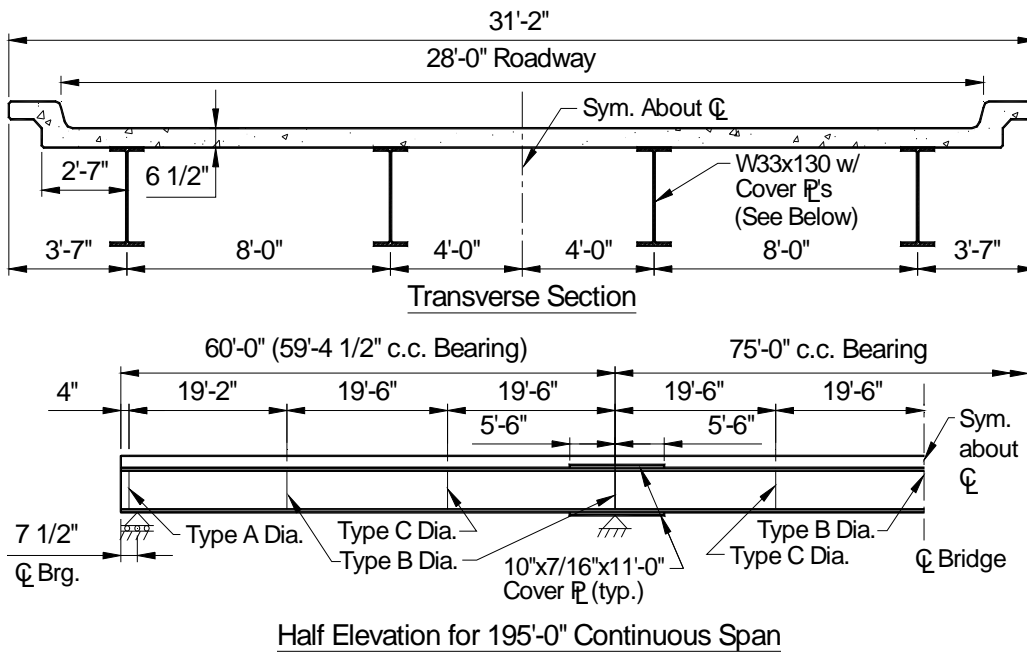


Figure 1.2: Example Bridge 2 Transverse Section and Half Elevation

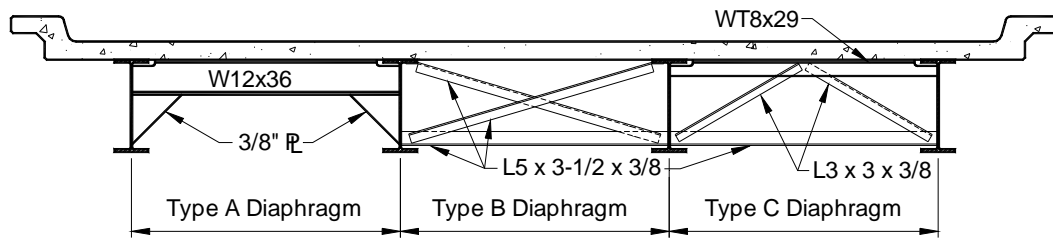


Figure 1.3: Diaphragm Layouts for Example Bridges 1 and 2

1.2.2. Study of Modern Bridge Design using AASHTO LRFD Edition 1

The third example design (Example Bridge 3), is a structure designed according to the first edition of the AASHTO LRFD Specifications. This design example was taken from an example design done by J. D. Carnahan, M. A. Grubb, and J. L. Hartmann.^[7] This bridge represents newly designed steel stringer bridges and shows effects of a larger stringer spacing on the distribution effects within a bridge structure. This modern bridge design is a two-span continuous, composite right I-girder design, with two 90-foot spans. Example Bridge 3 uses four compact unstiffened fully composite A709, Gr. 50W (AASHTO M270) weathering steel plate girders ($f_y = 50$ ksi), spaced 10 feet apart. The concrete slab ($f'_c = 4,000$ psi) spanning between the girders is 8-½ inches thick, with a minimum slab thickness of 8 inches, and the reinforcement is Grade 60. The slab overhangs each outside girder by 3'-6" and the bridge is symmetric about its centerline. The bridge structure provides a 34-foot roadway. The plate girders for this structure vary along their length and are shown in Figure 1.4.

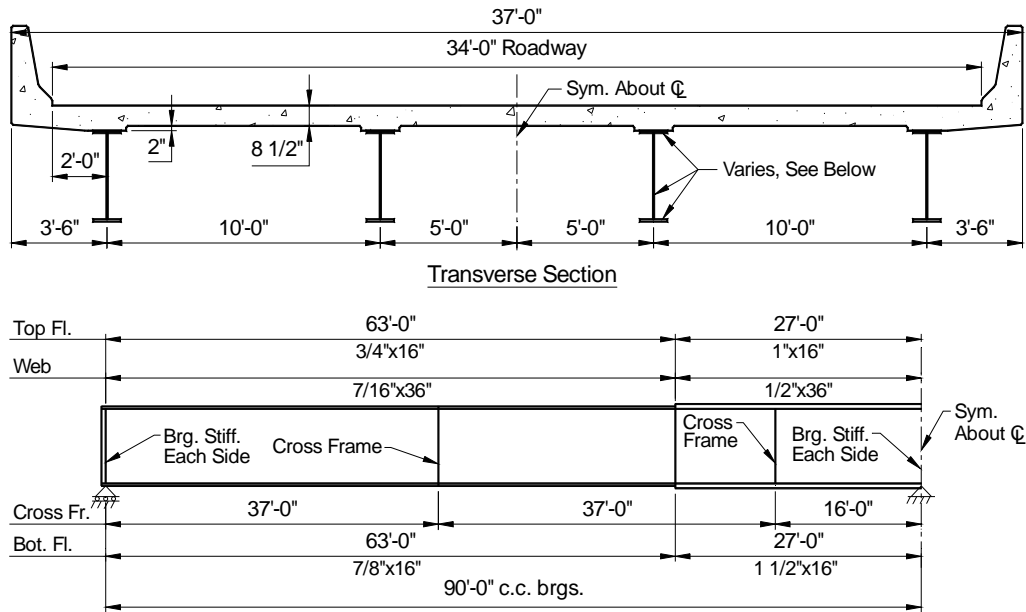


Figure 1.4: Example Bridge 3 Section and Half Elevation

These three actual bridge designs are used to demonstrate the benefits of using a refined analysis approach recommended by this research work, as opposed to relying on the AASHTO Manual alone for load ratings. Even though the structures focused upon within this thesis are steel structures, the principles and approaches discussed in this thesis are also applicable to extending the useful lives of bridge types such as concrete girder-slab bridges, flat-slab bridges, and prestressed/post-tensioned girder bridges. Steel stringer bridges were studied due to TxDOT correspondence stating that steel I-beam bridges are deemed most critical at this time.^[8]

1.3. OVERWEIGHT AND OVERSIZED TRUCKS IN TEXAS

The Central Permit Office (CPO) of TxDOT currently issues about 30,000 overweight/oversized permits a month. Of those permitted vehicles, it is estimated that about 10,000 are for overweight vehicles alone. In addition to these vehicles, the CPO also issues permits to vehicles covered under House Bill 2060. These “2060” permits allow vehicles to exceed legal gross loads by 5% and/or axle loads by 10%. With a “2060” permit, a vehicle is allowed to legally cross any bridge in the state of Texas, with the exception of interstate highway bridges, whether the bridge is load posted or not. In Fiscal Year 1995 alone, over 13,000 “2060” permits were purchased. With the recent North American Free Trade Agreement (NAFTA), it is estimated that the number of overweight vehicles will continue to increase on the Texas transportation system in the future. Recent research sponsored by TxDOT indicates that current legal limits for overloads will overstress certain bridge types.

For only a \$75 yearly permit and \$15,000 bond, vehicles weighing 80,000 pounds can be operated on state and county roads designed for around 58,000 pounds. Even heavier loads are allowed for agricultural vehicles. NAFTA alone will tend to increase the number of trucks requiring permits on the Texas highway system. Current analysis procedures based on AASHTO load distribution and impact factors indicate that stresses from current legal loadings and wheel patterns can exceed 0.9 F_y .

1.3.1. Related TxDOT Research Projects

Some current and completed projects sponsored under the TxDOT research program have addressed issues related to overloads, permitting, and load rating. TxDOT Project 1266, “Overload Permit Procedures” has defined criteria for issuing permits for overweight vehicles on simple span bridges of various types. The formulae developed allow for authorization of higher permit weights without additional engineering analysis. Some consideration of continuous spans was included in the project. The recommendations are based on a direct application of AASHTO design procedures of HS type trucks. No consideration was given to more realistic distribution of loads or for calibration to actual behavior. TxDOT Project 1323 addressed the Evaluation of Weight Tolerance Permits Authorized in House Bill 2060. The routing concerns of overweight vehicles have been addressed in TxDOT Projects 1482 and 1266.

TxDOT Project 7-2986 is ongoing to develop a Load Testing Program and was started in September of 1995. The objective of the project is to develop a bridge load-testing program for the State of Texas for assessing the load rating of a bridge. The intent is to establish procedures and evaluate the technology available for conducting tests of bridges to establish load ratings and help maximize the service lives of the State’s bridges. This thesis is sponsored under TxDOT Project 0-1746, which closely parallels Project 7-2986, and is designed to study the effects of permitted overloads on existing structures. This project is also designed to suggest additional analytical procedures to help maximize bridge

service lives. In short, Project 0-1746 attempts to do analytically what Project 7-2986 does experimentally.

1.4. BENEFITS OF FINITE ELEMENT ANALYSIS

A major part of the bridge rating problem is the determination of the Lateral Load Distribution Factors. The LLDF measures how heavily loaded an individual girder becomes due to one vehicle or a system of vehicles located on the bridge deck. Until recently, the LLDF's were obtained solely on AASHTO empirical criteria. The finite element method of analysis can be used today to do a rational, three-dimensional analysis of a bridge structure and determine a more accurate distribution of wheel loading than that given by empirical criteria alone. At the start of this research program, a decision needed to be made regarding the finite element program package that was most suited to bridge analysis and allowed for a rapid assessment of analysis results. The program package needed to be compatible for use on a personal computer to simulate the design office setting. The program also needed to allow users with limited experience in the use of finite element programs to efficiently prepare models of bridges and interpret the results. BRUFEM, a program package geared toward the analysis of girder-slab type bridge structures, was developed in a joint effort between FDOT and the Federal Highway Administration (FHWA) over a period of about ten years. The BRUFEM package is a set of four FORTRAN programs specifically developed to meet the bridge analyst's needs in the area of bridge rating. BRUFEM was also selected because its preprocessor allows for the rapid

generation of a finite element mesh and allows for the rapid modification of a bridge model when editing is necessary. SAP2000 was also considered and is a very powerful general purpose finite element program, however, BRUFEM has many features built-in that make it much more efficient for bridge engineers and it also addresses some modeling concerns that are unique to bridge structures. BRUFEM allows for shorter analysis times than SAP2000, and also formats its output with the bridge analyst in mind.

The first step in the creation of BRUFEM was a computer program developed by FDOT with FHWA titled Structural Analysis for Load Distribution (SALOD). The primary function of SALOD was to predict the flexural LLDF's for design and rating of simple span bridges. The use of SALOD has helped to keep adequate bridge structures from being posted when they are in good condition, even though they fail the rating criteria when using the AASHTO empirical methods.^[4] SALOD is a useful program, however, to keep its database of influence surfaces a reasonable size, simplifying assumptions are made when it models structures. Continuity of the girders, edge stiffening effects, skew effects, and other possibly significant effects were not considered by SALOD. Thus, the BRUFEM system was developed by FDOT. BRUFEM uses a system of programs to automate the rating of girder-slab bridges using a three-dimensional finite element analysis.

The BRUFEM system has the capability of directly rating prestressed and post-tensioned concrete bridges, reinforced concrete T-beam bridges, flat slab bridges, and steel girder bridges. All of the bridge types listed may contain

simple or continuous spans. Prestressed concrete bridges may be pretensioned or pretensioned and post-tensioned. Bridges may be skewed and stiffening elements such as parapets may be included in the model. Users can select from databases of standard sections and vehicle load configurations or use their own data. Using a minimum of input, a finite element model is automatically prepared using the BRUFEM pre-processor that can predict the dead and live load responses of bridges much more accurately than simple straight line (or line girder) models. One positive aspect of finite element analysis is that it allows an engineer to model unusual boundary conditions and geometries when simple formulas are not appropriate.

1.5. OVERVIEW OF TASKS COMPLETED DURING RESEARCH PROGRAM

Many tasks had to be completed to develop the conclusions shown within this thesis. The first task completed dealt with obtaining a large number of typical oversize or overweight permits from TxDOT and developing a database of critical truck information that would be useful in determining maximum force effects and trends in the truck records. A database of 119 TxDOT truck permits was developed that represents the typical trucks permitted on Texas highways daily. Also included in the database were 19 special vehicles that TxDOT classifies as Superheavy. TxDOT classifies vehicles as Superheavy when they have a total gross weight over 250,000 pounds (250 kips). These are special trucks designed to haul large pieces of machinery or other long and extremely heavy items. These special trucks were used to examine the effects of severely overloaded vehicles on bridges. The typical permitted trucks were used to study the effects of less severe

overloads that can occur on almost a daily basis on busy highways. These two types of truck records can parallel the AASHTO definitions of inventory and operating ratings. The inventory rating is designed to be used for the typical overloaded vehicles, while the operating rating is designed to account for the special Superheavy vehicles.

Once the permitted truck database was developed, the analysis began using a spreadsheet program developed by the author using Microsoft EXCEL. This spreadsheet modeled the response of a simple span line girder due to loads from arbitrary trucks with up to 13 axles. A 13-axle maximum was selected because the typical overload database contained trucks with 13 or fewer axles. The typical permitted trucks were analyzed using this EXCEL spreadsheet program and maximum moments and shears were calculated for simple spans of 50 feet, 75 feet, 100 feet, 125 feet, and 150 feet. These maximum force effects were then compared with those produced by four AASHTO design truck designations (H15-44, H20-44, HS15-44, and HS20-44). This spreadsheet program was also used to independently check the results of the SAP2000 program, which was also used to analyze line girder layouts.

SAP2000 allows for arbitrary axle spacing and weight without restriction of the number of axles on a specific truck. Many of the Superheavy vehicle designations had more than 13 axles and could not be accurately modeled by the spreadsheet program. SAP2000 was ideal for this type of analysis and produced rapid maximum force effect results. SAP2000 was also required to do analysis of bridges with continuous spans. The automated bridge rating program packages

SALOD and BRUFEM, developed by FDOT, were then utilized to develop finite element models to determine LLDF's for Example Bridges 1, 2, and 3. SALOD was helpful in positioning the critical vehicles for maximum effects on the three-dimensional (3D) model. SALOD gives a location based on a simple influence surface database to approximate the maximum response position, which is then a useful starting point from which the true critical position can be found using BRUFEM. Moving the critical truck through a range of positions close to the SALOD approximation allows a user to find the true critical position in BRUFEM. When analyzed in BRUFEM, the worst force effect cases are studied and compared with AASHTO code values for LLDF's. From these results, conclusions can then be drawn regarding the amount of conservatism contained within the code equations, and therefore reserve bridge capacities can be shown to exist. The usefulness of completing an accurate analysis is shown and conclusions are also formed regarding the steps necessary to perform a better bridge rating in a design office setting.

CHAPTER 2

TEXAS PERMIT TRUCK DATABASE

The first step in determining the effects of overloaded or oversized trucks was to develop a database of TxDOT permitted vehicles that would typify the oversized or overweight vehicles allowed in Texas. Trucks included within this classification are those for which TxDOT issues an overload permit after receiving a permit application. A large number of these vehicles were used to analyze typical bridge layouts with simple and continuous spans so that trends could be identified and the most critical trucks earmarked.

These permitted trucks include both the typical overweight permit applications as well as the TxDOT Superheavy vehicle classification permits, a total of 138 trucks. The database that was compiled contained 119 records of “typical” oversized or overweight trucks that were permitted between September 17, and October 8, 1996, by TxDOT. The majority of these trucks received permits on October 3, 1996. These records were received directly from the Central Permit Office (CPO) of TxDOT and contain permits for travel within various regions of the State of Texas. All vehicles in the database were given a record number for identification purposes, and the Record Numbers 5 to 123 represent the typical overweight permitted trucks. Record numbers 1 through 4 are used to identify four AASHTO design trucks used during analysis for comparison purposes. These four AASHTO design trucks are the H20-44, H15-

44, HS20-44, and the HS15-44. Schematic layouts for each type of design truck are shown in Figure 2.1.^{[1][2]}

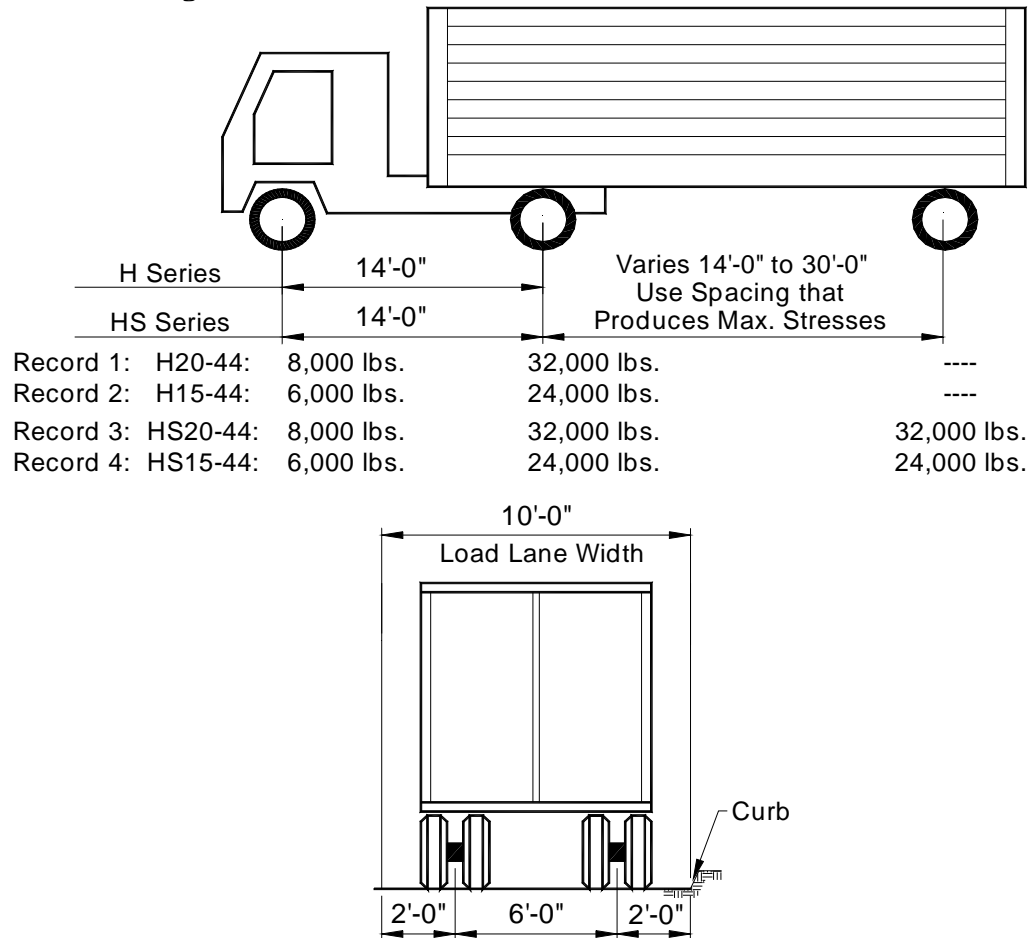


Figure 2.1: AASHTO H and HS Series Design Truck Layouts

Included in the database of permitted trucks are 19 vehicles that TxDOT classifies as Superheavy. Even though the 19 vehicles chosen by TxDOT for use in this project received permits in 1989, they are still representative of the special Superheavy vehicles that are seeking TxDOT permits at the present time. A vehicle with a total gross weight over 250 kips is grouped into the Superheavy

category. The minimum total gross weight of the Superheavy vehicles in this database is 295 kips, and the maximum total gross weight is 989 kips. All of the Superheavy vehicles have between 13 and 27 axles within this database. Superheavy vehicles are identified by database record numbers between 201 and 219.

2.1. FEATURES OF THE PERMIT TRUCK DATABASE

The TxDOT permit documentation papers contain quite a bit of information about the specific vehicle being permitted. Information included in the permit truck database consists of permit fee, permit number, load description, maximum width, maximum height, maximum length, gross weight, axle spacing, axle weights, tires per axle, and tire size. The information categories most critical for this research project were the axle spacing, axle weights, maximum width, maximum length, total gross weight, and the total number of tires per axle. Route descriptions and special conditions are also listed in TxDOT overload permit documentation, but none of this information was entered into the permit truck database. Total TxDOT permit fees varied quite a bit, with the average value of the permit fee equaling \$168. The lowest permit fee was zero dollars while the maximum permit fee reached \$4777.28 for these 119 overweight vehicles. Some permits show a rough breakdown of this permit fee, but none of this information was entered into the permit truck database. No permit fees were available for the 19 Superheavy TxDOT permits. Permit fees were not a primary focus of this research, however, it should be noted that almost all of these permit fees are quite inexpensive and do not provide a significant portion of the cost of damage these

vehicles cause. Figure 2.2 shows histograms of permit fee information for the typical overweight trucks only.

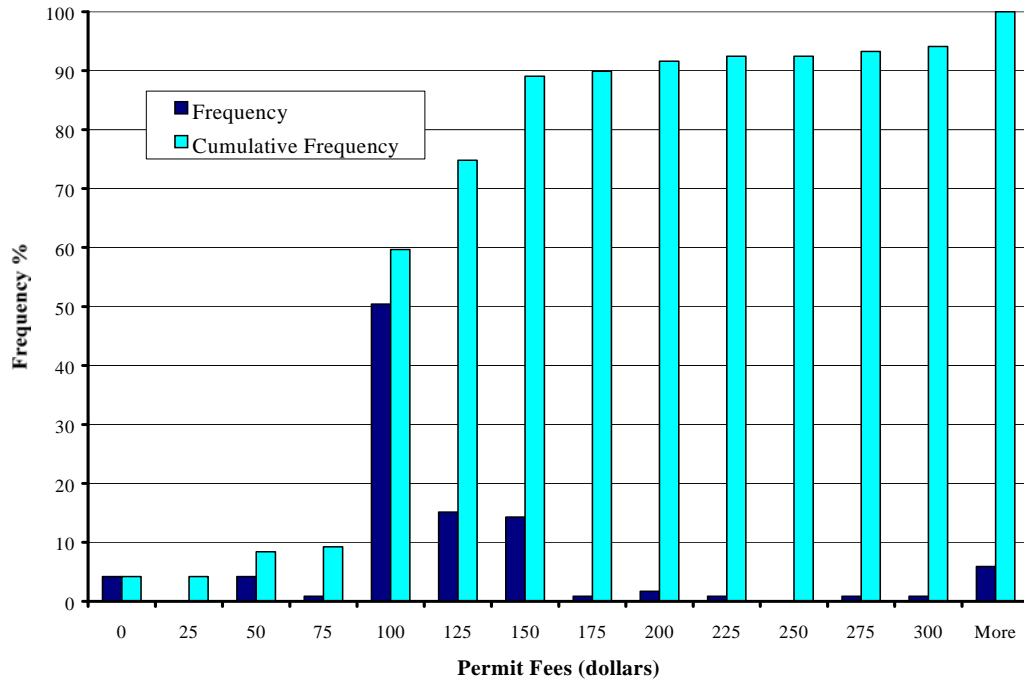


Figure 2.2: Histogram of Permit Fees (excluding Superheavy Vehicles)

Many graphs and histogram plots were constructed to help give a visual description of the vehicles used for these analyses. Most graphs are constructed with the typical permit trucks and the Superheavy vehicles separated, since these vehicle groups are not alike. Figure 2.3 shows all of the permit vehicles together on one graph and displays the relationship of each vehicle's total length to its total gross weight. Figure 2.3 shows the division of TxDOT truck designations at a weight of 250 kips. It is also interesting to see the range of truck lengths that fall within each of the TxDOT truck designations. The longest trucks in the Permit

Truck Database have lengths of 151 feet while the longest truck in the Superheavy Truck Database is 335 feet. The four data points labeled “Design Truck” correspond to the AASHTO H15-44, H20-44, HS15-44, and HS20-44 design truck specifications.

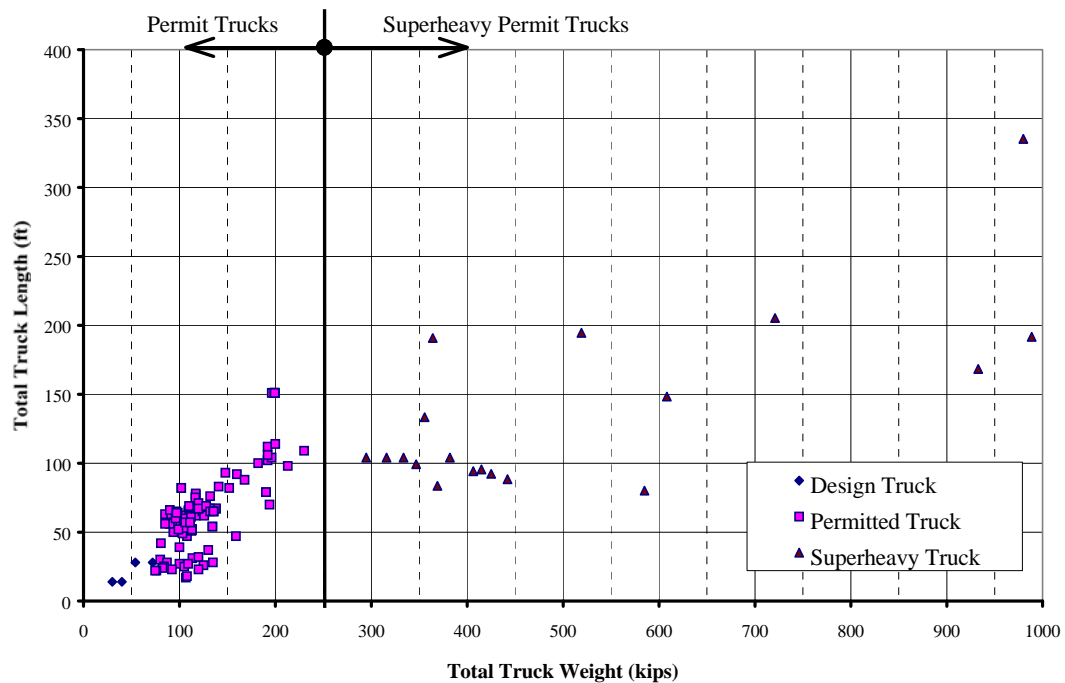


Figure 2.3: Permitted Truck Length versus Total Truck Gross Weight

As Chapter 3 describes in detail, maximum moment and shear values were calculated for each truck, along with design truck moment ratios, and included within the database. All information within this chapter deals with the truck characteristics and their trends alone, with no listing of moment ratio values. Chapter 3 describes the force effects produced by each of these trucks and compares these effects to those of AASHTO design vehicles.

2.3. TRENDS PRESENT IN THE TYPICAL PERMIT TRUCK DATABASE

Both histogram plots and graphs are helpful in identifying trends and generalizing the information found in the permit truck database. Some general trends that should be noticed are listed here:

1. All permitted trucks are heavier (total gross weight) than the heaviest AASHTO design truck contained in the database, the HS20-44. See Figure 2.3.
2. Generally, as truck lengths increase, so does the total gross vehicle weight. See Figure 2.3.
3. Within the permit truck database (excluding Superheavy), 93% of the vehicles have a maximum axle spacing less than 50 feet. The average maximum axle spacing for these vehicles is 32.6 feet. See Figure 2.4.
4. The minimum axle weight on 88% of these permitted vehicles (excluding Superheavy) is less than 20 kips. The average minimum axle weight is 14.0 kips. See Figure 2.5.
5. The maximum axle weight of 94% of these permitted vehicles (excluding Superheavy) is less than 24 kips. The average maximum axle weight is 20.75 kips. See Figure 2.6.
6. Within the permit vehicle database (excluding Superheavy), 76% of the vehicles were less than 80 feet in length. The average length of these vehicles is 64.5 feet. See Figure 2.7.

7. Within the permit vehicle database (excluding Superheavy), 81% of the vehicles had a total gross weight of 150 kips or less. The average weight of these vehicles is 124 kips. See Figure 2.8.

The heaviest record in the permit truck database (excluding Superheavy records) was Record 96, transporting a “Compressor”, and having a total gross weight of 230 kips. The truck records with the longest total vehicle length and the largest maximum axle spacing were Records 100, 101, 113, 114, 115, and 116. These six records were all described as vehicles for transporting a “Concrete Beam” and totaled 151 feet in length. The maximum axle spacing that these vehicles used was 99 feet. The truck record with the greatest axle weight was Record 21, for a “Mobile Crane”, which had axle weights of 27,000 pounds. For comparison purposes, the minimum total weight AASHTO design truck listed within this database, the H15-44, has a maximum axle weight of 24,000 pounds. The maximum total weight AASHTO design truck, the HS20-44, has a maximum axle weight of 32,000 pounds. The values assigned as truck “record numbers” were randomly assigned during the construction of the permit vehicle database to help identify input and output values. Any truck “record numbers” over 200 identify TxDOT Superheavy vehicles.

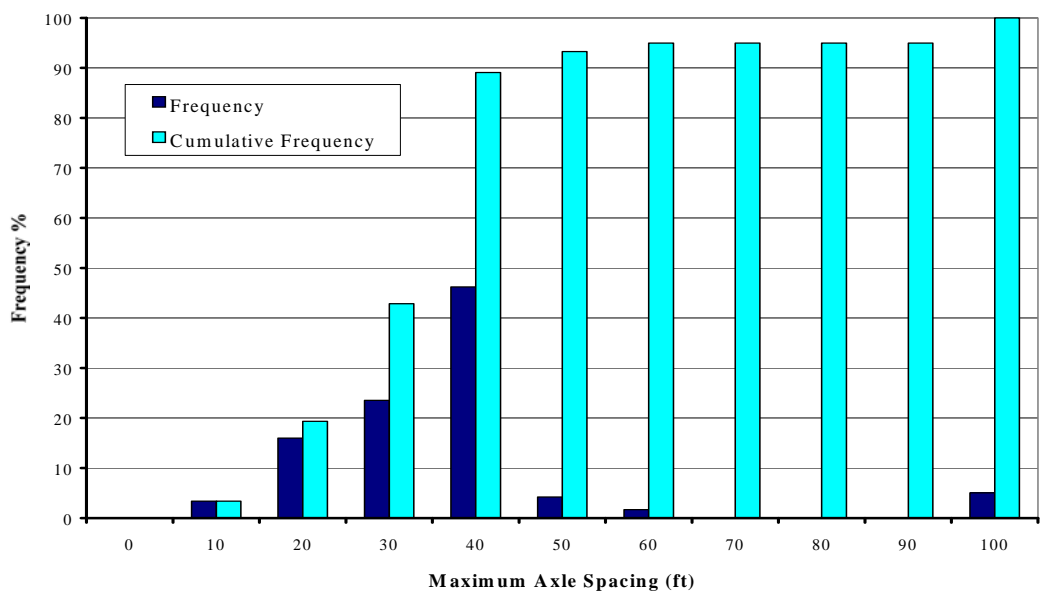


Figure 2.4: Maximum Axle Spacing Histogram of Permitted Vehicles (excluding Superheavy)

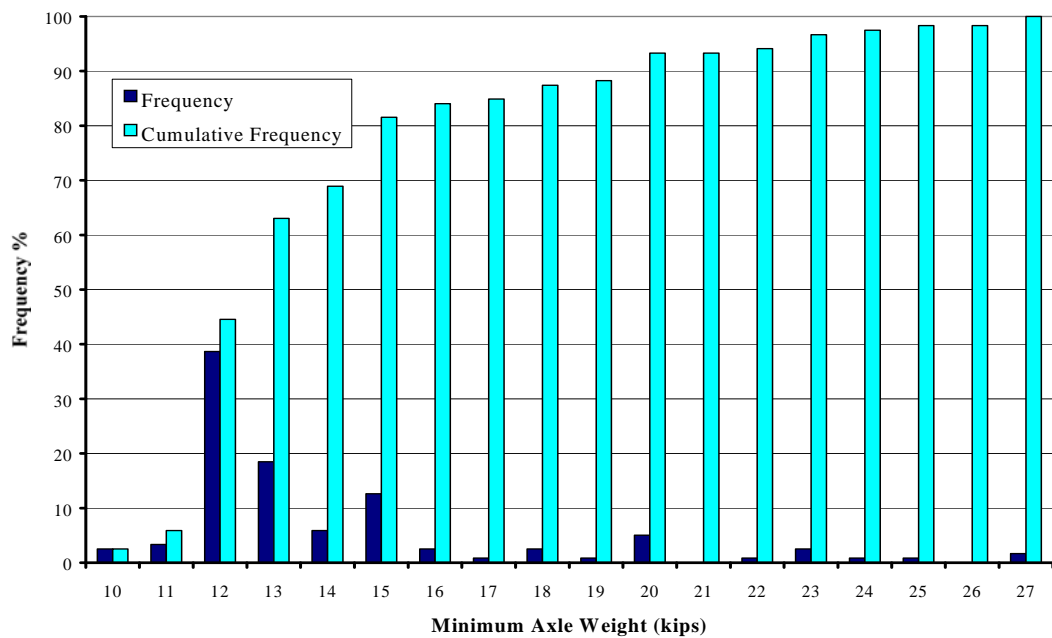


Figure 2.5: Minimum Axle Weight Histogram of Permitted Vehicles (excluding Superheavy)

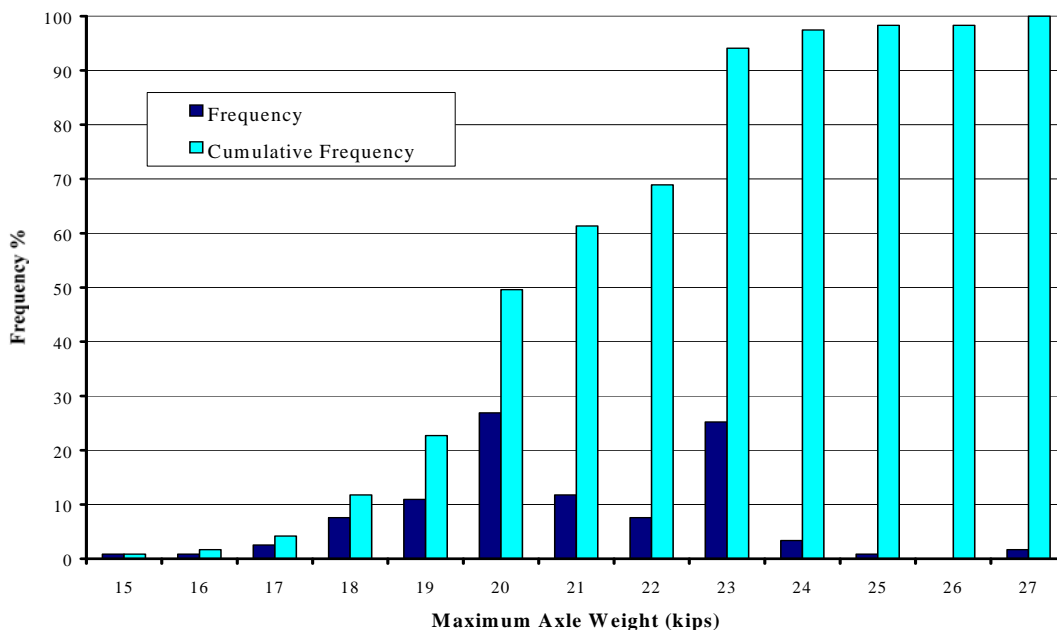


Figure 2.6: Maximum Axle Weight Histogram of Permitted Vehicles (excluding Superheavy)

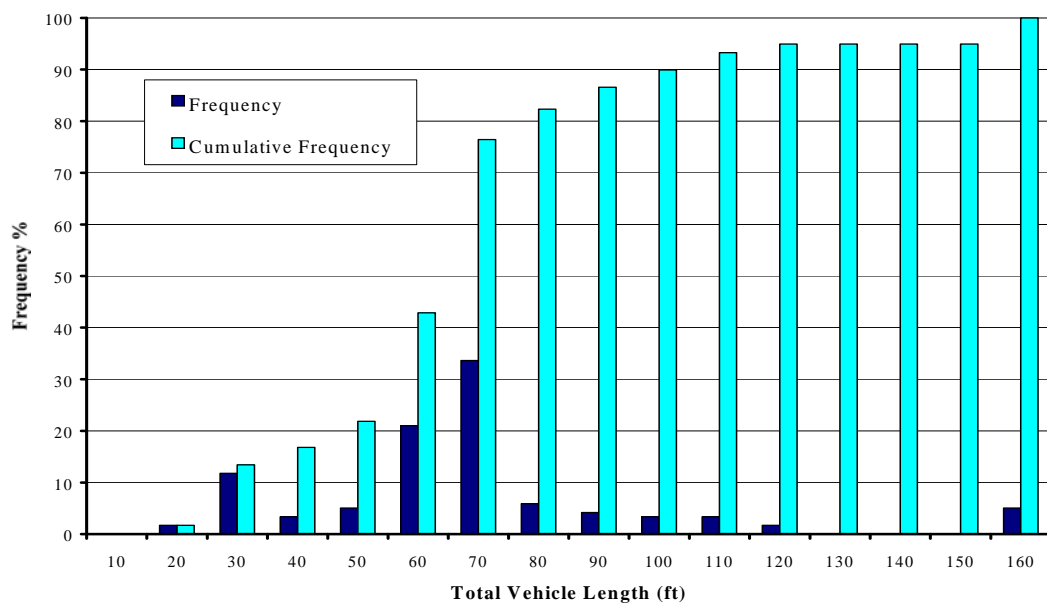


Figure 2.7: Total Length Histogram of Permitted Vehicles (excluding Superheavy)

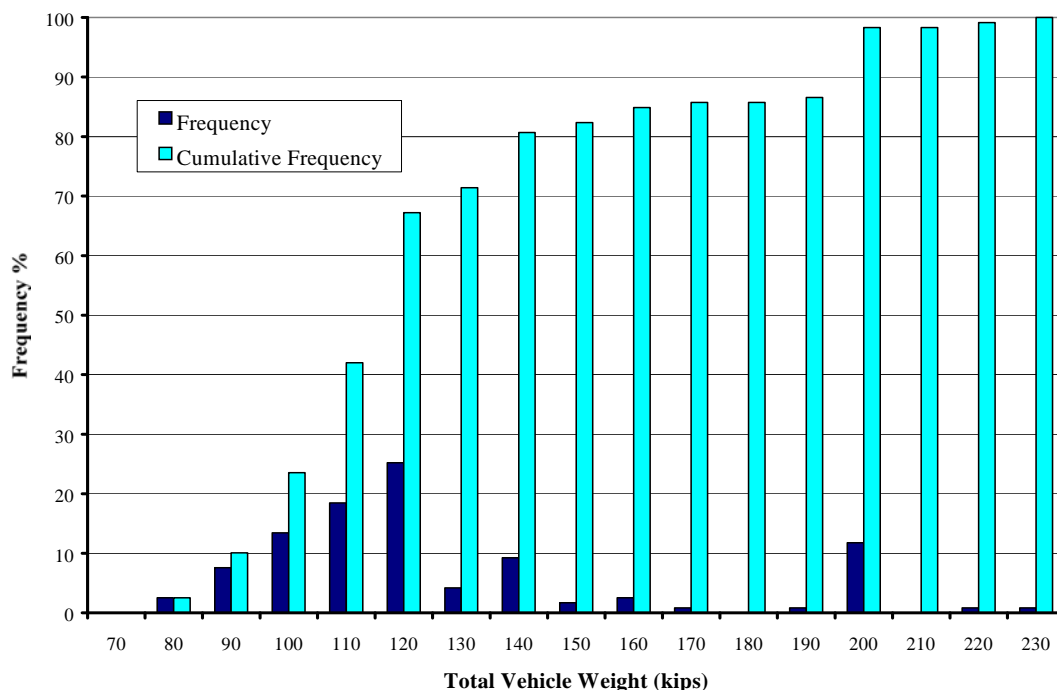


Figure 2.8: Total Weight Histogram of Permitted Vehicles (excluding Superheavy)

2.3. TRENDS PRESENT IN THE SUPERHEAVY TRUCK DATABASE

The most important trend to be noticed within the Superheavy vehicle category stems from the TxDOT Superheavy vehicle definition itself. All Superheavy trucks have a gross vehicle weight over 250 kips (see Figure 2.3). Some other important trends are listed below:

1. Within the Superheavy Vehicle Database, 79% of these vehicles weigh between 250 and 700 kips. The average weight of these vehicles is 515 kips. See Figure 2.9.

2. The minimum Superheavy vehicle length is 83.6 feet and 89% of the Superheavy vehicles have a vehicle length of 225 feet or less. The average length of the Superheavy vehicles is 138 feet. See Figure 2.10.
3. The maximum axle weight of 89% of the Superheavy vehicles is less than 50 kips. The lowest maximum axle weight in these Superheavy records is 21.5 kips. The average maximum axle weight of the Superheavy vehicles is 38.0 kips. See Figure 2.11.
4. The maximum axle spacing of 79% of the Superheavy vehicles is less than 60 feet. The average maximum axle spacing is 39.7 feet. See Figure 2.12.
5. Within the Superheavy vehicle category, 74% of the Superheavy vehicles have less than 16 axles, and 89% have less than 20 axles. Eleven axles are the fewest on any Superheavy vehicle. See Figure 2.13.

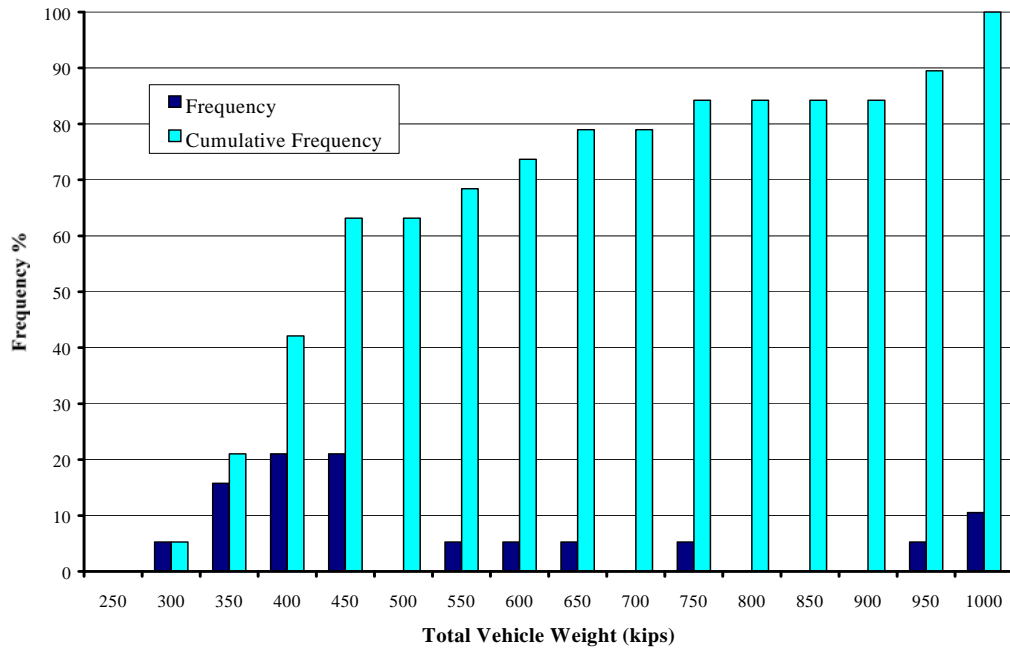


Figure 2.9: Total Weight Histogram for Superheavy Vehicles Only

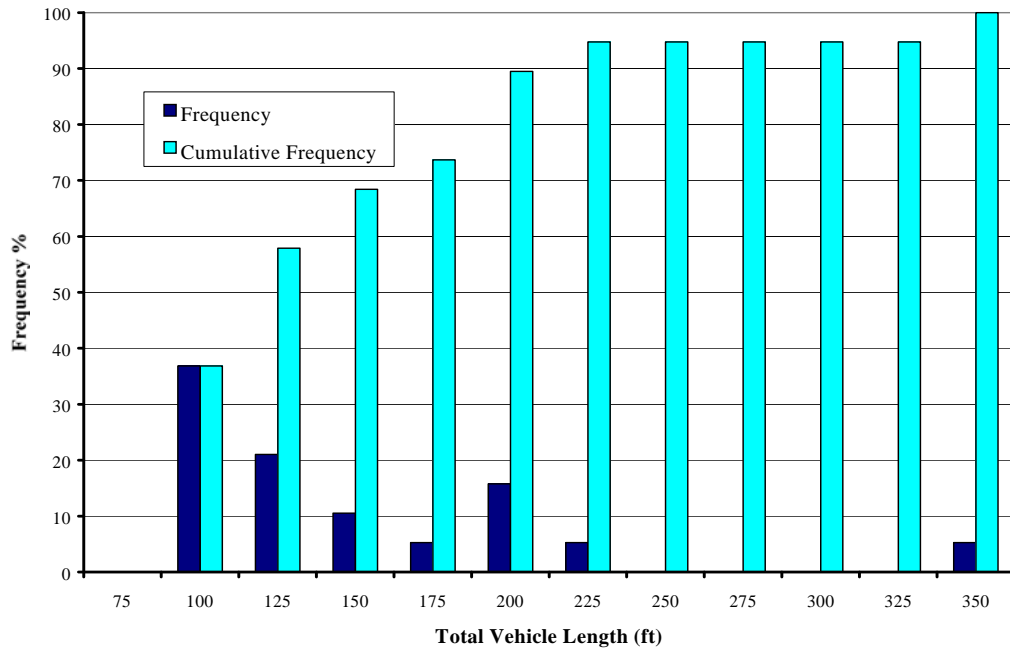


Figure 2.10: Total Length Histogram for Superheavy Vehicles Only

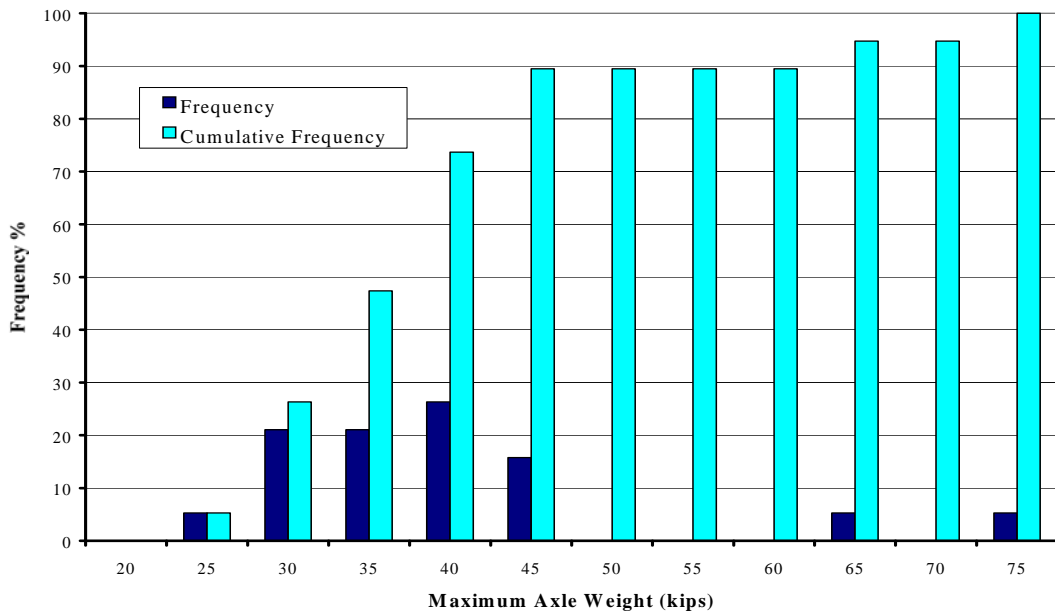


Figure 2.11: Maximum Axle Weight Histogram for Superheavy Vehicles Only

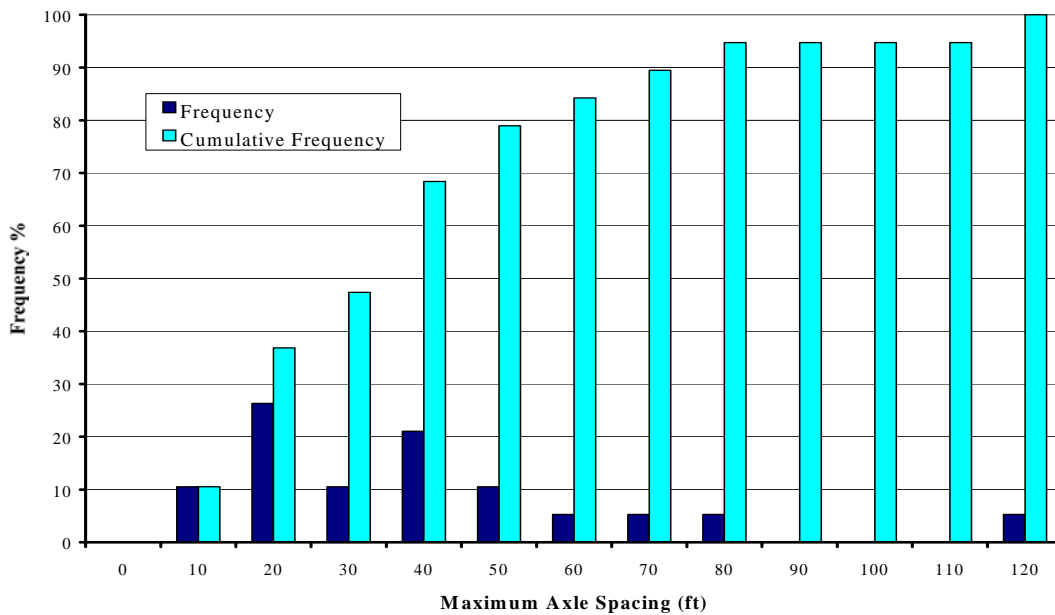


Figure 2.12: Maximum Axle Spacing Histogram for Superheavy Vehicles Only

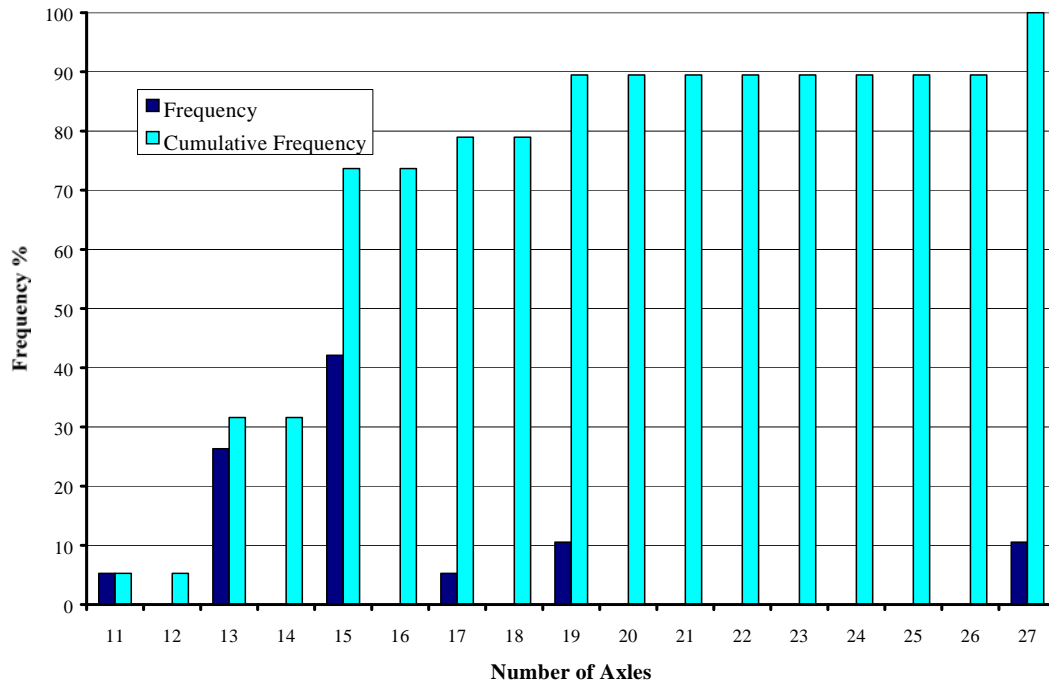


Figure 2.13: Number of Axles on Superheavy Vehicles Histogram

The heaviest record in the Superheavy truck database was Record 205, weighing 990 kips and carrying “McDermott Bridge Beam #2”. The record with the greatest vehicle length was Record 212, measuring 335 feet in length and carrying a Texaco petrochemical vessel. The vehicle with the greatest axle weight was also Record 212 with an axle weight of 70.0 kips. This axle weight alone is almost the total weight of an AASHTO HS20-44 design truck, whose total weight is 72,000 pounds. It is easy to imagine the type of overload this truck in particular could produce in a bridge designed for an HS20-44 truck configuration.

Table 2.1: Permit Vehicle Database Summary

Category		Permit Trucks	Superheavy Trucks	All Vehicles
Number of Axles	Min.	4	11	4
	Max.	13	27	27
	Ave.	6.6	16.1	8
Vehicle Length	Min.	17 ft	80.1 ft	17 ft
	Max.	151 ft	335.3 ft	335.3 ft
	Ave.	64.5 ft	137.7 ft	74.2 ft
Vehicle Weight	Min.	74.7 kips	294.7 kips	74.4 kips
	Max.	230 kips	988.6 kips	988.6 kips
	Ave.	124.1 kips	515.0 kips	177.1 kips
Max. Axle Weight	Min.	15 kips	21.5 kips	15 kips
	Max.	27 kips	70 kips	70 kips
	Ave.	20.75 kips	38.0 kips	23.1 kips
Min. Axle Weight	Min.	10 kips	12 kips	10 kips
	Max.	27 kips	20 kips	27 kips
	Ave.	14.0 kips	14.9 kips	14.2 kips
Max. Axle Spacing	Min.	7 ft	14 ft	7 ft
	Max.	99 ft	117 ft	117 ft
	Ave.	32.6 ft	39.7 ft	33.4 ft
Permit Fee	Min.	\$0.00	N / A	\$0.00
	Max.	\$4777.28	N / A	\$4777.28
	Ave.	\$168.07	N / A	\$168.07

It is not difficult to see the challenge of the truck permitting procedure when looking at the huge variation in the vehicles requesting permits today. TxDOT categorizes vehicles into “typical” and “Superheavy” groups to help separate these permit trucks somewhat, but even the variation of vehicle characteristics within each group is large. The purpose of developing this database was to help visualize the range of variations in permitted vehicles on Texas highways. The next step in the study of these vehicles’ effects on bridges

is performing line girder analyses on some simple bridge layouts using these truck records.

CHAPTER 3

LINE-GIRDER ANALYSIS TECHNIQUES

A line-girder analysis is an important first step in bridge design, and can prove to be quite useful in bridge rating and analysis also. For bridge rating purposes, line-girder analyses can be helpful in determining if a more detailed three-dimensional (3-D) analysis is required. Arbitrary truck layouts can be modeled as a series of point loads and moved across the bridge superstructure, idealized as one girder, to determine an estimate of the total bending moment and shear demand required of the bridge. If these moment and shear values are sufficiently beneath the nominal capacities of the structure, the line-girder analysis is sufficient to permit the vehicle in question.

This chapter outlines the line-girder analysis techniques available and gives examples of how this type of analysis can expedite the overweight truck permitting procedure. All line-girder analyses completed for this project were done using both a Microsoft EXCEL spreadsheet and the general purpose SAP2000 structural analysis program. The EXCEL spreadsheet was developed early in this project to analyze simply supported bridge spans only. It was also used as an independent check of SAP2000's output results to verify that SAP2000 was analyzing bridge structures in the manner required for bridge rating purposes. After verifying the SAP2000 results, further analyses were completed for continuous line-girder bridge layouts using SAP2000 only. All analyses involving trucks with more than 13 axles were also completed using

SAP2000 alone. It was deemed too time-consuming to develop a spreadsheet for these operations, and SAP2000 allowed the user to quickly generate results for such vehicles and structures. All continuous structures examined during this phase of the research were bridges comprising two equal span lengths. The span lengths were varied in each model; however, each model was symmetric about its interior support. This was done to identify trends in the results due to various truck layouts and does not assume that bridges must conform to these ideal geometries to be analyzed in this fashion. SAP2000 allows the user to model any type of bridge structure, from single to multiple spans of varied lengths, as required by the analyst.

3.1. DEVELOPMENT OF THE EXCEL SPREADSHEET PROGRAM

The development of an independent means of calculating maximum moment and shear response of an arbitrary truck layout on a simply supported line-girder structure was important to the verification of a commercial program's output. The spreadsheet developed for this project needed to be flexible enough to accommodate trucks that varied in size from 2 axles to 13 axles. This flexibility would accommodate every AASHTO design truck and all records within the Permit Truck Database, except for the Superheavy vehicle records. The spreadsheet program was designed to allow for arbitrary truck axle spacing and weight, and also accounted for various overall vehicle lengths.

The spreadsheet used an algorithm that marched each truck across the girder's span at intervals designated by the user. The overall truck length was calculated by using the individual axle spacing information, and the truck was

then moved incrementally, and analysis completed at each step, until the last truck axle was off the end of the span. A separate algorithm was generated to determine, at each interval, whether each axle was on or off the span. In the shorter span bridges, some truck axle spacings were such that some axles were already across the span while some others were not yet beginning to travel onto the span. The algorithm used in the spreadsheet program determined each axle's position and created a list of "effective" axles at each position in the truck's incremental movement across the span.

Using these "effective" axles, the principles of statics were used on these determinate structures to calculate the reaction forces at each end of the girder. Moments were summed about each end of the span to calculate the reactions at the opposite end due to the position of the "effective" truck axles. Since this analysis involves live loads only (permitted truckloads), the shape of the live load shear diagram can be determined. Since point loads are the only applied loads of interest on the girder, (no girder self-weight considerations, for example), the slope of the shear diagram is zero between these point loads. Further, we can check the shear diagram for correctness by making sure the values of internal shear match the reaction forces at each end of the line-girder.

Internal moments are easily calculated after determining the shear diagram, using the principle that the area under the shear diagram is the change in moment from point to point. The value of moment at each end of the simply supported beam is known to be zero by definition of a simply supported span. This also gives a check of the moment calculation procedure, by making sure

the moment at each end resolves to zero. It should be noted that the rear axle spacing of the AASHTO HS20-44 vehicle is variable between 14 and 30 feet. The 14-foot spacing is used in this example because it produces maximum moment and shear effects on these simple spans. (See Figure 3.1.)

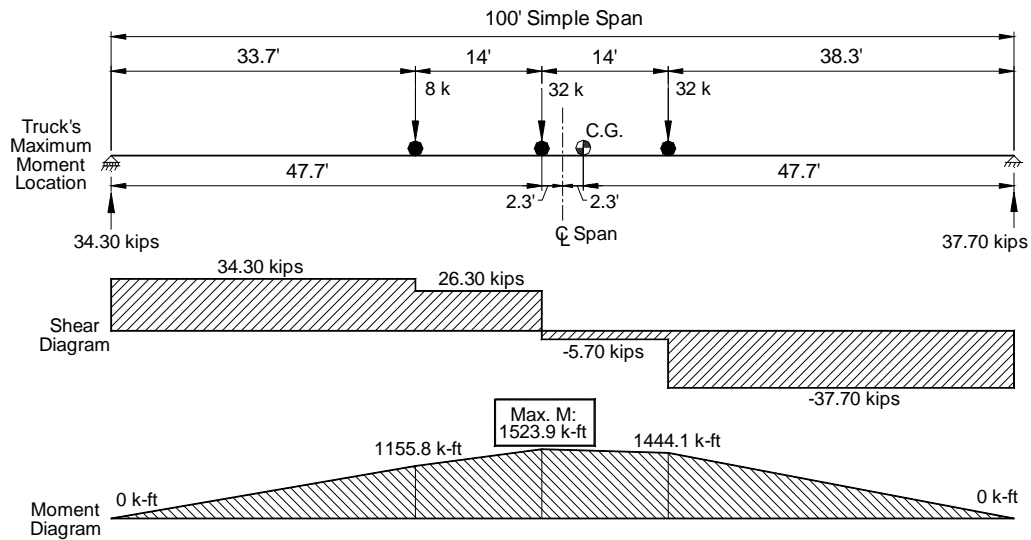
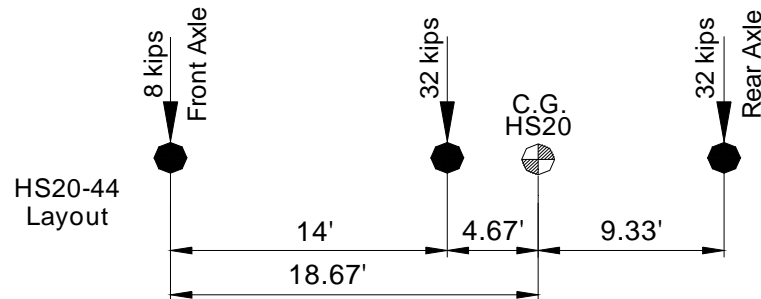


Figure 3.1: Loading, Shear, and Moment Diagrams for HS-20 Truck at Critical Moment Location on a 100-Foot Simple Span

These shear and moment diagrams are calculated at each interval of truck position to try and capture the point at which each truck produces maximum shear and moment values. Increment sizes are important when completing these calculations since one can specify too large an increment and miss the point where maximum shears and moments occur within the span. Maximum shear effects are produced on a simple span when an axle is located directly above a support. For that reason, we can be sure to capture this

position by specifying an interval that is a common factor of each axle spacing. If, for example, the truck axle spacings are all even numbers (in feet), we could simply use 2 foot segments as the spreadsheet increment and be sure to capture the maximum shear effect on the span. Unfortunately, the maximum moment positions are not as easy to pinpoint, especially when continuous spans or many truck axles are concerned.

On a simple span, if all truck axles are on the bridge simultaneously, the location of the truck that causes the maximum moment effect can be calculated by first finding the center of gravity of the vehicle's axles. An example of how this is done is shown in Figure 3.2.



Determination of the HS20 Truck's Center of Gravity			
	Distance from Front Axle	Axle Load	Load x Dist.
Front Axle	0'	8 kips	0 k-ft
Middle Axle	14'	32 kips	448 k-ft
Rear Axle	28'	32 kips	896 k-ft
		Sum = 72 k	Sum = 1344 k-ft
Truck C.G. Location = (1344 k-ft / 72 k) = 18.67 ft from Front Axle			

Figure 3.2: Example for Calculating a Truck's Center of Gravity

If a vehicle is too long for all axles to fit on the bridge simultaneously, this statement must be modified. In that case, the maximum moment can be calculated by finding the center of gravity locations of each set of “effective” axles on the bridge span as the truck is marched along the structure. The maximum moment occurs within the span when the centerline of the span is midway between the center of gravity of the effective point loads and the nearest concentrated load. Stated in another way, the maximum bending moment produced by moving concentrated loads occurs under one of the loads when that load is as far from one support as the center of gravity of all the moving loads on the beam is from the other support. These statements are better understood while looking at the illustration shown in Figure 3.1.

Due to the rapid personal computer processors available today, it was possible to use very small increments throughout these spreadsheet analyses (between 1/10 of a foot and 1/6 of a foot) to avoid the possibility of missing these maximum moment positions by more than 0.07 feet. The fractions are shown to emphasize the point made earlier describing the common factor technique to find maximum shear response. These increments are quite small, but only a small amount of extra processing time was added to the analysis of each vehicle in this manner, and this guaranteed miniscule errors in the spreadsheet output values for the maximum shears and moments recorded.

3.2. SELECTION OF SAP2000 FOR BRIDGE ANALYSIS PURPOSES

Obviously, the spreadsheet program was not developed to handle all possible cases of bridge geometry and truck layout. Instead, a commercial

program, SAP2000 was utilized to study a wider range of bridges and permit trucks. Many general purpose structural analysis programs are available to the bridge engineer, but very few possess a built-in interface for bridge-related analyses with a finite-element package. SAP2000 NonLinear Version 6.13 does handle bridge-related topics such as influence lines, truck induced moment and shear envelopes, and AASHTO travel lane concepts.^[6] AASHTO vehicles, along with typical CALTRANS vehicles and common railroad loadings, are available as standard vehicles within the program. Also available are user-defined vehicle generation techniques that allow the engineer to quickly input an uncommon or even Superheavy vehicle for permitting purposes. It was for this reason that SAP2000 was the program selected for this project, along with SAP2000's user-friendly finite-element pre-processor. A detailed step-by-step tutorial for performing a SAP2000 line-girder analysis is available in Appendix A.

3.2.1. Using Line-Girder Analyses to Identify Critical Bridges

Performing line-girder analyses are the first steps taken in the process of designing new bridge structures. Using the principles of Lateral Load Distribution Factors, line-girder results are extrapolated to each individual girder, estimating how much of the total bridge resistance must be supplied by each individual girder. During bridge analysis, the analyst needs to obtain similar information. For example, assume that the bridge in question is a two-lane structure, designed to carry AASHTO HS20-44 vehicles, showing no deterioration or distress. We know, from the design criteria alone, that the

structure is capable of carrying at least two HS20-44 vehicles at once (since it is a two-lane bridge), when each vehicle is located in the precise position required to produce maximum stress effects in one or more of the bridge girders. There is also some amount of reserve capacity in the structure, but for now we are concerned with only the minimum resistance available within the structure.

Reserve capacity can exist due to parapets, other additional stiffeners (such as curbs, railings, and sidewalks), and the neglected moment capacities within the slab. This thesis will focus on utilizing only the slab moments that are generated during bridge loading. The AASHTO LLDF calculation approach to bridge design assumes all live loads are distributed to the girders only. Of course, due to slab stiffness, slab moments are also generated under service loads, thus reducing the stresses in the girders. This effect can become quite significant, especially in short span bridges. The effects of sidewalks and railings on distribution factors in steel bridges are studied in a publication by Mabsout, Tarhini, Frederick, and Kobrosly.^[10] This thesis will focus primarily on the effects of the slab moments on LLDF calculation.

If a truck that is questionable due to its size or weight is to be driven across a questionable structure, it would be helpful to know how severe the overload possibility is. A line-girder analysis of the structure under the influence of a single design truck, compared with a line-girder analysis of the single truck in question would quickly estimate the degree of overload possible. Calculating the Maximum Moment Ratio of these two separate truck responses will quantify this overstress potential. The definitions of these Maximum

Moment Ratios for single trucks are shown in Equations 3.1, 3.2, and 3.3. The AASHTO H15 and HS20 vehicles are used for comparison in this thesis because they represent the lightest and the heaviest of the AASHTO design vehicles, respectively. The Moment Ratios calculated with these vehicles represent the extremes that exist for all vehicles in this database.

$$\text{Max. Moment Ratio (MR)} = \frac{\text{Max. Truck Line Girder Moment}}{\text{Max. AASHTO Truck Line Girder Moment}} \quad (3.1)$$

$$\text{Max. H15 MR} = \frac{\text{Max. Truck Line Girder Moment}}{\text{Max. H15 Line Girder Moment}} \quad (3.2)$$

$$\text{Max. HS20 MR} = \frac{\text{Max. Truck Line Girder Moment}}{\text{Max. HS20 Line Girder Moment}} \quad (3.3)$$

Since the example bridge under consideration was designed for HS20 vehicles, the HS20 MR would be calculated. This HS20 MR represents the scalar multiplier of the AASHTO HS20 vehicle's maximum moment effect required to calculate the permit vehicle's maximum moment effect. If the HS20 MR for this example bridge was found to be 2.0, for instance, it would mean that the truck in question was capable of producing twice the total moment produced by a single HS20 vehicle.

This calculation alone, however, does not guarantee that any of the bridge girders will be overstressed by the vehicle in question. How an individual bridge girder is loaded is a function of a vehicle's transverse

positioning as well as the longitudinal position where it will produce maximum moment. Obviously, a vehicle placed in its maximum moment position longitudinally will load each of the girders differently, depending on its transverse location. A truck placed nearest the curbs of a bridge will produce very different distribution effects than a truck straddling the bridge's transverse centerline.

In order to quickly determine the moment effect to one girder, say the exterior girder, this MR could be used with the AASHTO design LLDF's calculated for the bridge. These are conservative LLDF's, but they can be helpful in quickly determining of overload potential exists. Chapter 4 explains the technique for determining the AASHTO design LLDF's. For checking the exterior girder, the AASHTO LLDF calculated for the exterior girders only would be used as shown in Equation 3.4.

$$(LLDF_{AASHTO}) \times (HS20 MR) \times (Line Girder M_{HS20}) = Max. Girder M \quad (3.4)$$

This maximum girder moment developed under an overweight vehicle could be compared with the moment found in the exterior girder when the bridge is assumed fully loaded under AASHTO design criteria. If the maximum moment the exterior girder sees is less than the moments produced due to design loads, the vehicle in question is safe to pass. The vehicle may also be safe to pass if the maximum girder moment is greater than the design moments. This is due to the safety factors built into the AASHTO design code.

Using AASHTO Working Stress Design Criteria:

$$LL + DL \leq 0.55 F_y \quad (3.5)$$

Using Equation 3.5, it can be demonstrated that extra live load capacity exists before actual girder yielding would begin. This is also the case when checking using AASHTO Load Factor Design criteria.

Using AASHTO Load Factor Design Criteria:

$$1.3 DL + 2.17 LL \leq F_y \quad (3.6)$$

The live load multiplier in Equation 3.6 could be dropped in order to determine more accurate bridge girder capacities near girder yield stresses. The AASHTO design methods automatically place excess capacity into each bridge girder design. Under the passage of an overloaded truck, traffic patterns on a critical bridge can be modified so that the live loads present on a structure can be limited to the overweight truck only, and therefore accurately determined. The multipliers shown in the previous AASHTO design equations are necessary to handle the day-to-day loading pattern uncertainty that exists for each individual bridge structure designed. However, when the live load pattern can be controlled, as in this case, these load factors could be modified so that true bridge capacities are not under-estimated.

It must be noted that these approaches have used the AASHTO design LLDF calculation technique, which is also conservative in nature. Using this approach, slab moments are not considered and specific individual bridge characteristics were not used to generate the LLDF relationships. This thesis aims at using finite element analysis methods to more accurately calculate true LLDF's to increase bridge capacity estimates. By determining more accurate LLDF's, critical bridge structures, thought to be overstressed when checked using the AASHTO design LLDF's, may have the capacities to not be overstressed. While line-girder analyses are helpful in quickly identifying potential overloads, they must be combined with refined LLDF's to estimate true bridge capacities.

Using the finite element method, overweight trucks can be placed in any transverse bridge location, or where the actual travel lanes are located, rather than at the position that conservatively produces maximum moment effects for each girder. The true loading pattern can be modeled on the bridge, rather than using worst-case loading assumptions required during design. Chapters 4 and 5 explain the procedures and benefits related to the finite element analyses performed on three example bridges.

3.2.2. Simple Span Bridge Line-Girder Analyses

To get an idea of the potential overstress levels the TxDOT truck database could produce, many graphs were created to illustrate which vehicles caused the greatest maximum moment responses. Graphs were produced using the Maximum Moment Ratios plotted versus different truck variables to help

identify which truck characteristics affected the maximum moment each truck produced. These graphs were constructed for both the simply supported bridge spans and the continuous bridge spans, and the minimum weight (H15) and maximum weight (HS20) AASHTO trucks were used for comparison. Permitted trucks and Superheavy trucks were plotted separately, since the Maximum Moment Ratios were drastically different for some bridge layouts. The most obvious moment ratio trend is visible when plotted against each vehicle's total weight. Figures 3.3, 3.4, 3.5, and 3.6 show this trend, breaking up the total vehicle database into H15 Moment Ratio, HS20 Moment Ratio, Permit Vehicles excluding Superheavy, and Superheavy vehicles alone. The segregation between the typical permit trucks and the Superheavy trucks helps identify the overload potential for the majority of permitted vehicles on the Texas highways, separate from the rare Superheavy vehicles.

Figure 3.3 illustrates the relationship between Total Vehicle Weight and the maximum simple span moment ratio produced by each truck (excluding Superheavy vehicles) when compared with an AASHTO H15 vehicle (see Equation 3.2). Span lengths of 50 feet, 100 feet, and 150 feet are plotted, to show the increase in moment ratio as bridge span length is increased. For every vehicle, the moment ratio on the 50-foot simple span is the smallest, and the moment ratio on the 150-foot simple span is the greatest. In other words, as span lengths increase, the moment produced by each permitted vehicle increases more rapidly than the moment produced by the AASHTO H15 design vehicle. Looking at Figure 3.4, however, shows that this rule does not exist for

the comparisons with the AASHTO HS20 vehicle. For some of the lighter permitted vehicles, the maximum moment ratio when compared with the HS20 truck was actually produced on the shortest span, the 50-foot span.

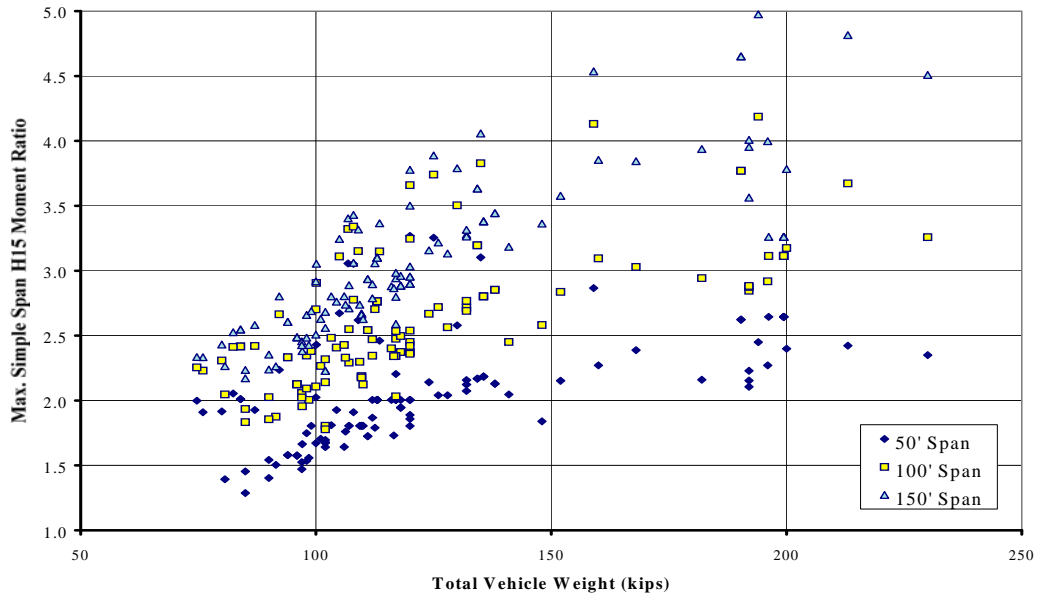


Figure 3.3: Maximum Simple Span H15-44 Truck Moment Ratio vs. Total Vehicle Weight Excluding Superheavy Vehicles

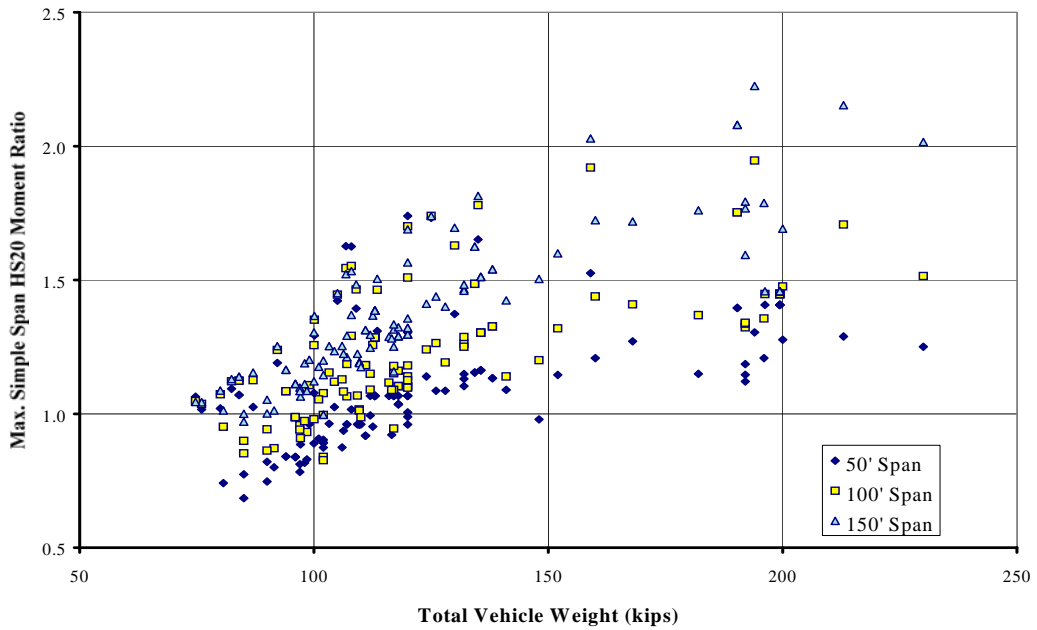


Figure 3.4: Maximum Simple Span HS20-44 Truck Moment Ratio vs. Total Vehicle Weight Excluding Superheavy Vehicles

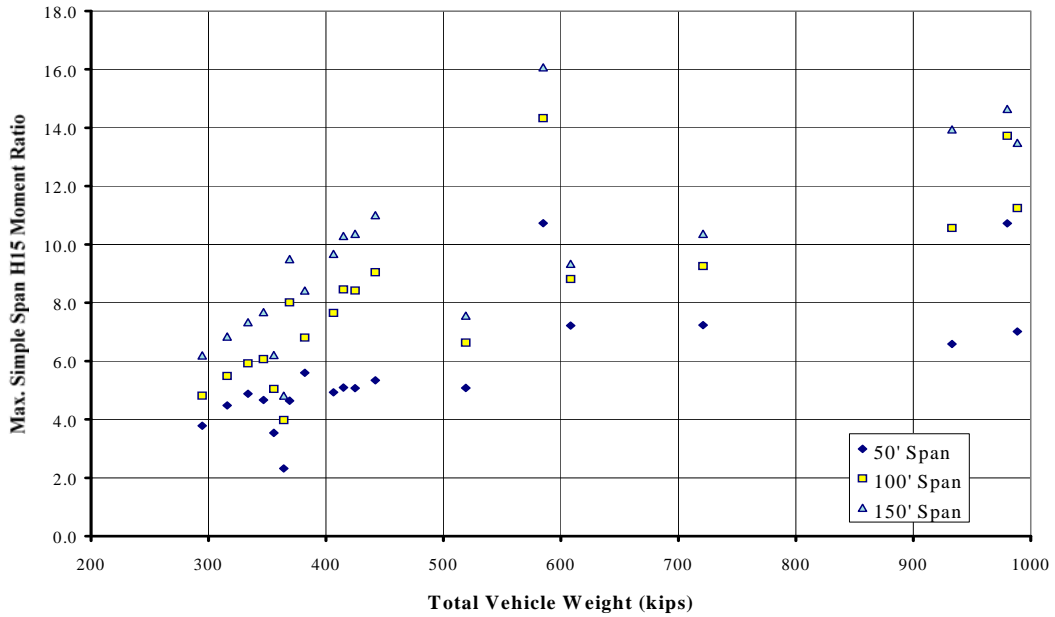


Figure 3.5: Maximum Simple Span H15-44 Truck Moment Ratio vs. Total Vehicle Weight – Superheavy Vehicles Only

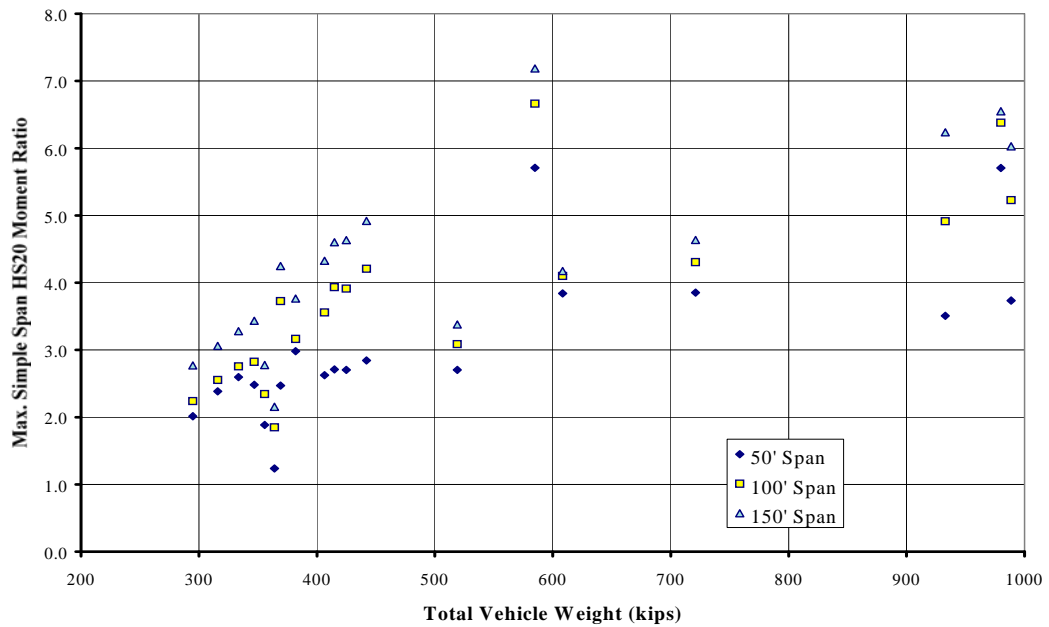
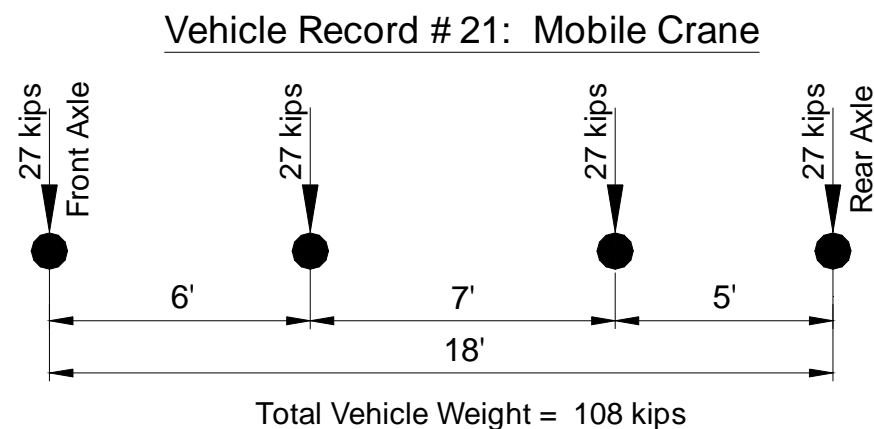


Figure 3.6: Maximum Simple Span HS20-44 Truck Moment Ratio vs. Total Vehicle Weight – Superheavy Vehicles Only



Max. Simple Span 50' Moment	Max. Simple Span 100' Moment	Max. Simple Span 150' Moment
1020 k-ft	2366 k-ft	3715 k-ft
Max. 50' HS20 Moment Ratio	Max. 100' HS20 Moment Ratio	Max. 150' HS20 Moment Ratio
1.62	1.55	1.53

Figure 3.7: TxDOT Database Vehicle Record #21 – “Mobile Crane”

A good example of a truck that produced the maximum HS20 moment ratio on the shortest span is Vehicle Record 21. This vehicle is described as a Mobile Crane and has 4 axles. Each axle load is 27 kips and the spacings of the axles from front to rear are 6 feet, 7 feet, and 5 feet, respectively. The total length of the vehicle is only 18 feet, and the total weight is 108 kips. Figure 3.7 shows the layout of Vehicle Record 21. The HS20 design vehicle has a total

weight of only 72 kips, and is spread over a minimum of 28 feet. Due to the fact that Vehicle Record 21 is both shorter and heavier than the HS20 design vehicle, this apparent reversal in the maximum moment trend becomes understandable. For these vehicles, as span lengths increase, the moment produced by the AASHTO HS20 design vehicle increases more rapidly than the moment produced by these permitted vehicles. These vehicles, which are both shorter and heavier than the design trucks they are compared with, comprise only a small percentage of all vehicles in the database. For most vehicles, the maximum moment ratios tend to increase as the span lengths increase.

Another important trend to notice is the fact that the maximum H15 moment ratio is always greater than the maximum HS20 moment ratio for each vehicle. This is simply due to the fact that the H15 vehicle is a two-axle truck with a total weight of only 30 kips and the HS20 vehicle is a three-axle truck with a total weight of 72 kips. The HS20 always produces a greater moment effect than does the H15 on these simple span lengths, causing the maximum moment ratios to vary accordingly.

A graph was produced to allow an analyst the opportunity to extrapolate the maximum moment ratios (MR's) on a simple span for all four AASHTO vehicles (the H15, HS15, H20, and HS20) from the determination of just one of these moment ratios. If, for example, line-girder results for an overweight vehicle were compared to those for an H15 vehicle on a simple span, this graph could be used, along with a 1.333 multiplier, to find the moment ratios for any of the design vehicles desired. The graph shown in Figure 3.8 is only useful on

simple spans, but allows an analyst the opportunity to generate all of the moment ratios by analyzing only one of the AASHTO design vehicles. This graph allows an analyst the opportunity to create a spreadsheet to generate all of the design truck moment ratios for a given simple span bridge length through the line-girder analyses of only one design truck and the permit truck.

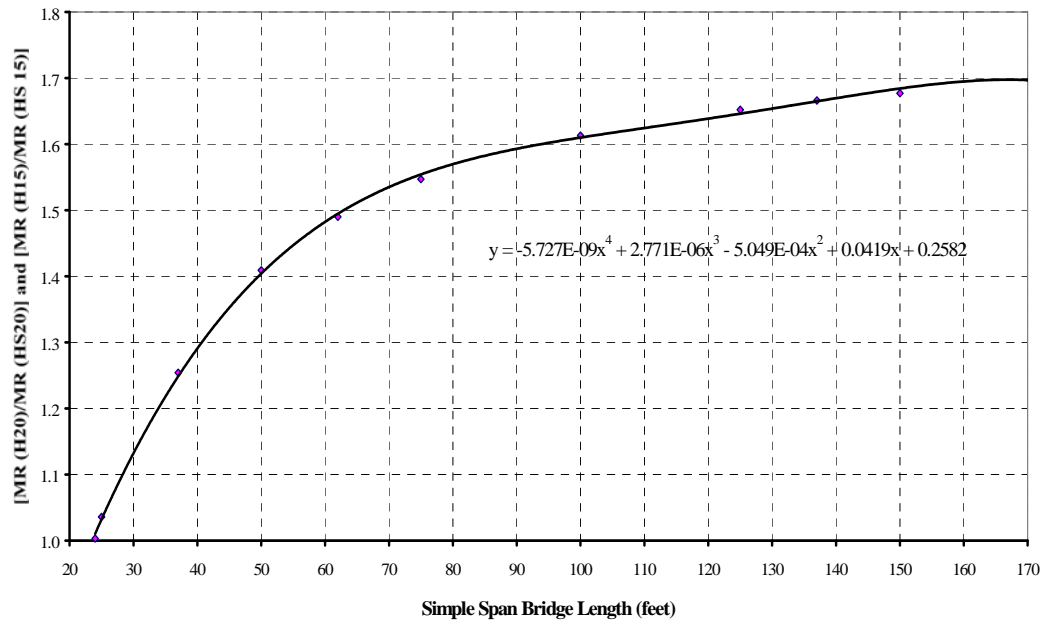


Figure 3.8: AASHTO H-Series and HS-Series Moment Ratio Conversion Chart on Simple Spans of Varied Length

$$\frac{MR (H20)}{MR (HS20)} = \text{Conversion Ratio, see Figure 3.8} \quad (3.7)$$

$$\frac{MR (H15)}{MR (HS15)} = \text{Conversion Ratio, see Figure 3.8} \quad (3.8)$$

$$\frac{MR (H15)}{MR (H20)} = 1.333 \quad (3.9)$$

$$\frac{MR (HS15)}{MR (HS20)} = 1.333 \quad (3.10)$$

Both the equation and graph shown in Figure 3.8 were developed by calculating the MR's produced by all vehicles in the vehicle database using the spreadsheet program. MR's for the H20 and HS20 vehicles were compared through simple division on span lengths of 25 feet, 37 feet, 50 feet, 62 feet, 75 feet, 100 feet, 125 feet, 137 feet, 150 feet, and 175 feet. The same procedure was used to compare the MR's of the H15 and HS15 vehicles. Using Microsoft EXCEL, these ratios were plotted, against simple span length, to generate the best-fit equation shown in Figure 3.8. An example of how to use these relationships will focus on Vehicle Record 21 (see Figure 3.7).

Table 3.1: Vehicle Record #21 Moment Values and Moment Ratios

	50' Simple Span	100' Simple Span	150' Simple Span
Vehicle #21 Max. Moment	1020 ft-k	2366 ft-k	3715 ft-k
H15 Max. Moment	334 ft-k	709 ft-k	1083 ft-k
HS15 Max. Moment	471 ft-k	1143 ft-k	1817 ft-k
H20 Max. Moment	446 ft-k	945 ft-k	1445 ft-k
HS20 Max. Moment	628 ft-k	1524 ft-k	2423 ft-k
Fig. 3.10 Conversion Value	1.41	1.61	1.68
H15 Moment Ratio	3.05	3.34	3.43
HS15 Moment Ratio	2.17	2.07	2.04
H20 Moment Ratio	2.29	2.50	2.57
HS20 Moment Ratio	1.62	1.55	1.53

Assuming we have a simple span bridge of 100 feet in length, it is possible to calculate the Maximum Moment Ratios for all four AASHTO design vehicles, knowing the maximum moment generated by only one design

vehicle. Assume we have already calculated the Maximum Moment Response due to an H15 design vehicle. The maximum moment value for an H15 vehicle, shown in Table 3.1, is found to be 709 ft-kips. Since the maximum moment produced by Vehicle Record 21 is 2366 ft-kips (also shown in Table 3.1), we can calculate the H15 Maximum Moment Ratio (MR) as shown in Equation 3.11.

$$\text{Max. H15 MR} = \frac{2366 \text{ ft} - k}{709 \text{ ft} - k} = 3.34 \quad (3.11)$$

It is not necessary to find the maximum moment positions for the HS15, H20, or HS20 vehicles and analyze their moment effects to calculate their Maximum Moment Ratios. Instead, the conversion ratios shown in Figure 3.8, along with the 1.333 conversion ratio, can be used to quickly achieve all desired Maximum Moment Ratios. If we needed to find the Vehicle 21 Maximum H20 MR from the previously calculated H15 MR, Equation 3.9 would apply. Rearranging Equation 3.9, the Maximum H20 MR would be 2.50, as shown in Equation 3.12.

$$\text{Max. H20 MR} = \frac{\text{Max. H15 MR}}{1.333} = \frac{3.34}{1.333} = 2.50 \quad (3.12)$$

At this point, both H-series trucks' MR's have been found, and the HS-series truck's MR's are desired. First, we need to determine the conversion

value from the graph in Figure 3.8. Since the bridge in question is 100 feet in length, we can either substitute “100” for variable “x” in the equation, or read the value from the graph directly. The conversion value is found to be 1.61. Using Equation 3.7, the Maximum Vehicle 21 HS20 MR is 1.55. Equation 3.13 illustrates this conversion.

$$\text{Max. HS20 MR} = \frac{\text{Max. H20 MR}}{1.61} = \frac{2.50}{1.61} = 1.55 \quad (3.13)$$

Finally, for the HS15 conversion, the same conversion ratio of 1.61 is utilized, since it is a function of span length alone. Since the maximum H15 MR has been determined to be 3.34, it can be used, along with the graph in Figure 3.8 to determine the Maximum Vehicle 21 HS15 MR. Using Equation 3.8, the Maximum Vehicle 21 HS15 MR is 2.07. Equation 3.14 illustrates this conversion.

$$\text{Max. HS15 MR} = \frac{\text{Max. H15 MR}}{1.61} = \frac{3.34}{1.61} = 2.07 \quad (3.14)$$

Table 3.1 verifies these MR’s on a 100-foot span as calculated through the EXCEL spreadsheet program’s line-girder analysis. The equation shown in Figure 3.8 can be easily programmed into a spreadsheet and utilized for span lengths between 24 and 170 feet. It is important to remember that the Equation shown in Figure 3.8 is valid only for simple span bridges. The 1.333 multiplier,

however, that converts MR's between H15 and H20 vehicles and HS15 and HS20 vehicles is valid for all MR's calculated on any structure. This is true because the number and spacing of axles for each H-series and HS-series truck are constant when compared with each other, and the axle weights of each series are all related by 1.333 to each other. With the number of axles and the axle spacing the same, increasing or decreasing each axle's weight by a scalar will change the moment produced by those vehicles by the same scalar.

Another important statistic to look at when trying to decipher the overload potential of all the vehicles in this database is the maximum, minimum, and average moment ratio values produced on varied span lengths. This information helps to identify which groups of vehicles are most likely to be critical, and the expected range of moment ratios that could be produced. Table 3.2 shows this data for all TxDOT database vehicles on simple spans of 50, 100, and 150 feet.

Table 3.2: Simple Span Moment Ratio Summary

		Permit			Superheavy			All		
		50' Span	100' Span	150' Span	50' Span	100' Span	150' Span	50' Span	100' Span	150' Span
H15 MR	Min.	1.29	1.78	2.17	2.32	3.98	4.81	1.29	1.78	2.17
	Max.	3.27	4.19	4.98	10.7	14.3	16.1	10.7	14.3	16.1
	<i>Ave.</i>	<i>2.05</i>	<i>2.64</i>	<i>3.07</i>	<i>5.73</i>	<i>8.12</i>	<i>9.67</i>	<i>2.55</i>	<i>3.38</i>	<i>3.97</i>
HS15 MR	Min.	0.91	1.10	1.29	1.65	2.46	2.87	0.91	1.10	1.29
	Max.	2.32	2.60	2.97	7.61	8.88	9.58	7.61	8.88	9.58
	<i>Ave.</i>	<i>1.45</i>	<i>1.64</i>	<i>1.83</i>	<i>4.07</i>	<i>5.03</i>	<i>5.77</i>	<i>1.81</i>	<i>2.10</i>	<i>2.37</i>
H20 MR	Min.	0.96	1.33	1.63	1.74	2.98	3.61	0.96	1.33	1.63
	Max.	2.45	3.14	3.73	8.04	10.8	12.1	8.04	10.8	12.1
	<i>Ave.</i>	<i>1.54</i>	<i>1.98</i>	<i>2.30</i>	<i>4.30</i>	<i>6.09</i>	<i>7.25</i>	<i>1.91</i>	<i>2.54</i>	<i>2.97</i>
HS20 MR	Min.	0.68	0.83	0.97	1.24	1.85	2.15	0.68	0.83	0.97
	Max.	1.74	1.95	2.23	5.71	6.66	7.19	5.71	6.66	7.19
	<i>Ave.</i>	<i>1.09</i>	<i>1.23</i>	<i>1.37</i>	<i>3.05</i>	<i>3.78</i>	<i>4.32</i>	<i>1.36</i>	<i>1.57</i>	<i>1.77</i>

Table 3.2 shows that for the majority of permitted vehicles (excluding Superheavy vehicles), the average moment ratios are under 2.5, except for the 100-foot or longer spans designed for an H15 truck. This shows that for the average permit trucks, on a structure with at least two lanes, it is unlikely that any overload potential exists. It is also unlikely that a 100-foot or longer simple span bridge would be designed for the lightest H15 trucks, making the average permitted vehicles safe to travel over bridges designed for anything heavier than the H15 design vehicle.

The largest overload potential exists with the Superheavy vehicle designations, with the worst vehicle in this database producing 6.7 times the maximum moment of an HS20 vehicle on a 100-foot simple span and 7.19 times an HS20 maximum moment on a 150-foot span. These Superheavy vehicles create an average of 3.8 times the maximum moment of an HS20 vehicle on a 100-foot span, the heaviest of the AASHTO design vehicles commonly used. It is these vehicles that are the perfect candidates for analysis using 3-D finite element techniques. The worst moment created by the typical permit vehicles was only 2.2 times the same HS20 vehicle's maximum moment. In other words, the Superheavy vehicles are the primary reason for needing a 3-D, finite element analysis. However, when the design truck used on a medium to long span bridge is less than the AASHTO HS20, a 3-D analysis may be warranted for a typical overweight truck as well. The best way to quickly discover this overload potential is to complete a simple line-girder analysis, to quantify the maximum moment potential.

3.2.3. Continuous Span Bridge Line-Girder Analyses

Just as simple span bridges can be modeled quickly and easily as line-girders to quantify the overload potential of certain overweight or oversized trucks, continuous spans can also be analyzed as line-girders effectively. The results of these analyses must be viewed a bit differently, however, since continuous span bridges contain more possible locations of maximum moment effects. Negative moment regions in continuous structures are often the critical regions, but that is not necessarily the case when a span is relatively long with

short adjoining spans. In that case, a short, heavy truck may produce maximum positive moment ratios that control when compared to the maximum negative moment ratios generated over the girder supports. The same TxDOT Superheavy vehicle database used for the simple span analyses was used for the continuous span line-girder analyses. This allows for a direct comparison of the magnitudes of the moment ratios generated when compared to the same four AASHTO design vehicles.

It is not possible to analyze every type of continuous span bridge that exists, even in Texas alone. Continuous bridge structures can vary greatly, having anywhere from two to over a dozen spans, with varied span lengths as site conditions dictate. It is not necessary, nor is it the focus of this project, to analyze numerous types of continuous span bridges to show the potential overloads that can occur due to permitted trucks. The relatively simple analyses done for this project are merely examples of what can be done to any structure, composed of simple and/or continuous spans. The analyst can use the same line-girder techniques to model both types of bridges effectively, showing the flexibility and power of the line-girder analysis technique. Two sets of symmetric, two-span continuous span bridges were studied, one set containing three bridges with girders of constant cross-section, and one set containing three bridges with increased girder stiffness in the region of the interior support.

3.2.3.1. Symmetric Two-Span Continuous Bridge Structures with Constant Cross-Sections

All of the continuous bridge structures modeled for use in this study were comprised of only two spans each. Furthermore, each bridge analyzed was modeled with equal span lengths. The models used during these analyses had span lengths of 50 feet, 100 feet, and 150 feet. Also, only the Superheavy vehicles were used for these analyses. Since Superheavy vehicles generate the greatest moment effects as shown in Table 3.2, they are the best at showing the differences between simple span moment ratios and continuous span moment ratios. Since Superheavy vehicles tend to also have longer maximum axle spacings, the negative moment effects often critical to continuous spans tend to be inflated. Separate sets of analyses were done on the same lengths of continuous structures, in an attempt to generalize the effects of cover-plated regions in continuous bridge girders. Figure 3.9 shows the three continuous girder bridge layouts with constant cross-section studied during this project.

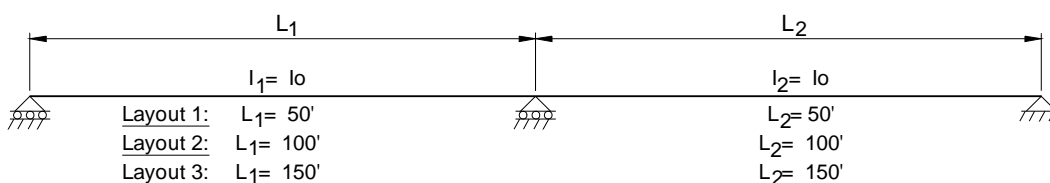


Figure 3.9: Three Continuous Girder Bridge Models with Constant Cross-Section

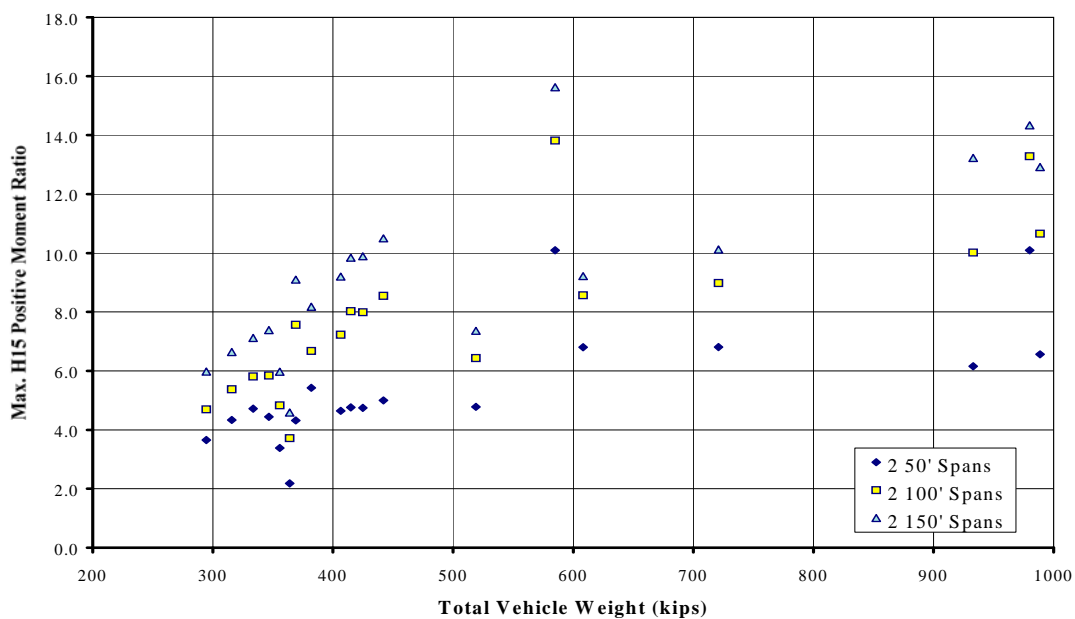


Figure 3.10: Maximum Continuous Span Positive H15 Truck Moment Ratio vs. Total Vehicle Weight – Superheavy Vehicles Only

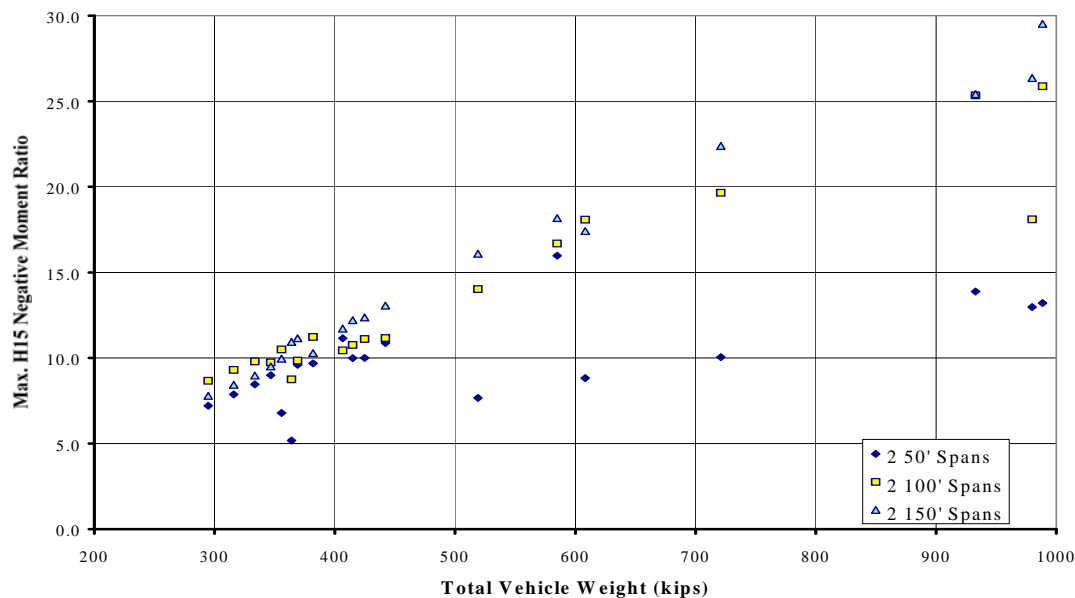


Figure 3.11: Maximum Continuous Span Negative H15 Truck Moment Ratio vs. Total Vehicle Weight – Superheavy Vehicles Only

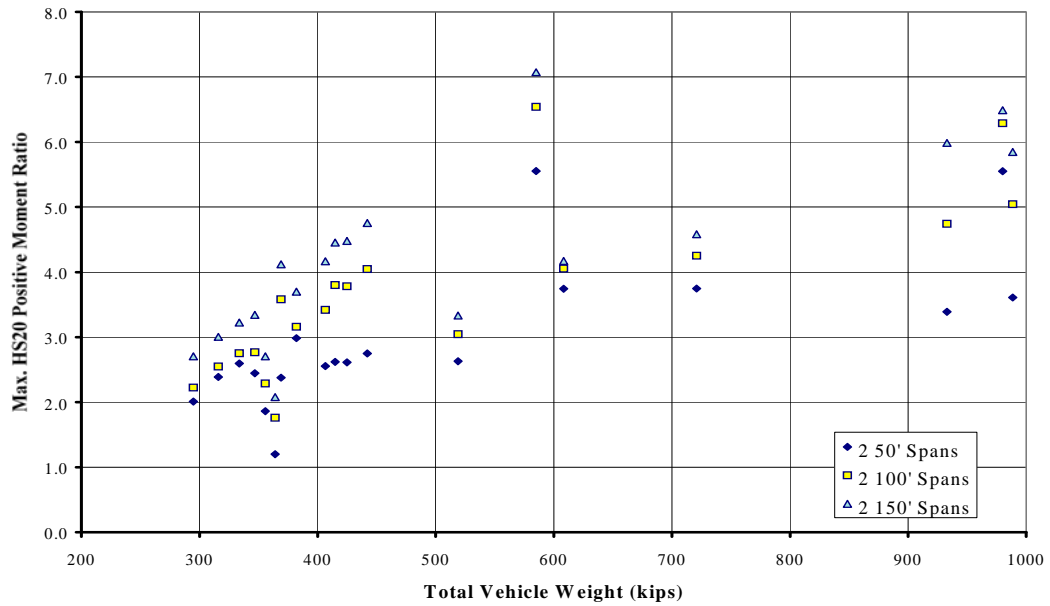


Figure 3.12: Maximum Continuous Span Positive HS20 Truck Moment Ratio vs. Total Vehicle Weight – Superheavy Vehicles Only

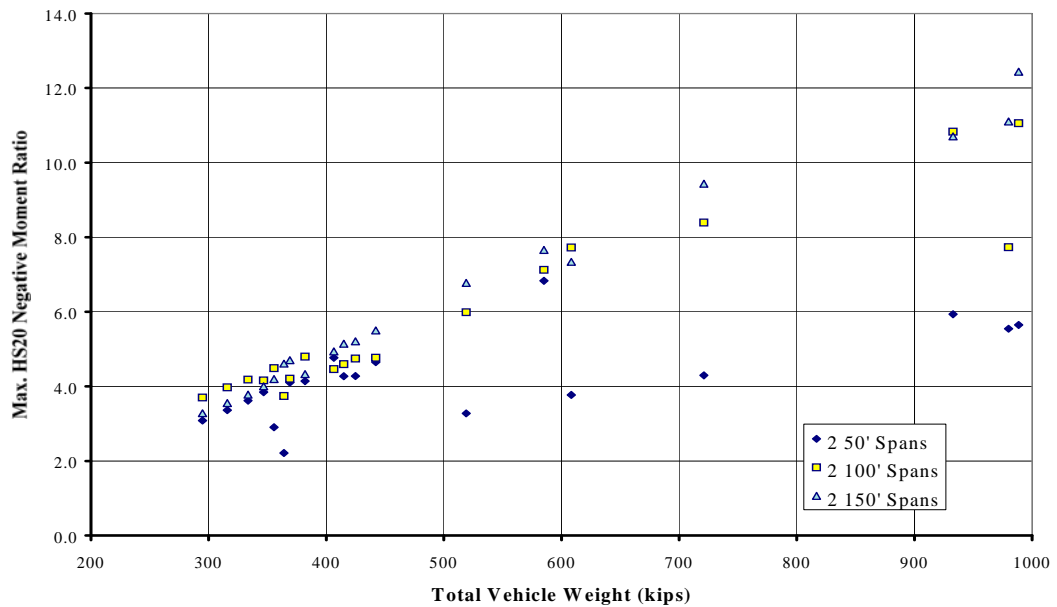


Figure 3.13: Maximum Continuous Span Negative HS20 Truck Moment Ratio vs. Total Vehicle Weight – Superheavy Vehicles Only

Table 3.3: Simple and Two-Span Continuous Moment Ratio Comparison

		Superheavy Vehicles Only								
		Simple Span			Continuous Span Positive Moment			Continuous Span Negative Moment		
		50'	100'	150'	50'	100'	150'	50'	100'	150'
H15 MR	Min.	2.32	3.98	4.81	2.18	3.72	4.59	5.17	8.66	7.79
	Max.	10.7	14.3	16.1	10.1	13.8	15.6	16.0	25.9	29.5
	Ave.	5.73	8.12	9.67	5.42	7.79	9.33	9.91	13.6	14.8
HS15 MR	Min.	1.65	2.46	2.87	1.60	2.35	2.77	2.95	4.93	4.37
	Max.	7.61	8.88	9.58	7.40	8.72	9.43	9.10	14.7	16.6
	Ave.	4.07	5.03	5.77	3.97	4.92	5.63	5.65	7.77	8.33
H20 MR	Min.	1.74	2.98	3.61	1.64	2.79	3.44	3.88	6.49	5.84
	Max.	8.04	10.8	12.1	7.57	10.4	11.7	12.0	19.4	22.1
	Ave.	4.30	6.09	7.25	4.06	5.84	6.99	7.43	10.2	11.1
HS20 MR	Min.	1.24	1.85	2.15	1.20	1.76	2.08	2.21	3.70	3.28
	Max.	5.71	6.66	7.19	5.55	6.54	7.07	6.83	11.1	12.4
	Ave.	3.05	3.78	4.32	2.98	3.69	4.22	4.24	5.82	6.25

Figures 3.10 and 3.11 show the magnitudes of the positive and negative H15 moment ratios generated in the homogeneous, two-span continuous line-girder analyses. When compared to Figure 3.5, showing the comparable simple span moment ratios, it is quickly noticed that the maximum positive moment ratios for both types of structures are almost identical in value. Some slight differences exist, however, the graphs look quite similar, each showing the trend of increased moment ratio with increased vehicle weight. When

comparing the maximum negative continuous span moment ratios with the maximum simple span positive moment ratios, one difference can be observed. The negative moment ratio values are about double the values for the simple span positive moment ratios. This shows the greater potential for overstress in the negative moment regions of continuous structures when compared to the simple span structures. Figures 3.12 and 3.13 also show the same trends when compared with Figure 3.6, except the magnitude of the moment ratio difference varies from about 1.5 to 2 for these HS20 comparisons.

Figure 3.13 shows a very interesting trend in the Maximum HS20 Truck Moment Ratios, using the Superheavy Vehicle classification only. The bulk of Superheavy Maximum Moment Ratios on these two equal span continuous structures fall into a linear pattern when plotted against Total Vehicle Weight (TVW). For the 150-foot span length condition, an equation relating these variables is shown as Equation 3.15.

$$\text{Max. HS20 Negative } MR_{150\text{ft}} = 0.013(TVW) - 0.546 \quad (3.15)$$

Although this equation only gives a rough estimate, it is a quick approach to finding the maximum MR over a support on a symmetric two-span structure. The Superheavy vehicles on the symmetric 100-foot spans also show linear relationships between Maximum Negative MR and Total Vehicle Weight. For the 100-foot span length condition, an equation relating these variables is shown as Equation 3.16.

$$\text{Max. HS20 Negative } MR_{100.ft} = 0.0112(TVW) + 0.403 \quad (3.16)$$

These equations are valid only if the two-span continuous structure is symmetric with constant beam stiffness throughout the bridge lengths shown. No relationship can be found for the 50-foot span length condition, typically due to a Superheavy vehicle's excessive overall length. Most short span bridges cannot hold all axles of a longer truck on the structure simultaneously, causing discontinuities in the Moment Ratio trends. Superheavy vehicles on the 50-foot span length structures act like separate, shorter bundles of "effective" axles rather than one truck with all axles "effective".

Table 3.3 shows these same observations in a different format, however the trends are the same. The average positive moment ratios can be seen to be quite close to the values calculated for the simple spans, while the negative moment ratios tend to be significantly greater. Generally, the continuous structures' moment ratios are controlled by the negative moment regions, assuming the layouts used in this project. These results could change depending on the layout of the spans in actual bridge structures. However, this information helps emphasize the important fact that the negative moment regions of continuous structures often control the behavior of these structures under overload patterns.

3.2.3.2. Symmetric Two-Span Continuous Bridge Structures with Modified Stiffness in the Negative Moment Region

The negative moment regions (cover plate regions) of each continuous span model were increased and analyzed under loads from the Superheavy vehicles to see the effects of this stiffness discontinuity on the generated moment ratios. The modeling of the region of increased stiffness near the interior support of each symmetric two-span model can be accomplished in SAP2000 by using any two AISC rolled steel sections that have a relative stiffness ratio (I_{xx} value ratio) of 1.5. The 1.5 stiffness ratio was selected as an estimate of a typical increase in stiffness in actual bridge structures. Figure 3.14 shows the three continuous girder bridge layouts with modified negative moment region stiffness studied during this project.

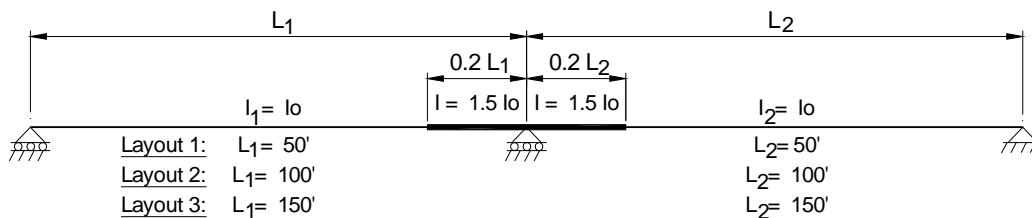


Figure 3.14: Three Continuous Girder Bridge Models with Modified Negative Moment Region Cross-Section

Table 3.4: Effects of Modified Negative Moment Region Girder Stiffness

Superheavy Vehicles Only								
Average Percent Difference in Moment and Shear Values Produced in Modified Girders when Compared to Constant Cross-section Girders								
Moment Values						Shear Values		
50' Span		100' Span		150' Span		50' Span	100' Span	150' Span
Pos. M	Neg. M	Pos. M	Neg. M	Pos. M	Neg. M			
-3.4	+13.1	-3.3	+12.9	-3.18	+13.1	+1.3	+1.0	+0.9

Table 3.4 shows that generally, when cover-plated wide-flange sections or stiffer beam sections, such as plate girders with larger plate sizes over support regions are used in continuous structures, the moment values (not moment ratios) generated in the negative bending region increase an average of 13%. This assumes the symmetric two-span layouts used for this project, but it does illustrate how the stiffer sections of continuous beams draw more bending moment into the stiffer region. The positive bending values for these two-span structures tend to decrease an average of about 3%. Shear values tend to remain about the same, showing only a 1% increase on average. It is important to realize that these changes in the moments and shears are seen in both the AASHTO design vehicle group and the Superheavy vehicle group. This means that the maximum moment and shear ratios should not be significantly altered when looking at cover-plated regions of continuous structures, or regions in plate girders with larger plate sections.

3.2.4. Truck Characteristics that Affect Maximum Moment Ratios

The goal of analyzing all of the truck records in the TxDOT database of permitted trucks was to determine which characteristics of these trucks could be pinpointed as a major contributor to maximum force effects. It has been established in this chapter that the key truck variable is Total Vehicle Weight. All graphs have shown the trend of increasing positive and negative moment ratios as the total vehicle weight increases. The rates of these changes vary according to the AASHTO trucks these permitted trucks are compared with, but the trends are constant across all plots.

Figure 3.15 shows the relationship between a truck's maximum axle weight and its positive moment ratio on a continuous span. It can be postulated that heavy trucks that are short in length will produce the maximum positive moment effects in continuous structures. Other factors make a difference in the moment ratios calculated, however, the maximum axle weight is shown to be an important variable when studying the positive moment ratio effects on continuous structures.

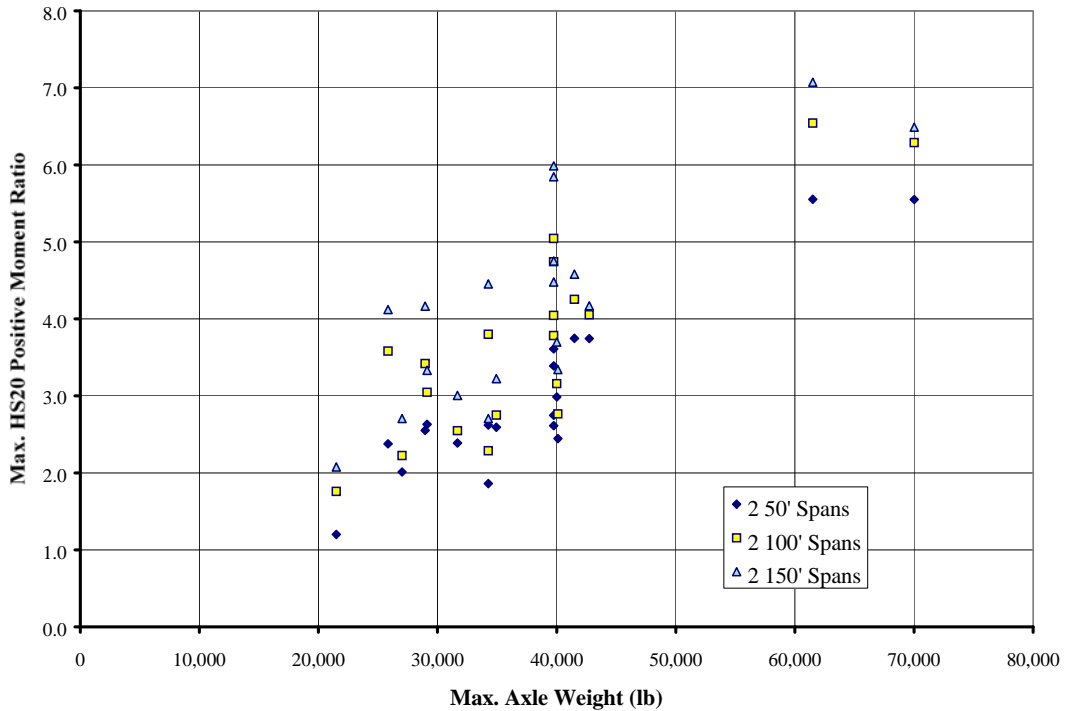


Figure 3.15: Maximum Continuous Span Positive HS20 Moment Ratio vs. Max. Axle Weight – Superheavy Vehicles Only

It can also be postulated that heavy groups of axles separated by a large distance will create large negative moment effects in continuous structures when these groups of axles straddle an interior support. Figure 3.16 shows the relationship between a truck's maximum axle spacing and the maximum negative moment ratio produced on a continuous span. It must be realized that the individual axle weights also play an important role in this case, but the maximum axle spacing is an important variable for continuous structure moment ratios. Figure 3.16 shows that the maximum axle spacing present on a vehicle alone is not the key to producing maximum negative moment ratios. It

also shows that vehicles with a maximum axle spacing greater than 40 feet tend to generate large negative moment ratios. It is rare to see a maximum truck axle spacing above 60 feet in this database of Superheavy vehicles.

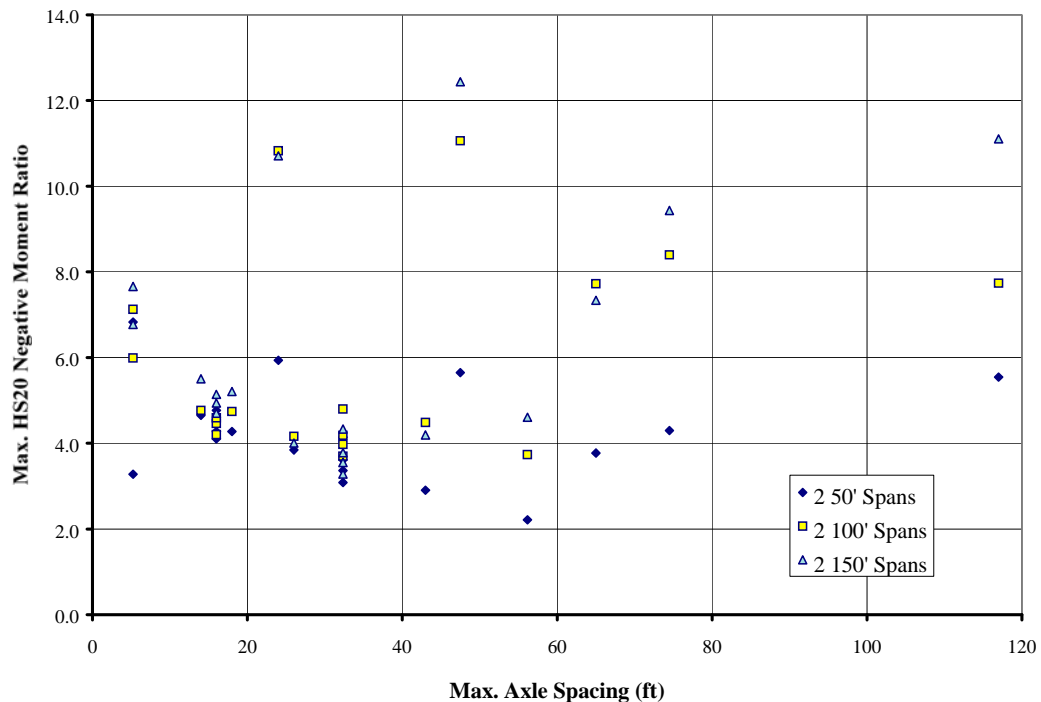


Figure 3.16: Maximum Continuous Span Negative HS20 Moment Ratio vs. Max. Axle Spacing – Superheavy Vehicles Only

Figures 3.17 and 3.18 are used to illustrate the vehicles that produced the maximum positive and negative moment ratios on the two span continuous line-girder models. Their positions are illustrated near the point where each truck would produce its maximum moment ratio. These figures illustrate the types of vehicles that control the positive and negative bending regions of a continuous structure. The truck producing the maximum positive moment ratio

has many heavy axles closely spaced, making up the bulk of the total truck load (see Figure 3.17). The truck producing the maximum negative moment ratio is quite heavy and has a large gap separating the two groups of axles that comprise the bulk of this vehicle's total weight (see Figure 3.18).

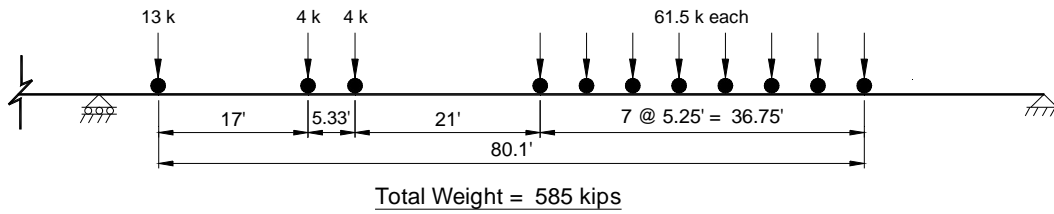


Figure 3.17: Superheavy Truck Record #213 Producing Max. Positive Moment Ratio

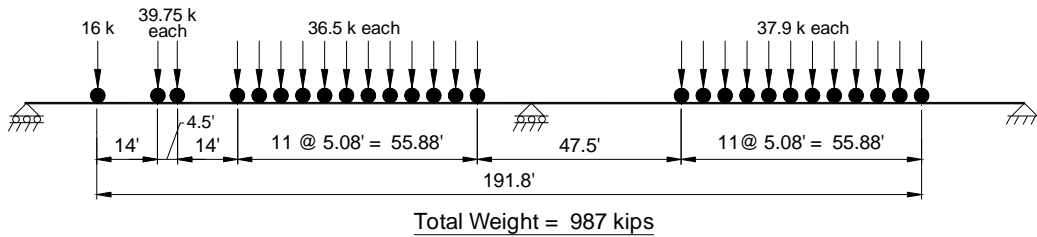


Figure 3.18: Superheavy Truck Record #205 Producing Max. Negative Moment Ratio

Just as moment values and moment ratios can be generated for simple and continuous span structures, shear values and shear ratios can also be generated using the same line-girder techniques. The examples shown in this chapter illustrate the power of the line-girder analysis technique for quantifying the potential overstress due to bending effects. These same principles can be used to quantify the overstress potential due to shear effects. Shear calculations

are quite important and can not be overlooked when analyzing a bridge for overloaded vehicles, however, the examples used in this thesis focus on the bending moment effects only. This is not intended to downplay the role of checking the shear stresses, but instead to focus on the flexibility of the line-girder analysis technique for quantifying both of these important force effects.

CHAPTER 4

AASHTO APPROACH TO LATERAL LOAD DISTRIBUTION FACTORS

Accurately calculating the Lateral Load Distribution Factors (LLDF's) for bridges deemed critical for overloaded truck passage is a challenging aspect of bridge rating techniques. While designers calculate LLDF's from AASHTO design equations, bridge analysts would be better served by a technique that allowed for less conservatism than what the design values generate. Consideration of a bridge's slab moment capacity, neglected in the determination of the AASHTO design LLDF's, would also help to more accurately determine the stresses developed in a bridge structure under actual overweight vehicle loads.

Many uncertainties regarding the loading patterns that may occur on a bridge structure do not exist when a permitted overweight truck is allowed to travel over a critical bridge. While it is important to include the worst-case scenarios when developing loading patterns for bridge design, it is not necessary to penalize the structure in this way while performing an overload analysis. Traffic control and strict instructions to overloaded truck operators can limit the live loads acting on a critical bridge structure at a particular point in time, allowing for more accurate estimates of load capacity. Controlling the transverse locations of overweight trucks during their passage over critical bridges can allow the bridge analyst to place the live loads expected in actual locations on the bridge slab, rather than always assuming the worst-case locations for girder stresses.

The advantages of a three-dimensional finite element analysis are obvious when these conditions are controlled. The question of whether or not the finite element analysis is too time-consuming to warrant its use can be answered only when it is known which programs are best suited for finite element analysis of girder-slab bridge structures. BRUFEM (Bridge Rating Using Finite Element Methods) is an analysis package specifically designed to model these types of situations.^[4] With some output modifications, as listed in this chapter, the BRUFEM package can generate more accurate estimates of girder stress levels much quicker than one would expect for a finite element package. BRUFEM uses a pre-processor that prompts the user for the required bridge information, and then generates the finite element mesh required for analysis.

The BRUFEM post-processor, though somewhat primitive when compared with the graphical interfaces available in commercial programs today, gives the information required to generate the actual LLDF's from the model due to a specific truck location or a combination of many truck locations on the bridge deck. The BRUFEM LLDF results are less conservative than the AASHTO design LLDF's, and can be used in conjunction with the line-girder analysis techniques discussed in Chapter 3 to estimate the actual girder stresses developed in all members of a bridge structure. By reducing the conservatism of the LLDF's and accurately modeling only a single truck's location on the bridge's deck, the apparent girder stresses can be lowered, thus improving the capacity a bridge structure can carry, with minimal extra time invested by the analyst. By utilizing spreadsheet programs and this personal computer based finite element program,

the procedures by which trucks are permitted can be improved and the capacities of the bridges in question can be more accurately calculated.

4.1. USING AASHTO DESIGN PROCEDURES FOR LLDF CALCULATION

Using the AASHTO empirical equations for calculating LLDF's is one approach available to a bridge analyst concerned about the performance of a critical bridge structure under the influence of an overweight vehicle. This section will explain how the AASHTO design LLDF approach can be modified to reflect the lateral load distribution pattern expected from the presence of only one vehicle on the bridge slab. The bridge that will be used to illustrate these ideas is Example Bridge 3 shown in Figure 1.4. Table 1.1 lists the characteristics of this bridge layout and contains information necessary for calculating the AASHTO LLDF's. In summary, Example Bridge 3 consists of four girders spaced at 10-foot centers with 3'-6" overhangs and a 34'-0" roadway width.^[7] The structure consists of two continuous spans, each of 90 feet, and has a minimum concrete slab thickness of 8 inches. This bridge layout has two critical flexural design sections, one in the positive flexure region and one at the interior pier section, or negative flexure region.

4.1.1. Working Stress Design Empirical Equations

Modifying the AASHTO LLDF calculation technique to account for only one truck on the bridge is done for this research to help eliminate the penalties that would be imposed during design for the possibility of more than one heavy vehicle on the bridge slab at a given time. We are assuming that the overweight

vehicle is the only vehicle that is present on the bridge structure, which can be enforced using traffic control or imposing travel time restrictions on the vehicle being modeled. Simple AASHTO LLDF's used in the Working Stress Design Specification can be calculated very quickly and follow the equations listed in Equations 4.1 and 4.2.^[2] The older WSD and LFD AASHTO Specifications deal with wheel loads rather than truck loads. Since we have computed moments due to whole trucks on line girders, it is proper to divide the wheel load distribution factors by a factor of 2 to get truck load distribution factors. This is equivalent to changing the calculated line girder moment from that of a design truck moment to that of a wheel line moment.

$$\text{Single Lane Wheel Load LLDF} = \frac{S}{7} \quad (4.1)$$

$$\text{Multiple Lane Wheel Load LLDF} = \frac{S}{5.5} \quad (4.2)$$

$$\text{Single Lane Truck Load LLDF} = \left(\frac{1}{2}\right) \cdot \frac{S}{7} = \frac{S}{14} \quad (4.3)$$

$$\text{Multiple Lane Truck Load LLDF} = \left(\frac{1}{2}\right) \cdot \frac{S}{5.5} = \frac{S}{11} \quad (4.4)$$

where: S = girder spacing = 10 ft

Since it is easy to calculate the multiple truck LLDF in this case, it is shown for use as a comparison later in this section. For Example Bridge 3, these simple LLDF's are shown for both a single traffic lane and multiple traffic lanes in Equations 4.5 and 4.6.

$$\text{Single Lane Truck Load LLDF} = \left(\frac{1}{2}\right) \cdot \frac{10}{7} = 0.71 \quad (4.5)$$

$$\text{Multiple Lane Truck Load LLDF} = \left(\frac{1}{2}\right) \cdot \frac{10}{5.5} = 0.91 \quad (4.6)$$

It should be noted that these AASHTO LLDF's were developed assuming the vehicles present on the bridge structures were the AASHTO design vehicles such as the H15-44, the HS15-44, the H20-44, and the HS20-44 vehicle layouts. Using these AASHTO LLDF's for analysis of very different trucks is not the intent of the AASHTO LLDF calculation technique. However, these values will be used for comparison purposes when the BRUFEM LLDF output is presented, and it also illustrates the techniques through which the design LLDF's are calculated.

The AASHTO LRFD Design Specification uses more complex equations to calculate these LLDF's in an attempt to reduce the amount of conservatism built-in to the empirical equations based on girder spacing alone. The LRFD Design Specification has incorporated Multiple Presence Factors into the LLDF equations it uses. These Multiple Presence Factors will be removed from our

LLDF's for this research because the overweight trucks in question will be the only vehicles assumed on the bridge structure at a time.

4.1.2. Interior Girder –LRFD Strength Limit State

The live-load distribution factor for an interior girder in positive flexure is shown in Equation 4.7.^[1] This equation holds for the situation where only one lane is loaded. AASHTO LRFD has a separate equation to account for two lanes loaded simultaneously.

$$LLDF = 0.06 + \left(\frac{S}{14}\right)^{0.4} \left(\frac{S}{L}\right)^{0.3} \left(\frac{K_g}{12.0 L t_s^3}\right)^{0.1} \quad (4.7)$$

where: S = girder spacing (ft)

L = span length (ft)

K_g = longitudinal stiffness parameter (see Eq. 4.8)

t_s = slab thickness (in.)

$$K_g = n \cdot (I + A \cdot e_g^2) \quad (4.8)$$

where: n = modular ratio of steel to concrete = 8

I = moment of inertia of girder alone (in^4) = 9280 in^4

A = area of girder alone (in^2) = 38.75 in^2

e_g = distance from slab CG to girder CG (in.) = 26.39 in.

$$K_g = 8 \cdot (9280 + (38.75) \cdot (26.39)^2) = 290,130 \text{ in}^4 \quad (4.9)$$

AASHTO LRFD limits the values that can be used for two of the variables necessary for calculating this moment LLDF. These limits involve the effective slab thickness, t_s , the girder span length, L , the girder spacing, S , and the longitudinal stiffness parameter, K_g . These limits are shown below:

$$3.5 \leq S \leq 16.0$$

$$20 \leq L \leq 240$$

$$4.5 \leq t_s \leq 12.0$$

$$10,000 \leq K_g \leq 7,000,000$$

Example Bridge 3 satisfies all of these limits, along with the additional requirement of the bridge having at least 4 girders. Using this approach, the interior girder AASHTO LRFD moment LLDF can be calculated. The value calculated using Equation 4.7 must be divided by 1.2 to account for the Multiple Presence Factor built-in to this LLDF equation. This approach of dividing by the Multiple Presence Factor is the same as the approach taken by AASHTO LRFD to analyze the fatigue limit state. The resulting LLDF is shown in Equation 4.10.

$$0.06 + \left(\frac{10}{14}\right)^{0.4} \cdot \left(\frac{10}{90}\right)^{0.3} \cdot \left(\frac{290,130}{(12) \cdot (90) \cdot (8)^3}\right)^{0.1} = 0.484 / 1.2 = 0.40 \quad (4.10)$$

4.1.2.1. Negative Moment Region Interior Girder LLDF

Since, in this example, the negative moment region of each girder is different in configuration than that of the positive moment region, the calculation of the LLDF for the interior girders must be recalculated. The term in Equation

4.7 that must be modified for the negative flexure region is the K_g term. This K_g term is based on the section properties of the interior pier section of the girder. The term containing K_g also contains the span length L . To compute the distribution factor for regions in negative flexure, the average of the adjacent span lengths is used for L . The value of L for Example Bridge 3 is therefore 90 feet, since both spans of Example Bridge 3 are 90 feet in length. Equation 4.12 shows the calculation of the negative flexure LLDF for the interior girders of Example Bridge 3. The calculation of the negative moment region K_g is shown in Equation 4.11.

$$K_g = 8 \cdot (15,454 + (58.00) \cdot (26.66)^2) = 453,423 \text{ in}^4 \quad (4.11)$$

$$0.06 + \left(\frac{10}{14}\right)^{0.4} \cdot \left(\frac{10}{90}\right)^{0.3} \cdot \left(\frac{453,423}{(12) \cdot (90) \cdot (8)^3}\right)^{0.1} = 0.503 / 1.2 = 0.42 \quad (4.12)$$

All other distribution factors at the negative flexure regions for the interior girder and for the exterior girder are independent of the span length and the stiffness of the girder. For that reason, all other LLDF calculations apply to both the positive and negative flexure regions of the girders.

4.1.3. Exterior Girder – LRFD Strength Limit State

The AASHTO LRFD live-load distribution factors for the design of exterior girders are determined as the governing factors calculated using a combination of approximate formulas, the Lever Rule, and a special analysis assuming that the entire cross section deflects and rotates as a rigid body.^[1] These

AASHTO LRFD methods have been modified to more accurately represent only one vehicle on the bridge structure at a time. Each method is illustrated using Example Bridge 3, and the Multiple Presence Factors are not included when using the Lever Rule analysis and the special Rigid Body analysis. These changes make this approach to calculating these modified AASHTO LLDF's similar to the design approach taken for the Fatigue Limit State in the AASHTO LRFD Specification.

4.1.3.1. Exterior Girder LRFD Moment Distribution Factor – Lever Rule

The lever rule involves the use of statics to determine the lateral distribution to the exterior girder by summing moments about the adjacent interior girder to find the wheel-load reaction at the exterior girder assuming the concrete deck is hinged at the interior girder (see Figure 4.1). A wheel cannot be closer than 2'-0" to the face of the curb. For the specified transverse wheel spacing of 6'-0", the wheel-load distribution to the exterior girder is computed as shown in Figure 4.1. No Multiple Presence Factor is added to the calculated LLDF. This value of lateral load distribution (0.70) must be compared to the values generated by the approximate formula and the Rigid Body analysis.

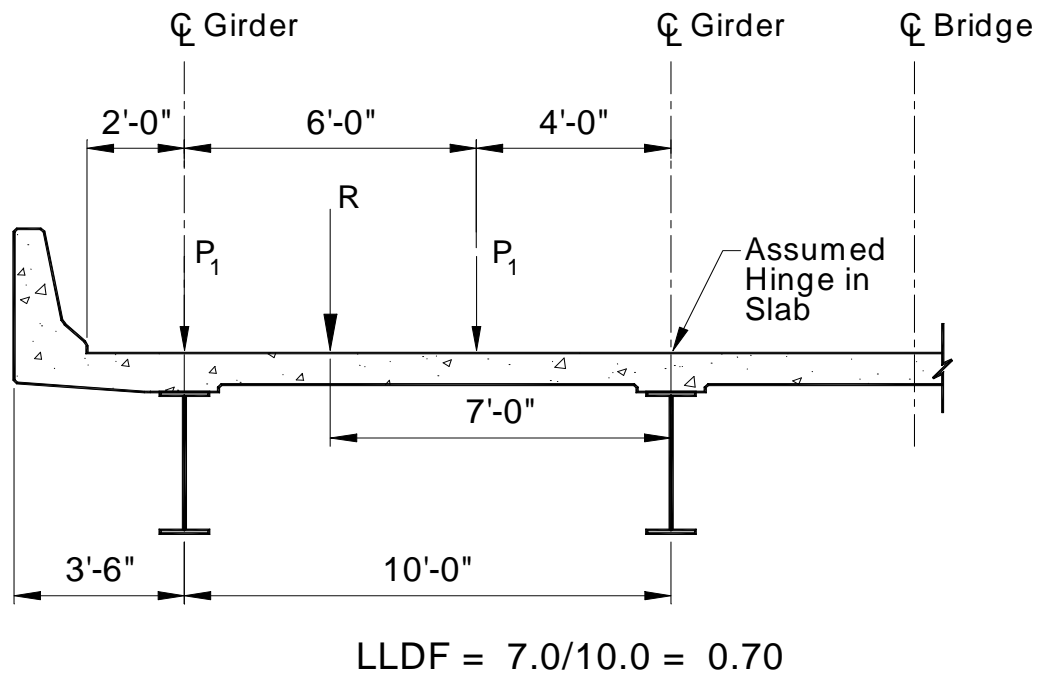


Figure 4.1: Exterior Girder LRFD LLDF – Lever Rule

4.1.3.2. Exterior Girder LRFD Moment Distribution Factor – Rigid Body Analysis

Assuming the entire cross section rotates as a rigid body about the longitudinal centerline of the bridge, distribution factors for the exterior girder are also computed for one lane loaded by the design vehicle. No multiple presence factor will be added to the calculated value since only one vehicle is assumed to be present on the bridge and the layout of the loads for this calculation is shown in Figure 4.2. The equation used for this calculation is shown in Equation 4.13. The LLDF calculated using this procedure is 0.61, as shown in Equation 4.14.

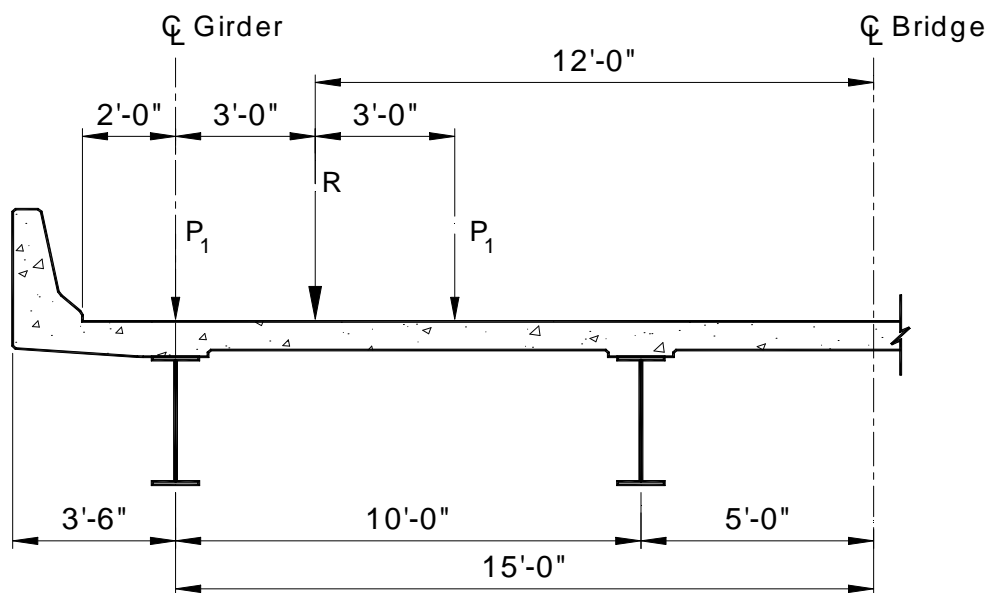


Figure 4.2: Exterior Girder Moment Distribution Factor – Rigid Body

$$R = \frac{N_L}{N_b} + \frac{X_{ext} \sum^{N_L} e}{\sum^{N_b} x^2} \quad (4.13)$$

where: R = reaction on exterior beam in terms of trucks

N_L = number of loaded lanes under consideration (= 1)

e = eccentricity of a lane from the CG of the girder pattern

x = horizontal distance from the CG of the girder pattern to each girder (ft)

X_{ext} = horizontal distance from the CG of the girder pattern to the exterior girder (ft)

N_b = total number of girders (= 4)

Referring to Figure 4.2:

$$R = \frac{1}{4} + \frac{(15.0) \cdot (12.0)}{2 \cdot (15.0^2 + 5.0^2)} = 0.61 \quad (4.14)$$

4.1.4. Summary of Single Vehicle AASHTO LLDF's

The resulting positive bending moment distribution factors used to check the strength limit state when only one vehicle is present on the bridge structure are shown in Table 4.1. It should be recognized that the procedure used for this thesis varies from the AASHTO methods since no multiple lane loading cases are checked and all impact factors are taken to be 1.0. The impact factor is omitted for these comparisons because overweight and Superheavy vehicles do not travel at normal highway speeds. It is rational to omit the impact factor for this reason. Multiple lane loading criteria often control these lateral load distribution factor values, however, since overweight vehicle analysis is not a design situation, these steps have been modified to compare the values calculated using these AASHTO-based approaches and the BRUFEM program. These methods are not valid for use in design situations and should not be construed to be substitutes to the AASHTO design specifications. However, if a strong correlation exists between these modified LLDF's and the calculated BRUFEM LLDF's, using these modified AASHTO LLDF's would be a faster approach to more accurate LLDF calculation.

**Table 4.1: Positive Flexure Region Single Vehicle AASHTO Truck LLDF's
(Ex. Bridge 3)**

	Exterior Girders	Interior Girders
WSD Empirical Equations:		
Single Lane (S/14)	0.71	0.71
Multiple Lanes (S/11)	0.91	0.91
LRFD Equation	N/A	0.40
LRFD Lever Rule	0.70	N/A
LRFD Rigid Body Equation	0.61	N/A
Governing LRFD LLDF	0.70	0.40

Looking at the results shown for positive flexure only, it can quickly be seen that using the AASHTO WSD empirical equations places a severe penalty on the estimated moments generated in each girder across the bridge structure. It is intuitive to estimate that the exterior girders of a structure will be required to supply more resistance to load simply because the exterior girders are only offered the immediate help of one other girder and not two. We would expect the interior girders to be able to share more of the applied loads to the other girders present in the structure, therefore reducing the applicable LLDF. The AASHTO LRFD approach produces similar exterior girder positive flexure LLDF's in this example, and produces an interior girder LLDF of almost half that of the exterior girder. Obviously, this is the more accurate approach to lateral load distribution, however, it may be more beneficial to use the BRUFEM approach to reduce these

values even further, especially when the actual travel lane positions are less penalizing than the design lane positions.

**Table 4.2: Negative Flexure Region Single Vehicle AASHTO Truck LLDF's
(Ex. Bridge 3)**

	Exterior Girders	Interior Girders
WSD Empirical Equations:		
Single Lane (S/14)	0.71	0.71
Multiple Lanes (S/11)	0.91	0.91
LRFD Equation	N/A	0.42
LRFD Lever Rule	0.70	N/A
LRFD Rigid Body Equation	0.61	N/A
Governing LRFD LLDF	0.70	0.42

The negative moment region modified AASHTO LLDF's are only different from the positive moment region values for the interior girders. As explained earlier in this chapter, this is due to the increased girder stiffness in the negative moment region, and is illustrated in Equations 4.11 and 4.12. The positive and negative moment regions LLDF's are calculated in this way for each of the three example bridges. Table 4.3 lists the modified AASHTO LLDF's for each example bridge.

Table 4.3: Single Vehicle LLDF Summary for Example Bridges 1, 2, & 3

	Bridge 1	Bridge 2			Bridge 3	
	(+ M)	60' (+M)	(-M)	(75' +M)	(+M)	(-M)
	Empirical Equations					
Single Lane	0.57	0.57	0.57	0.57	0.71	0.71
Multiple Lanes	0.73	0.73	0.73	0.73	0.91	0.91
LRFD Interior Girder LLDF	0.45	0.41	0.41	0.38	0.40	0.42
LRFD Lever Rule	0.63	0.63	0.63	0.63	0.70	0.70
LRFD Rigid Body Equation	0.59	0.59	0.59	0.59	0.61	0.61
Exterior Girder LLDF	0.63	0.63	0.63	0.63	0.70	0.70

4.1.4.1. TxDOT Reduction of AASHTO Design LLDF's for Overloads

The current TxDOT approach to permitting overloads on Texas bridges uses the AASHTO Design LLDF's with a reduction based on the overload vehicle's maximum axle gage. The reduction factor is multiplied by the AASHTO Design LLDF to create what this thesis calls a "TxDOT Reduction Factor". For a definition of the term "gage", see Figure 4.3. The TxDOT reduction value equation is shown in Equation 4.15.^[9] Table 4.4 lists the gage values for the overload vehicles used for analysis in this thesis. No gage values are listed for AASHTO Design Vehicles.

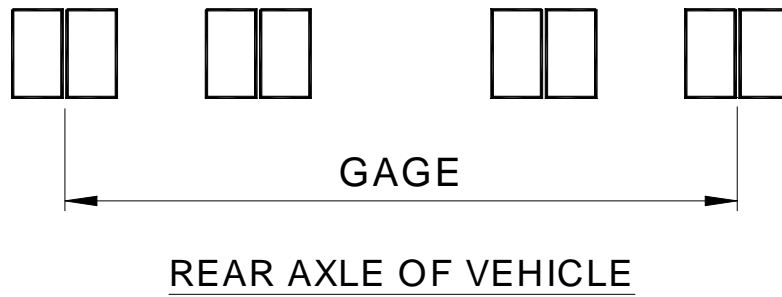


Figure 4.3: TxDOT Reduction Factor Gage Definition

$$\text{TxDOT reduction factor} = 1.2 - \left(\frac{\text{Gage}}{30} \right) \quad (4.15)$$

Table 4.4: Vehicle Gage Values and TxDOT Reduction Factors

Vehicle Record	Vehicle Gage	TxDOT Reduction Factor
Veh. #18	7.0 ft	0.97
Veh. #87	7.0 ft	0.97
Veh. #203	15.08 ft	0.70
Veh. #213	16.75 ft	0.64

CHAPTER 5

BRUFEM LATERAL LOAD DISTRIBUTION FACTOR STUDY

The next step in the comparison process of these modified AASHTO LLDF's and the finite element LLDF's is generating the input files required of the BRUFEM analysis package. It is necessary to calculate the LLDF's that exist at the particular cross-section in the bridge structure where the maximum bending stress effects are experienced for the truck in question. Every truck has a unique position at which it produces the maximum bending stress potential in the line-girder model. These positions vary and must be known beforehand, since the LLDF information taken from BRUFEM varies along the length of each bridge girder. The maximum negative moment effects for both Example Bridges 2 and 3 are seen at the points of interior support. The maximum positive moment effects in all three of these Example Bridges occur at different locations along the girder length, depending on the truck layout being analyzed.

5.1. DEVELOPMENT OF BRUFEM INPUT FILES

In order to find the correct cross-section of the bridge where these maximum moment effects occur, SAP2000 can be used, along with its influence line output feature, to pinpoint these critical moment locations. The BRUFEM suite of programs contains the SALOD (Structural Analysis for Load Distribution) program for generating influence surfaces. SALOD's primary function is to predict the flexural LLDF's for design and bridge rating on simple

span bridges. In order to make the database of influence surfaces developed for use within SALOD reasonable in size, many simplifying assumptions were made during the modeling. Significant effects not included in the SALOD program include girder continuity, edge stiffening effects of curbs and parapets, skew effects, as well as others.^[4] BRUFEM was developed to supercede the analysis capabilities of the SALOD program, but BRUFEM has no capacity to generate influence surfaces at this time.

The biggest concern during the analysis of these bridges under overloads is making sure to place the truck loads the bridge will see at the correct positions to create maximum moment effects. During this research, BRUFEM runs were made with trucks in both design lane locations and actual travel lane locations in order to compare the results obtained. The longitudinal truck locations are a function of the truck axle layout only. The design and travel lane transverse locations are independent of the truck's axle layout.

5.1.1. Summary of BRUFEM Input Cases

In all, 15 BRUFEM analyses were carried out, 5 such analyses on each of the three Example Bridges. Both AASHTO design vehicles and vehicles from the TxDOT Permit Database (including the Superheavy vehicles) were used to analyze the LLDF's in each of these three example bridges. The vehicles selected from the TxDOT database for BRUFEM analysis were chosen because each produced the maximum positive or negative moment in the Example Bridges analyzed during this research. Both positive and negative moment effects are studied to see if trends exist in the LLDF's depending on the regions of the bridge

most affected. Table 5.1 lists the characteristics of each BRUFEM run, including the transverse vehicle location, longitudinal vehicle location causing maximum bending moment, and the value of the maximum moment produced on a line-girder model of each configuration. Table 5.1 also lists the Figures illustrating the tested vehicles and their transverse and longitudinal positions. It must be realized that in many instances, all of the vehicle axles are not on the structure at the time when the vehicle produces its maximum moment effect. This is especially true for the Superheavy vehicle designations, since these vehicles tend to be quite long.

Table 5.1: Breakdown of 15 BRUFEM Runs on Example Bridges 1, 2, & 3

Run ID #	Vehicle Type	Transverse Lane Location	Longitudinal Location	Max. M_{LG} (k-ft)
Bridge 1:				
Run 1	H20-44 (Fig. 5.1)	Actual (Fig. 5.7)	Figure 5.16	+446
Run 2	HS20-44 (Fig. 5.2)	Actual (Fig. 5.7)	Figure 5.17	+628
Run 3	HS20-44 (Fig. 5.2)	Design (Fig. 5.8)	Figure 5.17	+628
Run 4	Veh. #18 (Fig. 5.3)	Actual (Fig. 5.9)	Figure 5.18	+1092
Run 5	Veh. #213 (Fig. 5.4)	Actual (Fig. 5.10)	Figure 5.19	+3584
Bridge 2:				
Run 6	HS20-44 (Fig. 5.2)	Design (Fig. 5.8)	Figure 5.20	-470
Run 7	HS20-44 (Fig. 5.2)	Design (Fig. 5.8)	Figure 5.21	+643
Run 8	Veh. #87 (Fig. 5.5)	Actual (Fig. 5.11)	Figure 5.22	+1107
Run 9	Veh. #203 (Fig. 5.6)	Actual (Fig. 5.12)	Figure 5.23	+2351
Run 10	Veh. #203 (Fig. 5.6)	Actual (Fig. 5.12)	Figure 5.24	-3488
Bridge 3:				
Run 11	HS20-44 (Fig. 5.2)	Design (Fig. 5.13)	Figure 5.25	+1110
Run 12	HS20-44 (Fig. 5.2)	Design (Fig. 5.13)	Figure 5.26	-715
Run 13	Veh. #87 (Fig. 5.5)	Actual (Fig. 5.14)	Figure 5.27	+1885
Run 14	Veh. #203 (Fig. 5.6)	Actual (Fig. 5.15)	Figure 5.28	+4698
Run 15	Veh. #203 (Fig. 5.6)	Actual (Fig. 5.15)	Figure 5.29	-6835

5.1.1.1. BRUFEM Truck Wheel Layout Input

This section contains Figures 5.1, 5.2, 5.3, 5.4, 5.5, and 5.6. These figures show the axle layouts in plan view of all trucks analyzed using the BRUFEM

suite of programs. The spacing dimensions shown are the values used in the program as either BRUFEM Standard Vehicles or User-Input Vehicles. The User-Input Vehicles need to have input text files named "Veh.dat" created before running the BRUFEM pre-processor.^{[4][5]} These input files are documented in Appendix B. If the user wishes to use a Standard Vehicle, such as the AASHTO design vehicles, there is no need to create a "Veh.dat" file before running the program. When using a Standard Vehicle, the user can interactively input the type of vehicle desired while using the BRUFEM pre-processor.

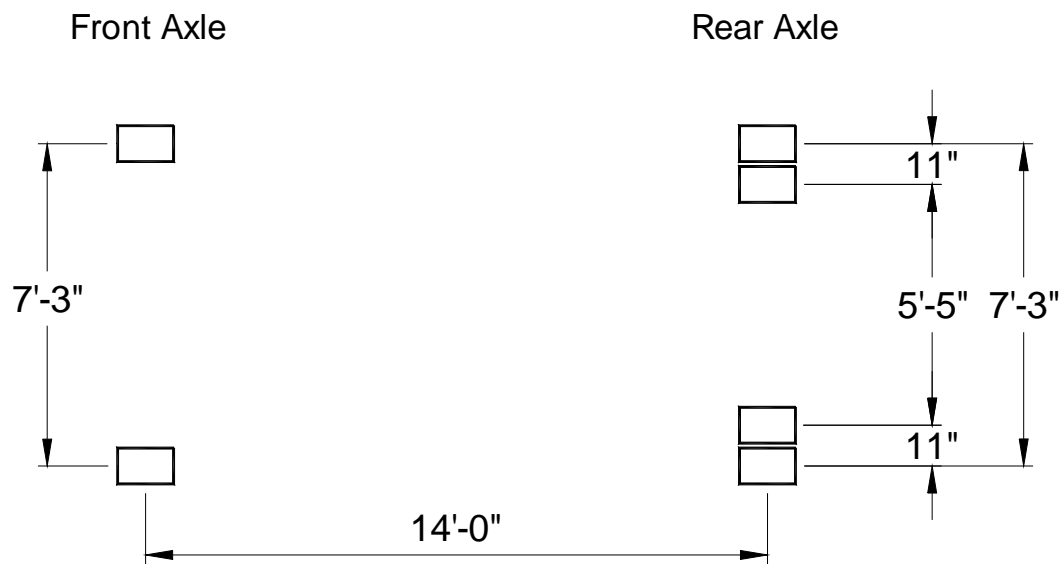


Figure 5.1: BRUFEM Standard H20-44 Wheel Configuration

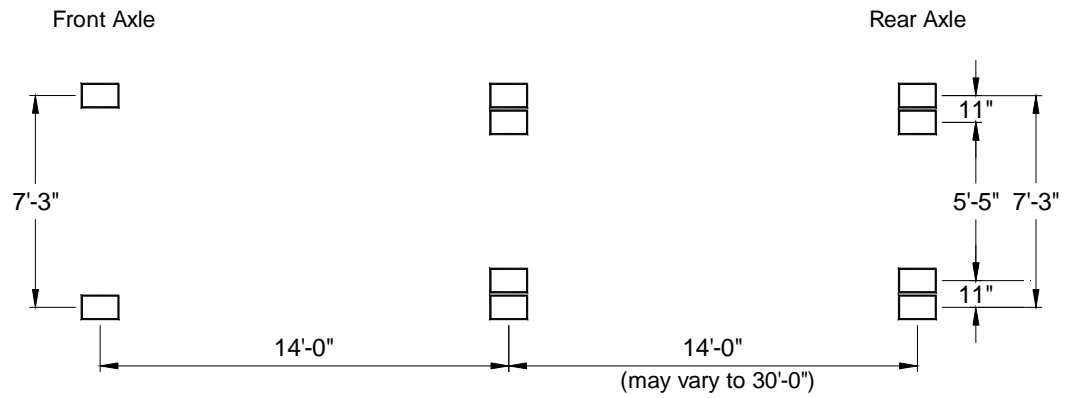


Figure 5.2: BRUFEM Standard HS20-44 Wheel Configuration

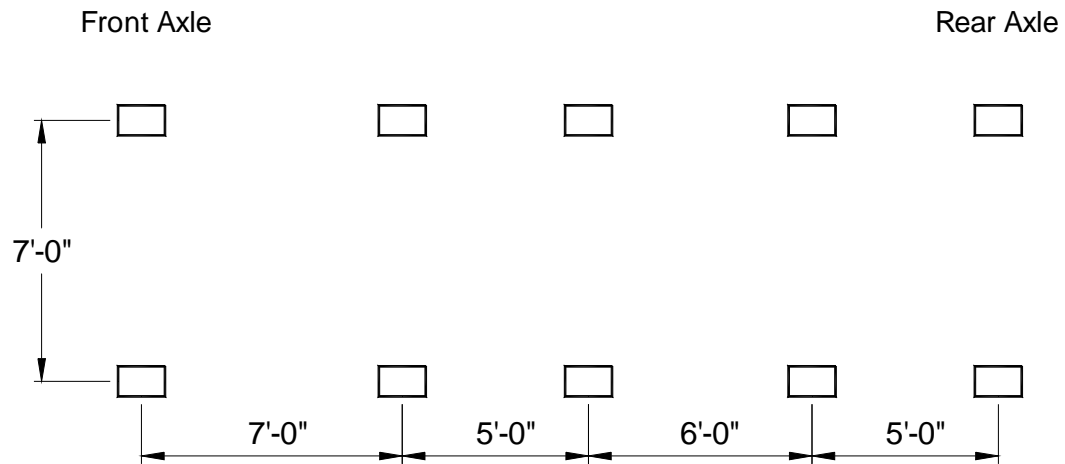


Figure 5.3: BRUFEM Vehicle #18 Wheel Configuration

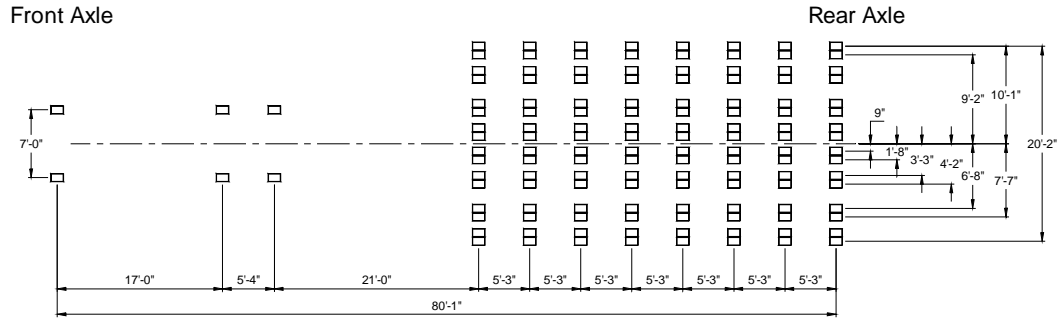


Figure 5.4: BRUFEM Vehicle #213 Wheel Configuration

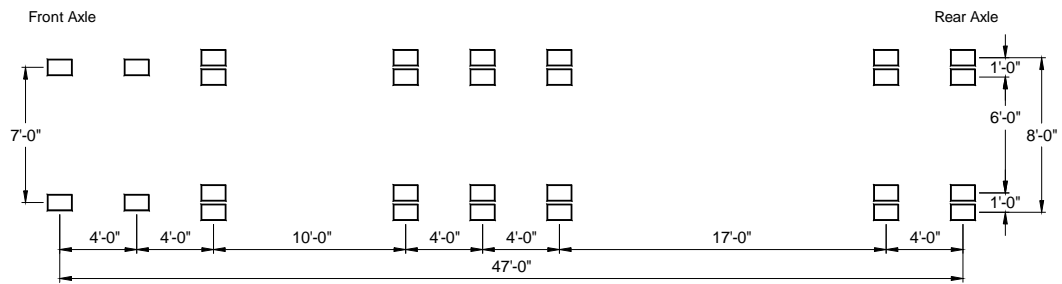


Figure 5.5: BRUFEM Vehicle #87 Wheel Configuration

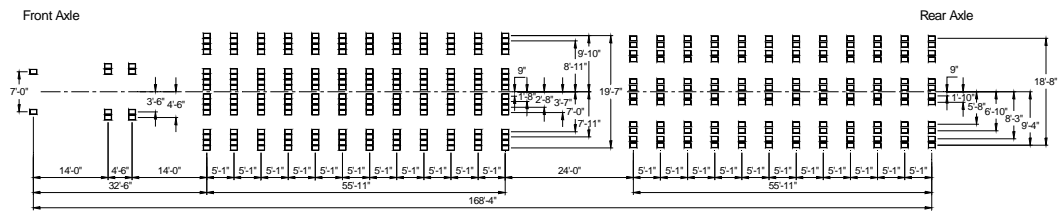


Figure 5.6: BRUFEM Vehicle #203 Wheel Configuration

5.1.1.2. BRUFEM Transverse Truck Position Input

This section contains Figures 5.7, through 5.15. These figures illustrate all of the various transverse truck locations used as BRUFEM input during this research. The “Travel Lane” positions were selected to be a likely location where that specific truck would travel on the selected bridge structure. Using these locations, rather than the “Design Lane” transverse locations, should prove to spread the truck’s load out over more girders. This also more accurately represents the load’s position on the bridge slab, allowing for the BRUFEM program to accurately estimate the actual stresses and LLDF’s under these conditions. The “Design Lane” locations place the vehicles the minimum distance away from the face of the curb as defined by the AASHTO design specification. For the Superheavy vehicles studied in this research, the travel lane is assumed to be a lane located at the centerline of the bridges in question. This is done to distribute the maximum amount of load to each of the available girders in each structure. Also, since these Superheavy vehicles are so wide, this travel lane is the one that would most likely have to be used to cross bridges the widths of those selected as Example Bridges 1, 2, and 3.

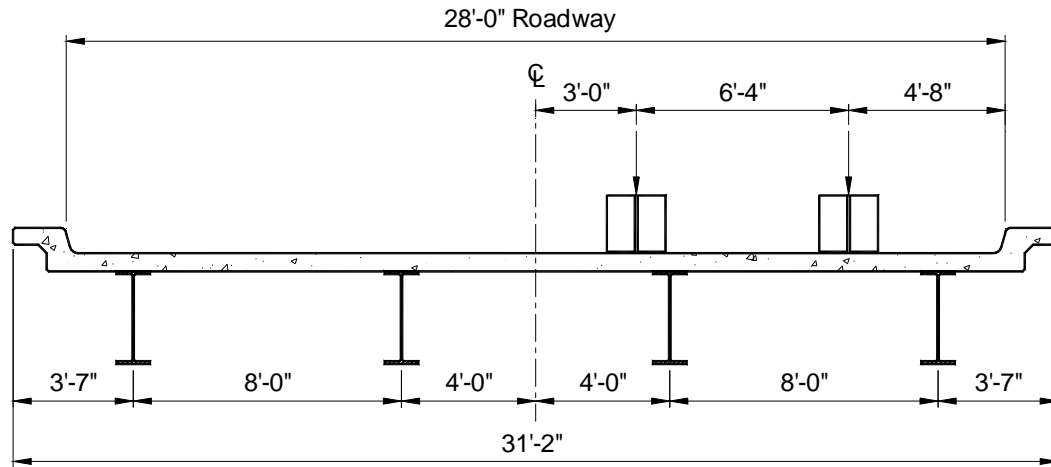


Figure 5.7: H20 and HS20 Rear Axle Travel Lane Position on Ex. Bridge 1

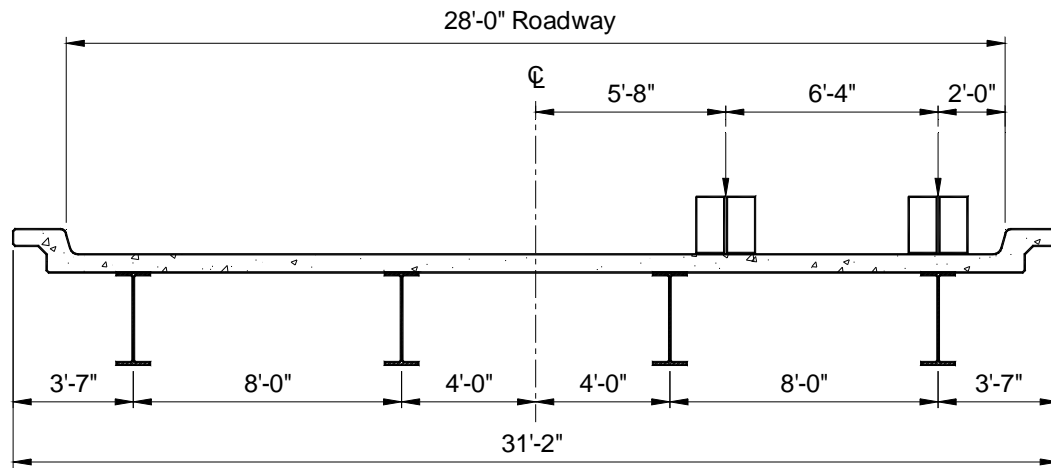


Figure 5.8: HS20 Rear Axle Design Lane Position on Ex. Bridges 1 and 2

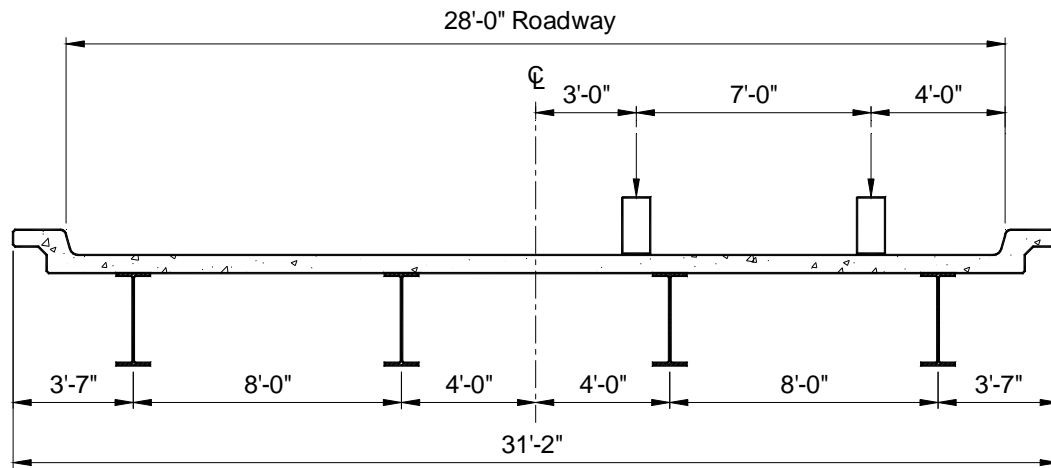


Figure 5.9: Vehicle #18 Rear Axle Travel Lane Position on Ex. Bridge 1

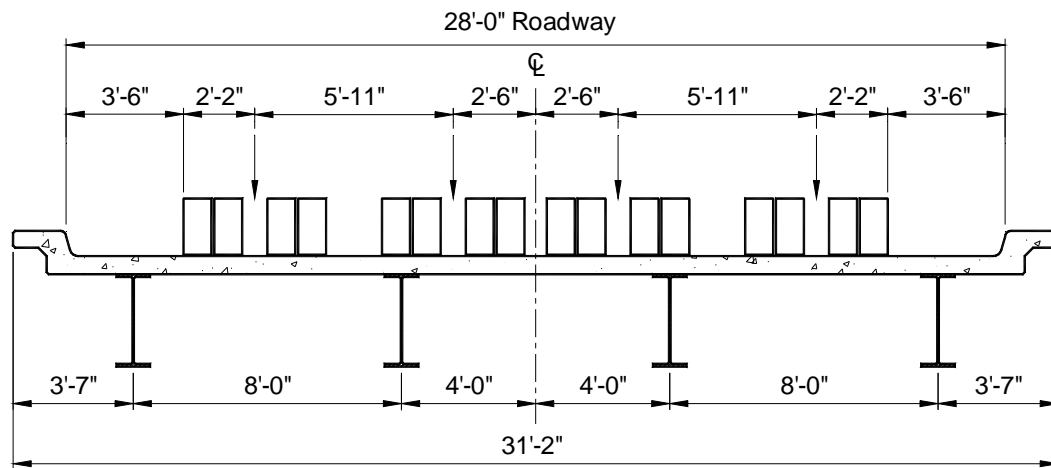


Figure 5.10: Vehicle #213 Rear Axle Travel Lane Position on Ex. Bridge 1

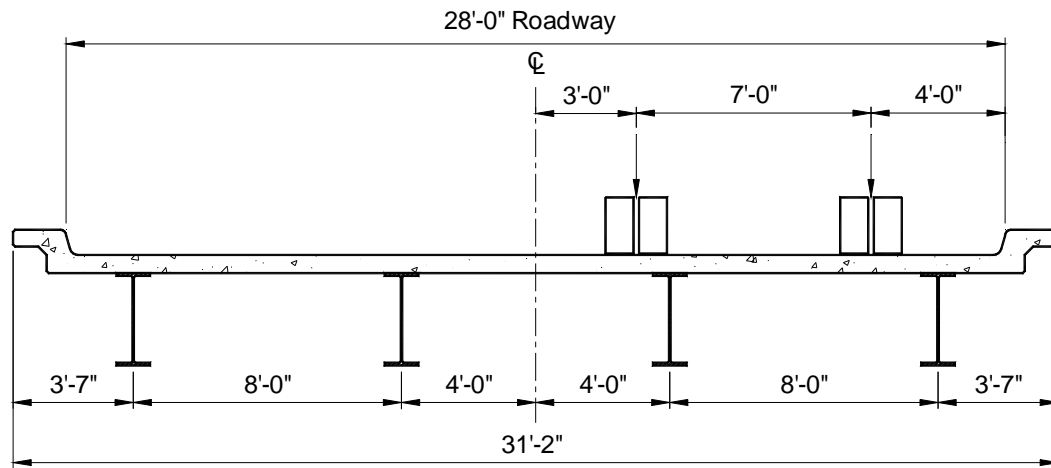


Figure 5.11: Vehicle #87 Rear Axle Travel Lane Position on Ex. Bridge 2

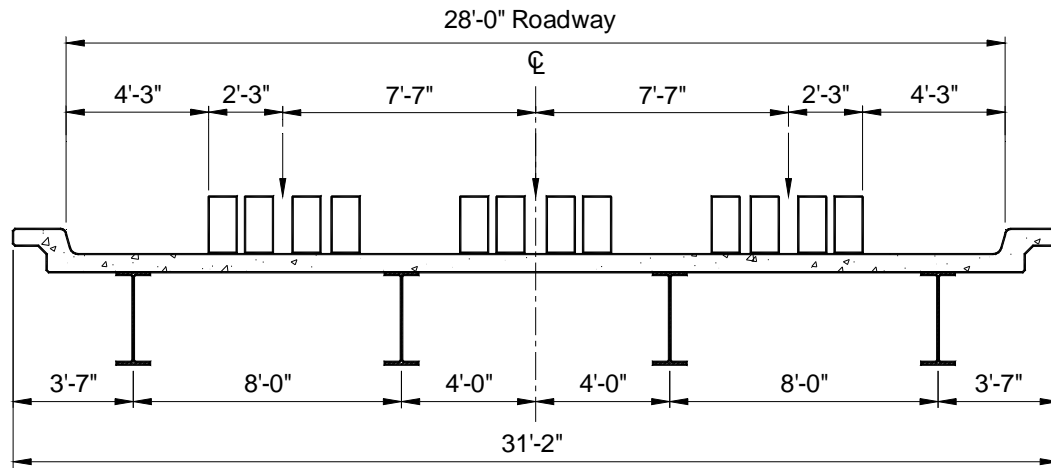


Figure 5.12: Vehicle #203 Rear Axle Travel Lane Position on Ex. Bridge 2

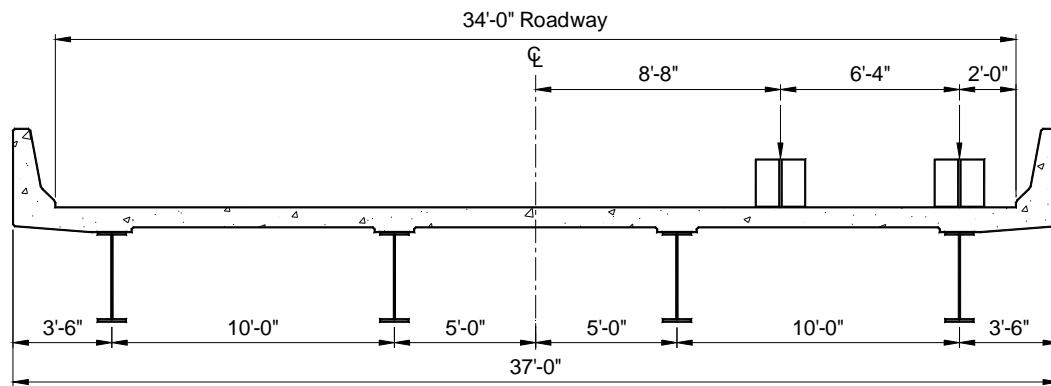


Figure 5.13: HS20 Rear Axle Design Lane Position on Ex. Bridge 3

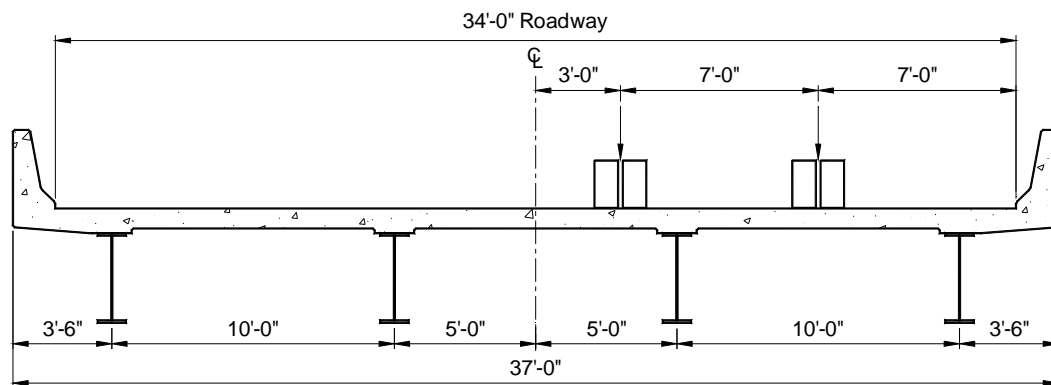


Figure 5.14: Vehicle #87 Rear Axle Travel Lane Position on Ex. Bridge 3

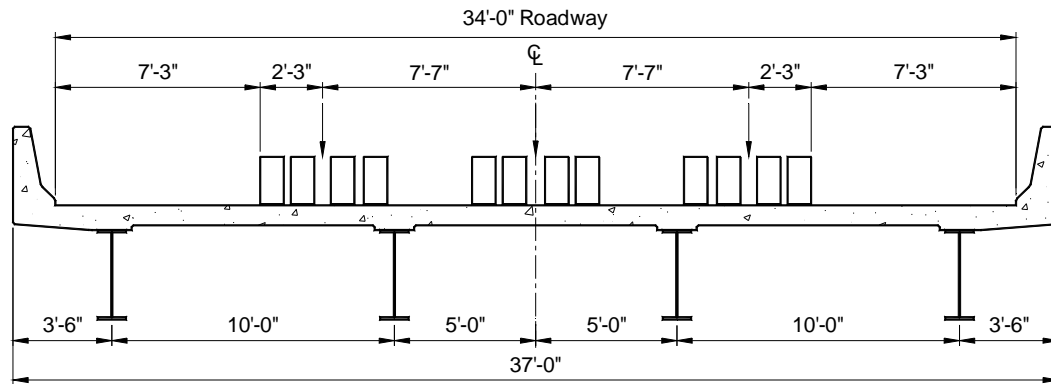


Figure 5.15: Vehicle #203 Rear Axle Travel Lane Position on Ex. Bridge 3

5.1.1.3. BRUFEM Longitudinal Truck Position Input

This section contains Figure 5.16 through Figure 5.29. These figures illustrate all of the longitudinal truck positions used as BRUFEM input during this research. Each position was found before going into BRUFEM to minimize the output created by the program. This was done because BRUFEM's post-processing capabilities are limited and because of the input technique required to analyze non-standard vehicles. When inputting a non-standard vehicle into the BRUFEM program, it is only necessary to place the "effective" axles into the "Veh.dat" input file. Another valid technique would be to input all axles of each overweight vehicle, and incrementally move the vehicle across the bridge span to determine the worst moment effects. The incremental technique would have to generate a great deal of output, due to the small increment sizes necessary and the

long truck lengths possible when dealing with Superheavy vehicles. It is much more efficient to let SAP2000 do this type of analysis in the form of a line-girder technique, as discussed in Chapter 3. Utilizing the SAP2000 program to find the longitudinal maximum moment positions and BRUFEM to analyze each exact truck position for LLDF calculation is the most efficient use of both programs. Section 5.1.2 describes the process by which each of these longitudinal truck positions was calculated, using the influence lines generated by the SAP2000 line-girder analyses.

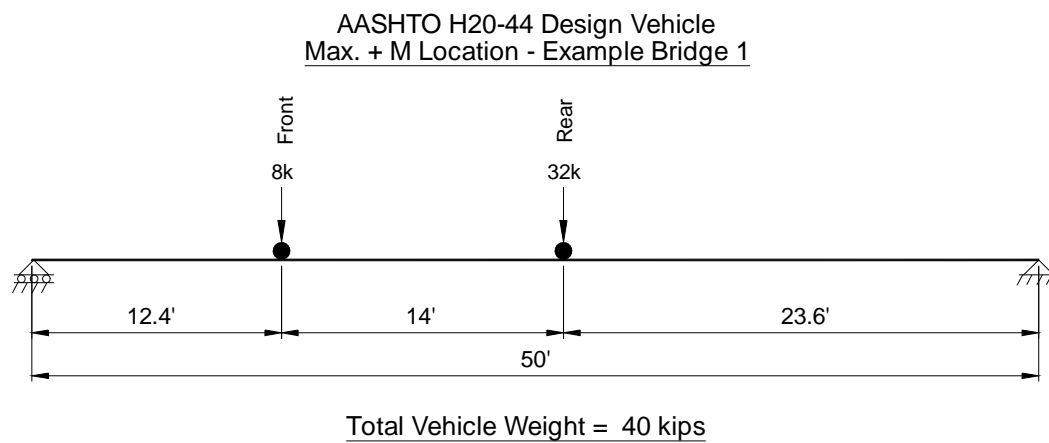


Figure 5.16: H20-44 Max. Positive Moment Location on Ex. Bridge 1

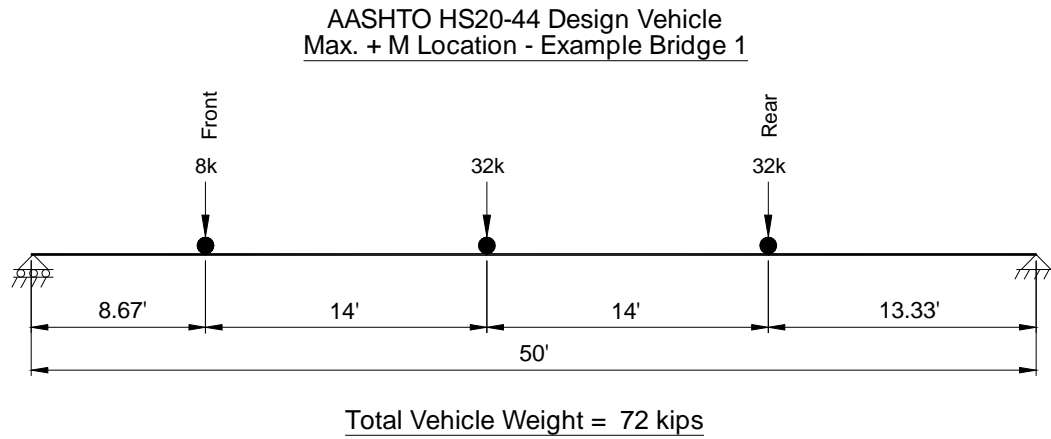


Figure 5.17: HS20-44 Max. Positive Moment Location on Ex. Bridge 1

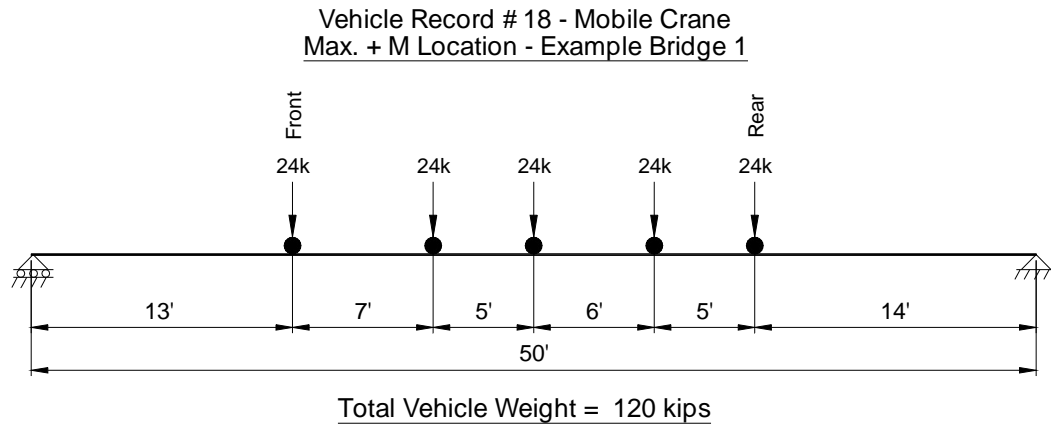


Figure 5.18: Vehicle #18 Max. Positive Moment Location on Ex. Bridge 1

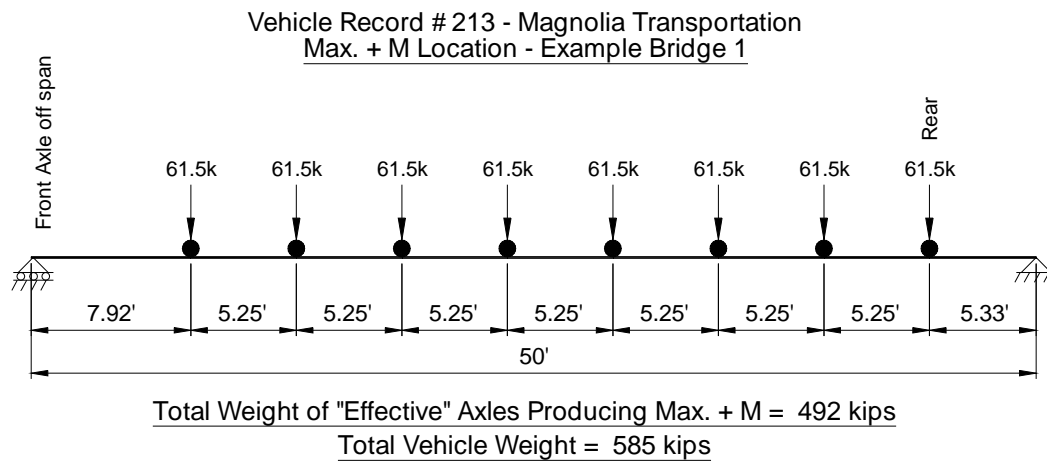


Figure 5.19: Vehicle #213 Max. Positive Moment Location on Ex. Bridge 1

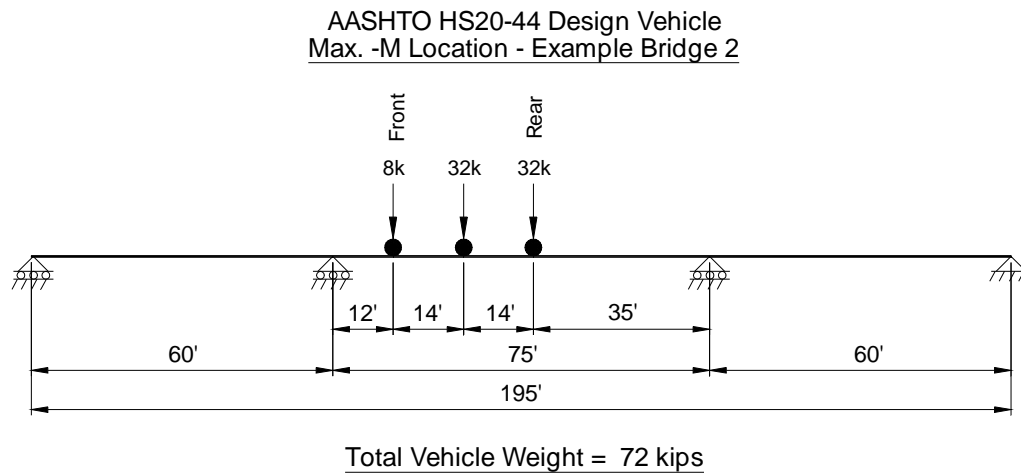


Figure 5.20: HS20-44 Max. Negative Moment Location on Ex. Bridge 2

AASHTO HS20-44 Design Vehicle
 Max. + M Location on End Span - Example Bridge 2

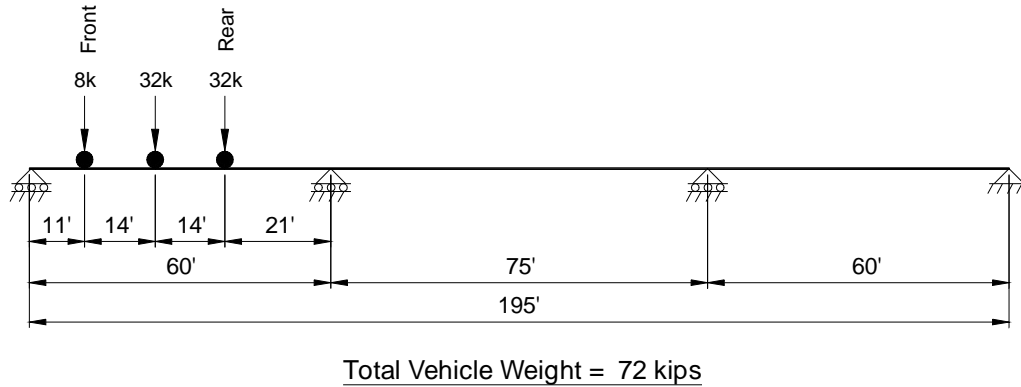


Figure 5.21: HS20-44 Max. Positive Moment in End Span Location on Ex. Bridge 2

Vehicle Record # 87 - Mobile Crane
 Max. + M Location on Interior Span - Example Bridge 2

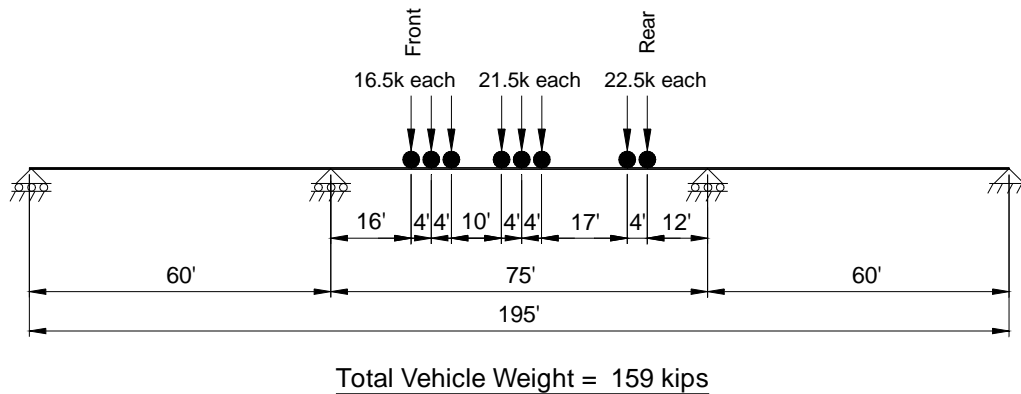


Figure 5.22: Vehicle #87 Max. Positive Moment in Interior Span Location on Ex. Bridge 2

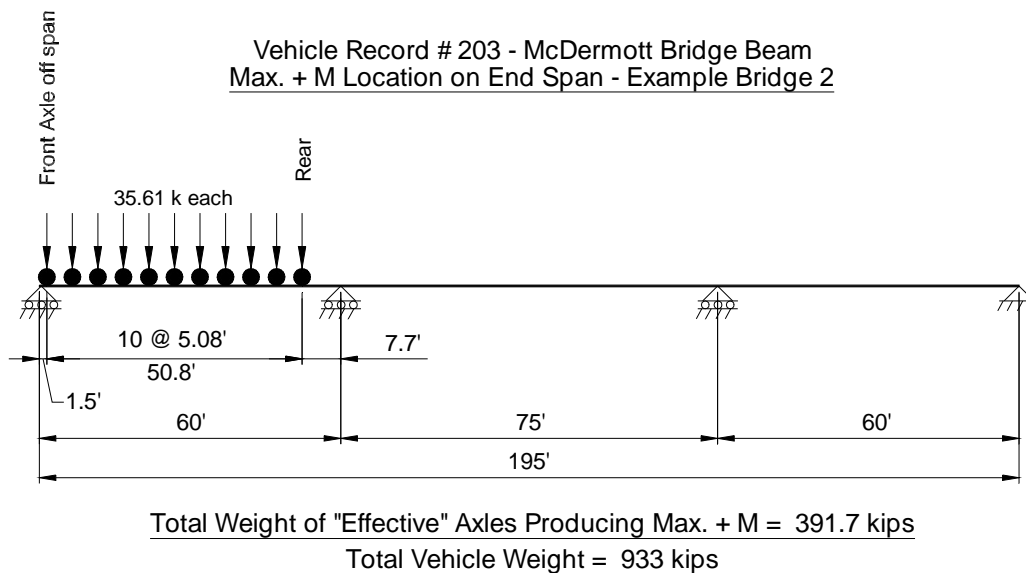


Figure 5.23: Vehicle #203 Max. Positive Moment in End Span Location on Ex. Bridge 2

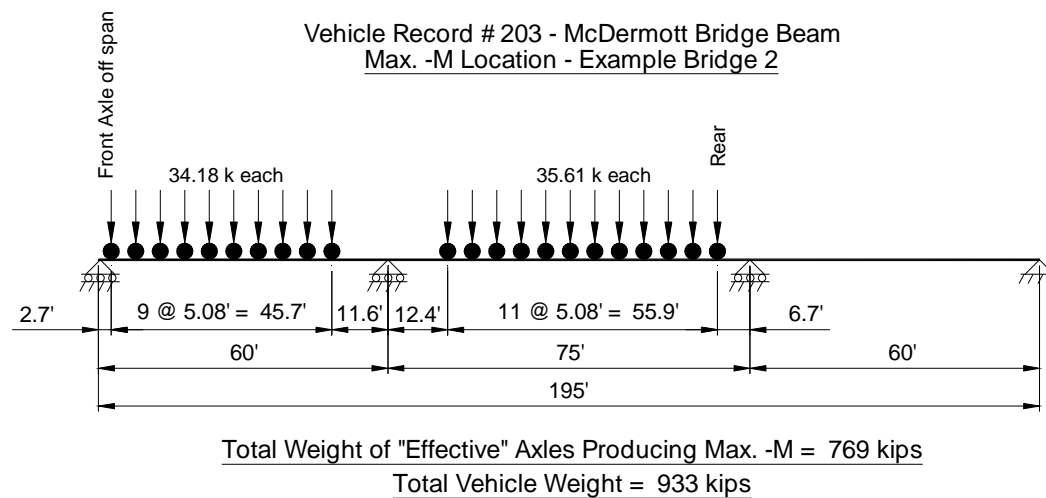


Figure 5.24: Vehicle #203 Max. Negative Moment Location on Ex. Bridge 2

AASHTO HS20-44 Design Vehicle
 Max. + M Location - Example Bridge 3

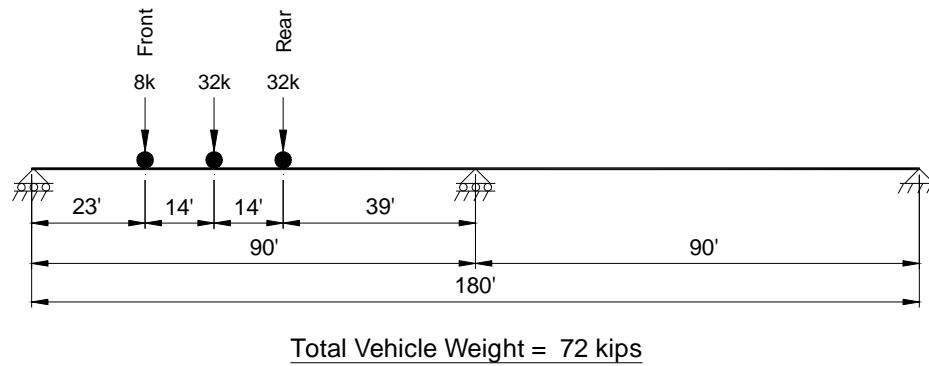


Figure 5.25: HS20-44 Max. Positive Moment Location on Ex. Bridge 3

AASHTO HS20-44 Design Vehicle
 Max. -M Location - Example Bridge 3

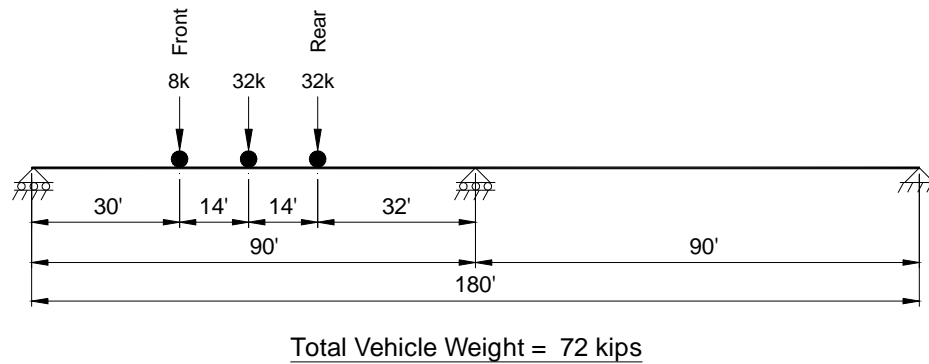


Figure 5.26: HS20-44 Max. Negative Moment Location on Ex. Bridge 3

Vehicle Record # 87 - Mobile Crane
 Max. + M Location - Example Bridge 3

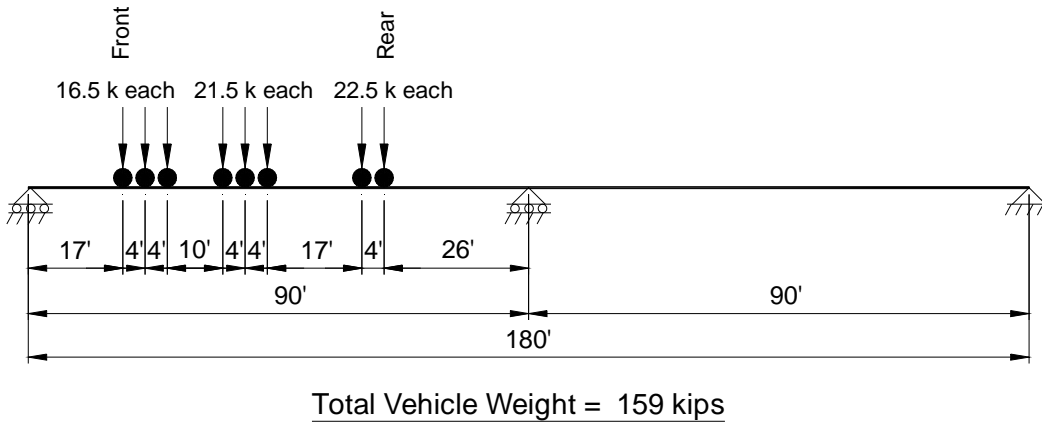


Figure 5.27: Vehicle #87 Max. Positive Moment Location on Ex. Bridge 3

Vehicle Record # 203 - McDermott Bridge Beam
 Max. + M Location - Example Bridge 3

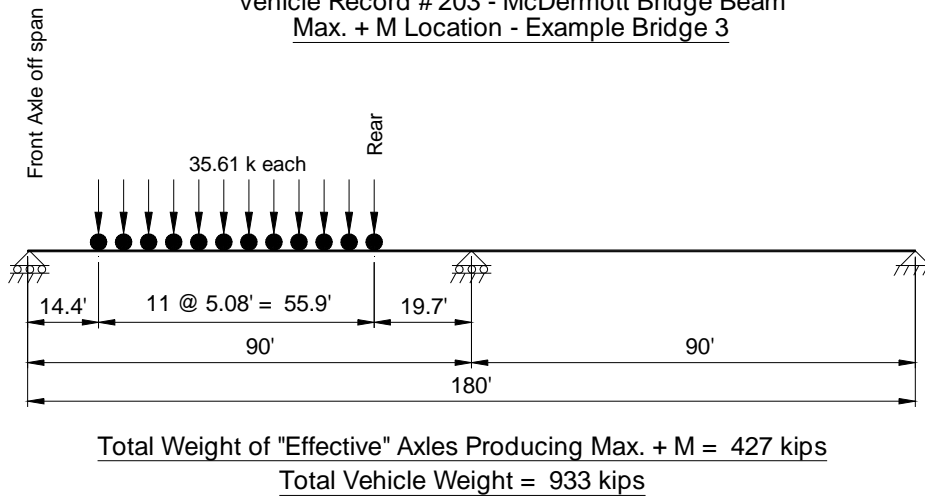


Figure 5.28: Vehicle #203 Max. Positive Moment Location on Ex. Bridge 3

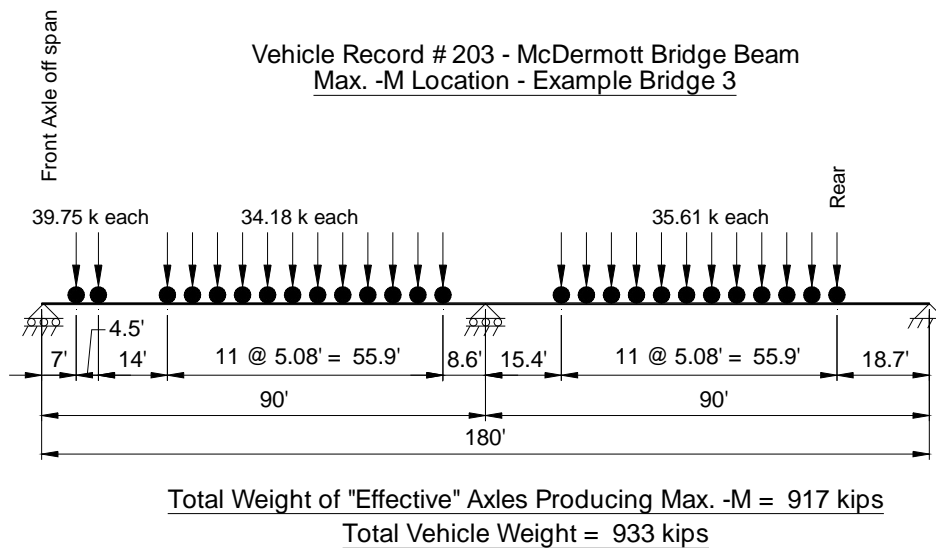


Figure 5.29: Vehicle #203 Max. Negative Moment Location on Ex. Bridge 3

5.1.2. Determination of Critical Longitudinal Truck Positions

As stated earlier, the BRUFEM package is best suited for analysis of LLDF's and calculating bridge ratings. BRUFEM is not set up to efficiently generate the maximum moment response envelopes required to correctly identify the longitudinal location at which a vehicle will produce maximum bending moments in a bridge structure. The BRUFEM pre-processor can be forced into calculating these responses by incrementally shifting all axle loads along the bridge structure, however, this would create output files too large to manage. A better approach to finding the critical longitudinal vehicle positions is to use the features of SAP2000's bridge analysis options. Once the SAP2000 analysis is complete, the user needs to input just the "effective" truck axles acting on the bridge in their critical moment position for BRUFEM LLDF calculation.

The best method of explaining the process of determining the critical moment location on a bridge structure is to use Example Bridge 1 to describe the procedure. Example Bridge 1 is a 50-foot simple span structure. Assume we want to find the location at which the largest value of moment is created somewhere along the span for an AASHTO HS20 vehicle. Rules exist for simple spans (as explained in Chapter 3) for determining these locations by finding the center of gravity of the truck's axles. From this information, the vehicle can be accurately placed on the span, and bending moments calculated to determine the maximum moment produced in the span. Unfortunately, not all vehicles or bridge layouts are as easy to analyze as an HS20 on a 50-foot simple span.

Continuous structures have no simple rules available to calculate the maximum moment positions of any moving load system. Long trucks also pose a problem since many sets of "effective" axles can exist within the same truck if the truck is longer than the total bridge length or has many sets of axles of varying weight. For these reasons, a SAP2000 line-girder analysis is the best method available to determine the maximum moments generated by an arbitrary truck. Using the line-girder analysis techniques discussed in Chapter 3, output of maximum positive and negative moments can be generated at each node or output segment of the structure. A simple search through the SAP2000 output will give the maximum positive moment on any span, as required. Looking at the SAP2000 output at any interior supports of continuous structures will give the maximum negative moments at that support. These moment values are tabulated

with their location along the element length, giving the user the point within the structure at which the maximum moment occurs.

Now the user knows the point in the structure where the maximum positive and negative bending effects occur, however, that is not an indicator of the truck position necessary to produce such effects. To determine the truck position that causes the maximum moment effect at a certain joint or node in the line-girder model, an influence line can be generated. SAP2000 can generate the moment influence line at any joint, as requested by the user. The calculated position of maximum moment is the joint at which the user must request the moment influence line in order to find the critical truck position. The moment produced by each axle of a vehicle can be found by multiplying the ordinate of the moment influence line at that axle's position on the structure by the weight of that axle. A summation of these values for each vehicle axle gives the total moment produced at the node previously specified by the user.

SAP2000 output tables can be exported as text files and imported as data into a spreadsheet to calculate the vehicle location that will produce the maximum moment in the structure. Once these moment influence values are placed in the spreadsheet, the truck's axles can be marched along the structure, with the spreadsheet calculating the total moment produced until the maximum moment value found from the original SAP2000 analysis is duplicated. When these total moments match, the critical vehicle location has been determined.

It is important to input many nodes or output segments into the SAP2000 model to generate a smooth moment influence line. The research presented for

this thesis used about one output segment per foot of bridge span length. Understanding and using the moment influence lines can also narrow down the possibilities of truck locations that can cause maximum moment effects. Qualitative assessments can be made quickly to determine which axles of the vehicle will generate the most moment potential. This can help to avoid placing the vehicle at locations that will obviously not create the maximum moment desired.

For this research, all simple span truck locations were found using the simple rules available and discussed in Chapter 3. All continuous span truck locations (for Example Bridges 2 and 3) were calculated using the influence line technique. The influence lines used to generate these critical truck locations are shown in Figures 5.30 through 5.34. This influence line technique can be programmed into a spreadsheet and utilized to prevent the user from filtering through a large amount of BRUFEM post-processor output and inputting more information than necessary in the BRUFEM “Veh.dat” files.

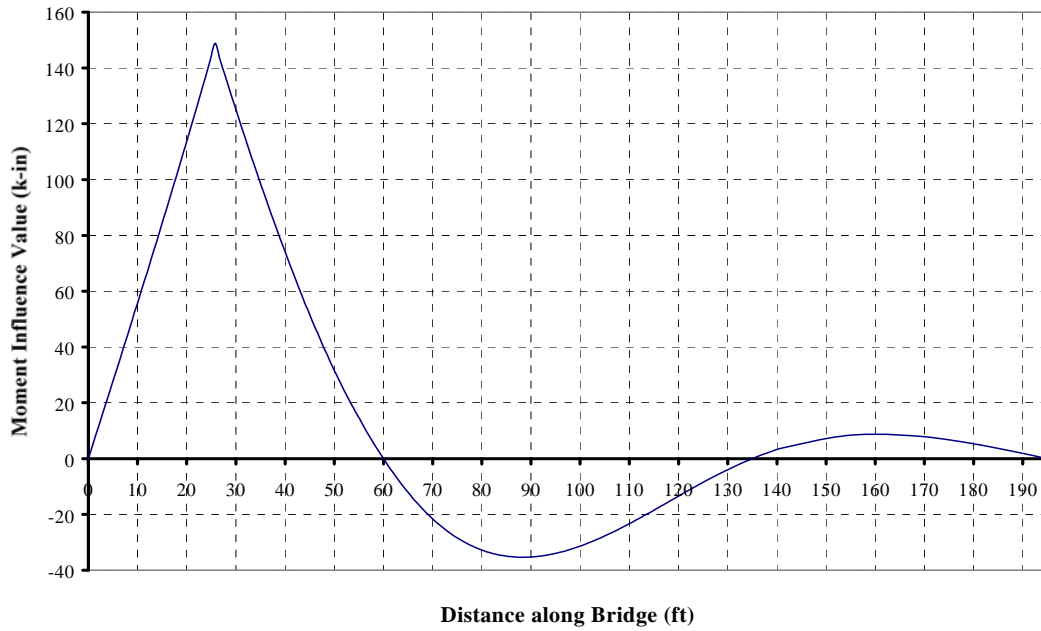


Figure 5.30: Maximum Positive Moment Influence Line in End Span of Ex. Bridge 2

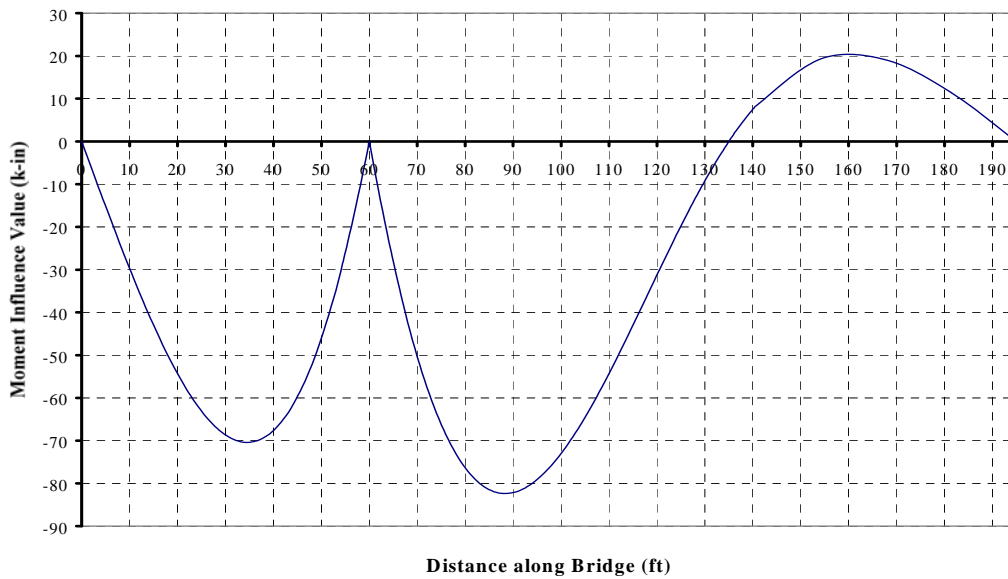


Figure 5.31: Maximum Negative Moment Influence Line at Interior Support for Ex. Bridge 2

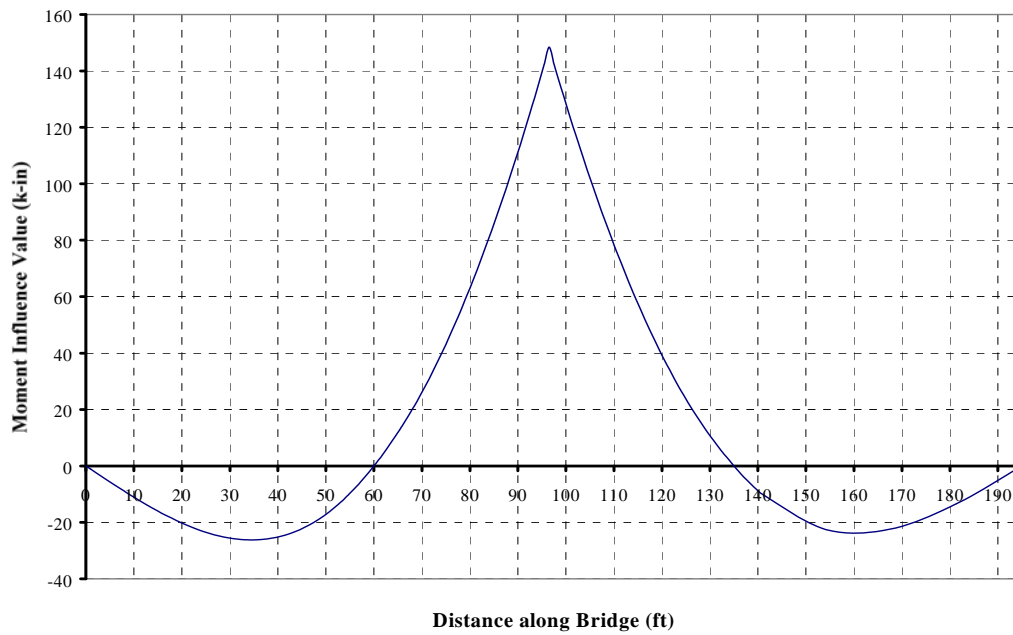


Figure 5.32: Maximum Positive Moment Influence Line in Interior Span of Ex. Bridge 2

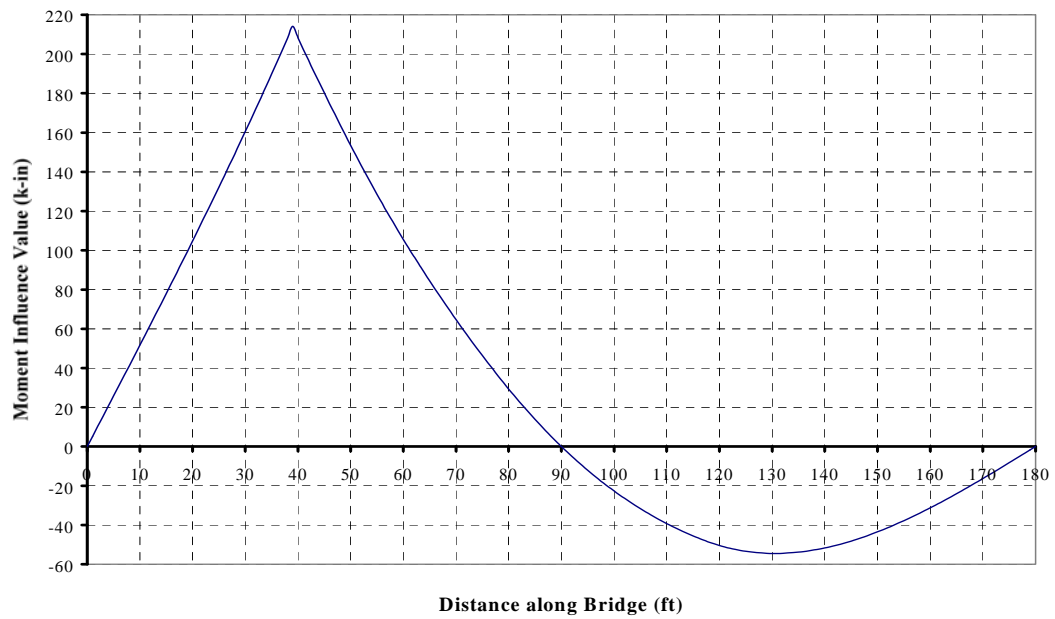


Figure 5.33: Maximum Positive Moment Influence Line for Ex. Bridge 3

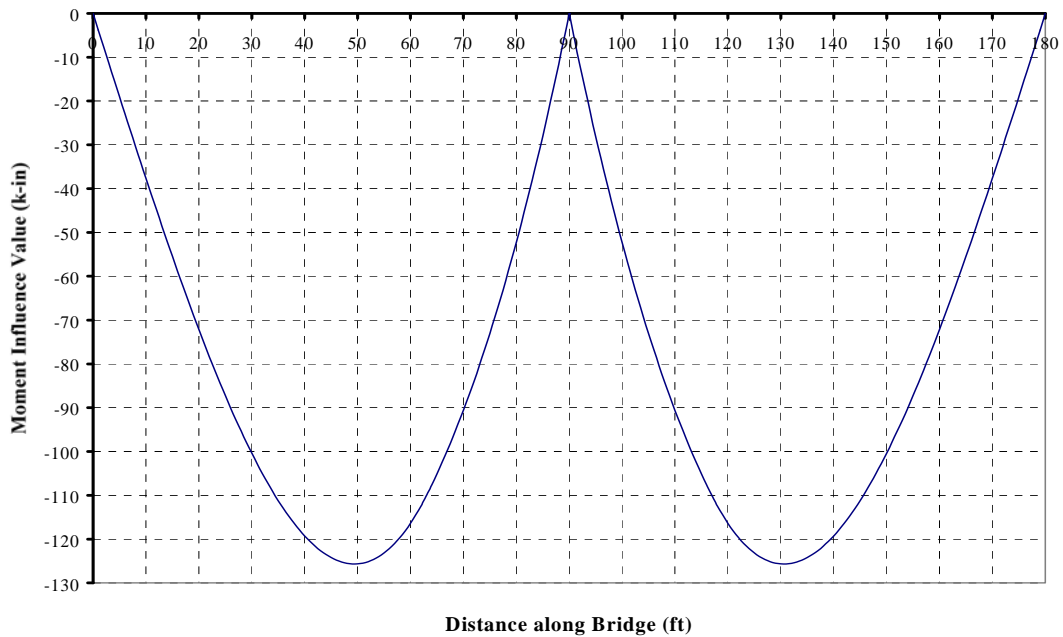


Figure 5.34: Maximum Negative Moment Influence Line for Ex. Bridge 3

The location of the maximum positive moment will vary in the same bridge structure, depending on the vehicle under consideration. In this research, all of the maximum positive moment locations in both Example Bridges 2 and 3 were almost identical for the different truck layouts chosen for analysis. The maximum positive moment influence lines shown in Figures 5.30, 5.32, and 5.33 can be used for each vehicle analyzed in this thesis since the maximum deviation from these critical moment locations was at most one foot. Since the values for the influence lines vary slightly over such a small distance, it is not detrimental to the results of the critical truck location analysis to use only the curves shown in Figures 5.30, 5.32, and 5.33.

In actual practice, the locations of maximum moment in a span may vary significantly from truck to truck depending on specific bridge or vehicle axle layout. Negative moment influence lines, on the other hand, need to be developed only at the interior support locations since the maximum negative moments will always occur at these points. Appendix B shows the input files that were generated to model the non-standard truck layouts (Veh.dat) and the girder characteristics (Bar.dat) for Example Bridges 2 and 3. The “Veh.dat” files include only the axles located on the bridge structure for each critical moment-producing position as described in this chapter.

5.1.3. Running the BRUFEM Pre-Processor

Once all the input files required of BRUFEM for non-standard girder geometry and vehicle layout were generated, the BRUFEMNT pre-processor was launched for each of the 15 runs. This section will describe the modeling techniques used for each Example Bridge and will explain the input used to generate the “History.pre” files for each run. While the general concepts of the modeling are discussed in this chapter, none of the input files are listed here. All of the 15 “History.pre” files are listed in Appendix B along with the “Bar.dat” files required for Example Bridges 2 and 3 and the required “Veh.dat” files for non-standard vehicles.

5.1.3.1. BRUFEM Modeling of Example Bridge 1

Example Bridge 1 is a non-composite 50-foot simple span bridge with a layout shown in Figure 1.1. Diaphragms are modeled using the interactive

BRUFEM pre-processor input technique at each of the locations shown in the Elevation View of Figure 1.1. BRUFEM automatically places diaphragms at the support points if they are used in any bridge, but additional locations can be input as required by the user. BRUFEM allows the user two options for modeling all diaphragms in the bridge. The two options for diaphragm modeling are steel beam diaphragms and X-brace diaphragms. It was found during the development of the BRUFEM programs that the X-brace type of diaphragms behaved similarly to the K-brace diaphragm type. For this reason, all diaphragms modeled in this research consisted of the X-brace type. Only the end supports of Example Bridge 1 have the steel beam type of diaphragms and BRUFEM only allows one type of diaphragm throughout the bridge model.

When diaphragms are present in the actual bridge structure, they must be modeled to get valid results from BRUFEM. Also, when modeling the diaphragms in a bridge structure, the BRUFEM post-processor, POSTNT, increases the live load moments, shears, and their corresponding LLDF's by 5% before displaying any results. The reasoning behind this 5% increase is explained in the BRUFEM User's Manual in detail, and this increase is unnecessary for this research. It is also important to note that the BRUFEM finite element output files do not include this 5% increase. Only the post-processor output reflects this 5% increase.

The BRUFEM basic model for Example Bridge 1 consists of four W33x141 girders, with zero skew, spaced at 8'-0" centers. Since the cross-section of the girders is constant throughout the length of the bridge, a "Bar.dat"

file is not required for Example Bridge 1. No additional stiffeners are added to account for parapets or curbs. Other research has been done to study the effects of this type of stiffening, and it is not included in this research. BRUFEM prompts the user for either a full analysis or a live-load analysis only. A live-load analysis is sufficient in these cases since only LLDF's are required in the BRUFEM output. A full bridge rating can be done if the full analysis is completed, however, additional information is included in the output files that is not required for this research.

The concrete slab thickness in this model is 6 ½ inches and the f'c of the concrete is 3,000 psi. Four elements are used to model the slab between the girders, as recommended in the BRUFEM Manual. Since this bridge consists of only one 50-foot segment, 50 nodes were used to model the bridge in the longitudinal direction, one element per foot length. The edges of the bridge slab, or overhangs, extend 3'-7" beyond the centerlines of the exterior girders. This information is input to the BRUFEM pre-processor directly and three elements are used to model these portions of the slab on each side of the bridge. BRUFEM prompts the user for the distance from the edge of the bridge to the travel lanes on both sides of the bridge being modeled. This is to check travel lane edge clearances during post-processing. For Example Bridge 1, both edge distances are input as 1'-6".

During the live load description portion of the BRUFEM pre-processing, both the interactive input methods and the "Veh.dat" file input methods were used, depending on the vehicle being modeled. Only one of each vehicle was

placed on the bridge simultaneously, however, BRUFEM does allow for up to three. All of these BRUFEM runs specified only one input vehicle position, as described earlier in this chapter. BRUFEM does allow the user to specify incremental shifts in the live loads on the slab, but these options were not used in this research. No lane loads were added during these LLDF analyses, but BRUFEM allows the user to input these types of loads also, if desired.

5.1.3.2. BRUFEM Modeling of Example Bridge 2

Only minor differences exist between Example Bridges 1 and 2. Example Bridge 2 is a 3-span continuous structure, 195'-0" in length, rather than a 50-foot simple span bridge (see Figure 1.2). Since Example Bridge 2 has longer spans than Example Bridge 1, the diaphragm locations are spaced differently, even though their make-up is similar. Example Bridge 2 has a varying girder cross-section also, using W33x130 sections with cover-plated interior pier sections. This varied cross-section is modeled using the "Bar.dat" file shown in Appendix B. The other characteristics of Example Bridge 2 match those of Example Bridge 1, and only the differences in the BRUFEM models will be discussed in this section.

The BRUFEM model for Example Bridge 2 still uses four elements between girders to model the slab, but uses a different element scheme in the longitudinal direction. BRUFEM only allows the user to use 150 elements to model a bridge in the longitudinal direction. The span lengths of Example Bridge 2 are 60 feet, 75 feet, and 60 feet, respectively, and our model contains the maximum amount of elements allowed by BRUFEM. The 60-foot spans have 45

elements each longitudinally and the 75-foot span has 60 elements longitudinally. This element layout was done in an attempt to keep the aspect ratios similar throughout the structure, while utilizing the maximum number of longitudinal elements allowed by BRUFEM. The BRUFEM pre-processor also prompts the user for any hinges in the continuous structures. No hinges were used during the modeling of Example Bridge 2.

5.1.3.3. BRUFEM Modeling of Example Bridge 3

The modeling of Example Bridge 3 is quite different than the modeling of the other two Example Bridges. This is due to the fact that Example Bridge 3 is a fully composite bridge structure. The roadway width is 34'-0" for this two-span continuous structure and both the steel and concrete is of a higher strength than that of Example Bridges 1 and 2. The specified concrete f'_c is 4,000 psi, and the minimum slab thickness is 8 inches. The slab overhangs the centers of the exterior girders by 3'-6" on each side of the bridge as shown in Figure 1.4. All four girders of the structure consist of plate girders rather than rolled sections, spaced at 10'-0" centers with zero skew. The interior pier section of each girder has an increased bending stiffness due to larger plate sections in this region. The total length of the bridge is 180 feet, consisting of two 90-foot spans. Cross frames, modeled as X-braces, are also included in the BRUFEM model.

The BRUFEM pre-processor allows the user the choice of two types of composite action modeling techniques. The girder-slab interaction models available in BRUFEM are illustrated in Figure 5.35 and Figure 5.36. Non-composite action is modeled as shown in Figure 5.35. In the BRUFEM non-

composite model, the centroid of the girder is at the same elevation as the slab centroid. Section properties specified for the girders are those of the girders alone. In the non-composite model, the function of the slab elements is mainly to distribute the wheel loads laterally to the girders.

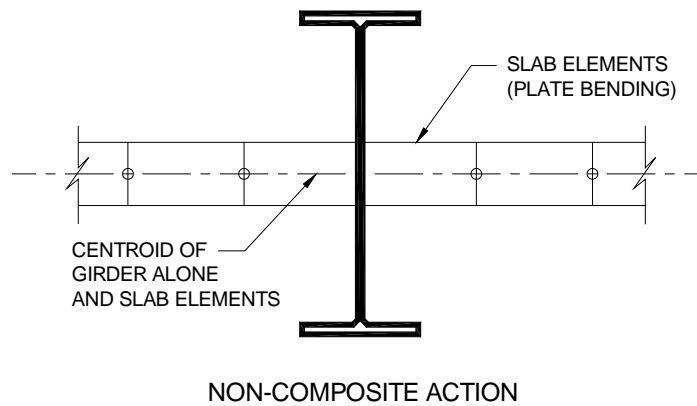


Figure 5.35: BRUFEM Model of Non-Composite Slab-Girder Interaction

Figure 5.36 shows the two methods by which BRUFEM can model composite action. One method of modeling involves the use of a composite girder model (CGM) and the other involves the use of an eccentric girder model (EGM). When using the CGM method, BRUFEM specifies composite properties for the girders. The centroid of the composite girder section is located at the same elevation as the centroid of the slab in the finite element model. The CGM composite girder is the combination of a stand-alone girder and an effective width of slab.

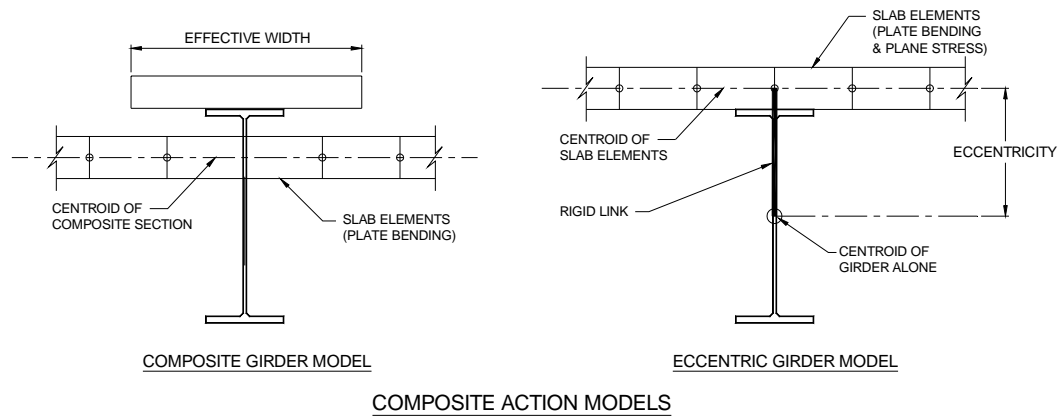


Figure 5.36: BRUFEM Models of Composite Slab-Girder Interaction

The second method available in BRUFEM for modeling composite action between the slab and girders involves what the BRUFEM manual calls a three-dimensional analysis. BRUFEM’s three-dimensional analysis, the eccentric girder method (EGM), uses the non-composite section properties of both the girders and the slab, along with a vertical eccentricity of the girders from the mid-depth of the slab (see Figure 5.36). The eccentricity of the girders is calculated internally while running the SIMPAL analysis portion of BRUFEM. Modeling the composite action in this way takes the in-plane stresses developed in the slab into account by using shell elements. These shell elements consider membrane behavior as well as bending behavior, accounting for the effects of shear lag directly, without the use of the effective width calculation done in CGM modeling.

The EGM assumes what BRUFEM calls a “rigid link” between the mid-depth of the slab and the centroid of the girder. The EGM modeling technique is

generally considered to be more accurate than the CGM technique.^[4] The CGM is considered less accurate because it approximates the effective width required to determine the composite section properties of the girders. This research used the EGM method of modeling composite action, however, these results must be interpreted a bit more carefully than results generated from the CGM technique. In the EGM analysis, the effect of the axial girder forces must be taken into consideration when computing the total moment in the girder section. Also, the user must use sufficient numbers of longitudinal elements when modeling with EGM. If the EGM model does not contain enough elements longitudinally, the compatibility of longitudinal strains between the girder and slab is not achieved. The BRUFEM User's Guide recommends at least 20 longitudinal elements per span, and the model generated for Example Bridge 3 used 75 elements per span to utilize the maximum number of 150 longitudinal elements in the model.^[4]

5.2. SUMMARY OF BRUFEM OUTPUT FILES

BRUFEM creates many files necessary to complete the analysis that remain after a run has been completed. The four most important of these output files for the user are explained here to assist in finding the most useful BRUFEM output information quickly. The "History.pre" file is a history file containing all data interactively input by the user. "History.pre" is a useful file to view when checking a model's input values. It expedites the editing of any incorrect input files by allowing the user to change only the incorrect input values while allowing the user to run the analysis again using the "Restart" pre-processor command.

Another useful output file is the file titled “Input.in1”. The “Input.in1” file is the finite element bridge model file created by the BRUFEM pre-processor that contains truck wheel locations, wheel loads, properties of the finite element model members, and joint coordinates. The “Input.in1” file is useful for checking the truck positions during analysis, especially when the vehicles being analyzed are not standard AASHTO design vehicles.

The two most important files generated by BRUFEM for the user are the “Brate.out” file and the “Input.ou1” file. “Brate.out” is the BRUFEM bridge rating output file containing both bridge rating information and LLDF results, as requested by the user. For this research, only the LLDF results were requested during analysis. The “Input.ou1” file contains detailed finite element output such as number of joints in the model, number of load conditions, nodal coordinates, boundary conditions, element definitions, load data, displacements, forces, and stresses. The “Input.ou1” file is a large file, but contains all results that are later interpreted and presented in a less cumbersome manner in “Brate.out”.

It should be noted that the BRUFEM post-processor (POSTNT) sometimes takes the true finite element analysis results from “Input.ou1” and alters them when certain conditions exist in the bridge model. For this reason, the user should exercise caution before blindly using the “Brate.out” results from the POSTNT program. The user should refer to the BRUFEM User’s Manual for a discussion on the reasons behind these variances.^[4] Section 5.3 discusses the differences between the SIMPAL finite element analysis results (Input.ou1) and the “Brate.out” file for steel stringer bridges with intermediate diaphragms only.

5.3. DIFFERENCES BETWEEN SIMPAL OUTPUT AND POSTNT OUTPUT

When modeling steel stringer bridges with intermediate diaphragms, BRUFEM's POSTNT program modifies the finite element results and presents this modified information in the "Brate.out" file. One modification that is made to the finite element output is a 5% increase of both the calculated shears and moments used in calculating BRUFEM's LLDF's. This increase is included because while developing the BRUFEM package, the authors found a small percentage of steel stringer bridges where the moment and shear values were underestimated by as much as 5% when compared to results of more expensive finite element programs. This anomaly was present only in steel stringer bridges with intermediate diaphragms present. All three of the Example Bridges studied during this research are steel stringer bridges with intermediate diaphragms. Since all three of these bridges are very common, right-girder bridges, of common span lengths, these 5% increases in shears and moments have been removed from the calculated BRUFEM LLDF's. All BRUFEM LLDF results presented in this thesis have been modified from the values shown in "Brate.out" to remove this 5% increase.

Another modification made to the BRUFEM LLDF values was in the manner of defining a girder LLDF. BRUFEM defines a moment LLDF as shown in Equation 5.1.

$$DFM_i = \frac{M_i}{\left(\frac{\sum M_i}{2N} \right)} \quad (5.1)$$

where: DFM_i = Lateral load moment distribution factor for girder i

M_i = Live load moment in girder i

$\sum M_i$ = Total moment in the girders across the section of the bridge

N = Number of vehicles on the bridge

The BRUFEM post-processor (POSTNT) evaluates the lateral moment and shear distribution factors for every load case output by SIMPAL. The post-processor first reads the moments, axial forces and shears in the girder and stiffener members, the axial forces in truss members and the stresses in slab elements for a load case and calculates the total moment and shear acting on either side of the girder and stiffener elements.^[4] POSTNT then evaluates lateral moment and shear distribution factors for the girders considering the total moment and shear acting on the girders and stiffeners across the bridge for the load case in question. The BRUFEM LLDF's use "2N" in the denominator to formulate wheel line LLDF's rather than truck LLDF's. All moments and LLDF's reported in Chapter 6, as well as the modified AASHTO design LLDF's reported in Chapter 4, are truck LLDF's.

The LLDF's reported in Chapter 6 are also modified from the BRUFEM LLDF output to reflect only the forces resisted by the girders of the bridge structures studied. The results reported by BRUFEM lump all forces taken by the

slab into the girder LLDF's. The focus of this research was to isolate the load effects on the girders only, thus accounting for the slab capacity that is assumed to be zero during AASHTO design procedures. The procedures used to isolate the girder force effects are outlined in Section 5.4. These modifications allow for a direct calculation of the maximum moment required of a bridge girder under these overweight vehicles. Directly using the BRUFEM LLDF calculation procedure slightly overestimates the force effects actually seen by the bridge girders alone.

5.4. USER MODIFICATIONS REQUIRED FOR POSTNT RESULTS

Two separate modification techniques are required to report the girder moment LLDF's in this research. Two techniques are necessary because both non-composite and composite girder construction techniques exist in the three Example Bridges studied here. The methods by which BRUFEM calculates the total girder moments for each type of model will be discussed, along with the user modifications required to separate all sources of total girder moment from the output.

5.4.1. Modifications Required for Non-Composite Girder Models

In order to separate the girder moment from the slab moment at each girder section, the user must enter BRUFEM's "Input.ou1" file. Located about halfway through this output file is the section titled "Forces – Three-D Frame Members". From this listing, all girder element forces can be determined, given the element number. Knowing the location where the maximum moment occurs in the span from statics or SAP2000 output, the user can find the moments in the

steel section only from the “1-3 Plane – (M2)” column in this file. You will notice that the moment listed here is less than the moment listed for the girder in question in BRUFEM’s “Brate.out” file. This is because BRUFEM adds any moment taken by the slab into this girder moment output.

According to the BRUFEM User’s Manual, the program’s post-processor takes the finite element output for the slab members and numerically integrates the internal forces to develop a total slab moment.^[4] It is very time-consuming and difficult to pinpoint all of this slab moment data in the finite element output, however, since the only sources of moment capacity come from the slab and girder in the non-composite model, the slab moment can be quickly determined.

The slab moments listed in Chapter 6 for the non-composite girder models were calculated by subtracting the girder moment (from “Input.ou1”) from the total girder moment listed in the “Brate.out” file. It should be noted that the total girder moment listed in the “Brate.out” file is divided by a factor of 1.05 to remove the 5% moment increase built in to those values. Equation 5.2 illustrates this calculation.

$$M_S = \left(\frac{M_{TOTAL}}{1.05} \right) - M_{GIRDER} \quad (5.2)$$

where: M_s = Slab moment

M_{total} = “Brate.out” moment value

M_{girder} = “Input.ou1” girder moment alone

The user can also approximate the slab moment value for the non-composite girder model by assuming an effective width of concrete over each steel girder. This technique assumes that the curvature in both the concrete slab and the steel girder are equal at the cross-section in question. The effective width of the concrete slab is required to calculate the moment of inertia of the slab section assumed to act with each girder. Equation 5.3 illustrates the general curvature relationship, and Equation 5.4 solves directly for the slab moment, given the girder moment.

$$\left(\frac{M}{EI}\right)_{SLAB} = \left(\frac{M}{EI}\right)_{GIRDER} \quad (5.3)$$

$$M_{SLAB} = M_{GIRDER} \left(\frac{E_{SLAB} \cdot I_{SLAB}}{E_{GIRDER} \cdot I_{GIRDER}} \right) \quad (5.4)$$

5.4.2. Modifications Required for BRUFEM EGM Composite Girder Models

A similar technique is used to calculate the slab moments in composite girder models. BRUFEM's finite element output supplies enough information to calculate the moments carried by the slab. In the composite girder model, however, the couple generated by the axial forces in both the slab and the girder creates an added component to the total moment capacity of the section. The only additional information that is required from BRUFEM for this condition is the axial load in the girder. The axial load in the girder is listed in the rightmost column of the "Input.ou1" output. When reading the girder moment, the girder

axial load can also be quickly located at the same joint. Using this added information, and the eccentricity of the slab centroid from the girder centroid (which is known by bridge geometry), all the necessary components are available to calculate the slab moment directly.

Equation 5.5 shows how BRUFEM calculates the total girder moment for LLDF purposes, and Equation 5.6 illustrates the formula for calculating the moment in the slab alone. Equation 5.6 divides the total BRUFEM post-processor output value by a factor of 1.05 to remove the 5% increase built in to those values. Figure 5.37 illustrates these forces and moments used to calculate the slab moments in Chapter 6.

$$M_{TOTAL} = M_{SLAB} + M_{GIRDER} + (P \cdot e) \quad (5.5)$$

$$M_{SLAB} = \left(\frac{M_{TOTAL}}{1.05} \right) - M_{GIRDER} - (P \cdot e) \quad (5.6)$$

where: M_{total} = “Brate.out” total girder section moment

M_{slab} = Moment in slab only

M_{girder} = Moment in girder alone

P = Axial force in both the slab and girder elements

e = Eccentricity from slab centroid to girder centroid

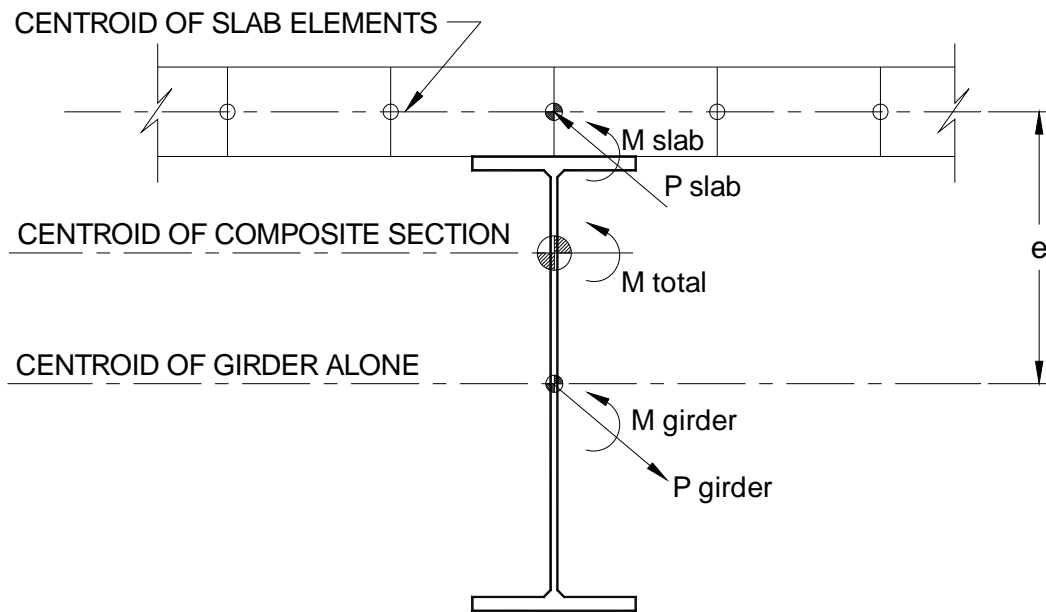


Figure 5.37: Total Moment on EGM Steel Girder Section

The moment LLDF values listed in Chapter 6 calculated from the BRUFEM analysis are calculated differently for the non-composite model and the composite girder model. Equation 5.7 shows the calculation technique used for the non-composite girder models. Equation 5.8 shows the calculation technique used for the composite girder models.

$$\text{Non - Composite LLDF}_i = \frac{M_{GIRDER i}}{\left(\frac{\sum M_{TOTAL}}{1.05} \right)} \quad (5.7)$$

$$\text{Composite LLDF}_i = \frac{M_{TOTAL i} - M_{SLAB i}}{\left(\frac{\sum M_{TOTAL}}{1.05} \right)} \quad (5.8)$$

where: $LLDF_i$ = Lateral Load Distribution Factor for girder i

$M_{girder i}$ = Moment in girder i alone

$M_{slab i}$ = Moment in slab at girder i

$M_{total i}$ = “Brate.out” girder i moment and slab moment

ΣM_{total} = Total “Brate.out” moment across section of bridge

CHAPTER 6

SUMMARY AND COMPARISON OF BRUFEM LLDF'S

The results from 15 separate BRUFEM analyses are presented in this chapter. These results are presented in three groups of 5 analysis runs, sorted by the Example Bridge each represents. A few cursory checks of these data were made to see if the trends matched what was expected of the analyses. One condition that can be verified quickly is totaling the BRUFEM moments across a bridge section and making sure this sum equals the total static moment produced by the vehicle in that location. This summation was checked for each of these 15 runs and the errors found ranged from 0.2% to 2.5%.

The error in total moment was caused by the difference in location of the maximum moment within a member and location of the nodes in the BRUFEM model. Also, BRUFEM limits the user to a relatively small number of nodes and elements, and this can become a concern when longer multi-span continuous structures are involved. As the models get longer, the length of the elements must increase in size, due to the restrained number of members and joints allowed. Increasing the size of the elements increases the possibility of error due to missing the maximum moment location. Another source of error stems from the numerical integration techniques used by BRUFEM to calculate slab moments. As element sizes increase, force gradients present in the model are less accurately captured by the numerical integration technique used by BRUFEM. Errors can also arise when the wheel locations do not match nodal locations. Vehicle wheel

loads applied to an element are spread out to the corner nodes of the element. The model sees these wheel loads only at the nodal locations, causing slight errors to arise. Since all of these errors are applied evenly across the bridge model to each girder, they do not affect the LLDF's.

6.1. LLDF AND SLAB MOMENT RESULTS FOR EXAMPLE BRIDGE 1 (RUNS 1 THROUGH 5)

This section presents the analysis results obtained analyzing Example Bridge 1. This structure is a 50-foot, simply supported, non-composite stringer bridge. See Table 1.1 and Figure 1.1 for more detailed Example Bridge 1 layout information. Table 5.1 lists the figures that diagram the vehicle locations for each run made on Example Bridge 1 (Runs 1 through 5). Vehicle location information and the analysis results are listed in Table 6.1. In Runs 1 through 3, AASHTO design trucks were used to load this structure at the location causing the maximum moment effect in a line-girder analysis. Run 4 uses a vehicle from the TxDOT Overload Vehicle Database (Vehicle #18). This vehicle was selected because it produced the highest moment of any vehicle in the Overload Vehicle Database on the simple span bridge layouts summarized in Chapter 2. Run #5 uses a vehicle from the TxDOT Superheavy Vehicle Database (Vehicle #213). This vehicle was selected because it produced the highest moment on the simple span bridge layouts of all vehicles studied. This reasoning was followed to select the TxDOT Vehicles used for each bridge layout during this research.

Table 6.1: Example Bridge 1 Analysis Results (Non-Composite)

	Vehicle	Vehicle Type	Lane Used	M_{\max} (Line Girder) (k-in)	Max. M Location from End of Span		
Run 1	H 20	Design	Travel	5352	23.6 ft		
Run 2	HS 20	Design	Travel	7536	22.7 ft		
Run 3	HS 20	Design	Design	7536	22.7 ft		
Run 4	Veh. #18	Overload	Travel	13104	25.0 ft		
Run 5	Veh. #213	Superheavy	Center	43008	23.7 ft		
All Moments listed in (kip-inches)							
	Girder	M_{Total}	M_{Girder}	M_{Slab}	Girder M%	Slab M%	LLDF
Run 1	1	199.1	192.5	6.6	96.7	3.3	0.037
	2	902.9	866.5	36.4	96.0	4.0	0.165
	3	1895.2	1792.0	103.2	94.6	5.4	0.341
	4	2258.1	2156.5	101.6	95.5	4.5	0.410
	<i>Sum</i>	<i>5255.2</i>	<i>5007.5</i>	<i>247.7</i>	<i>95.3</i>	<i>4.7</i>	<i>0.953</i>
Run 2	1	318.1	309.0	9.1	97.1	2.9	0.041
	2	1325.7	1276.0	49.7	96.3	3.7	0.171
	3	2572.4	2446.0	126.4	95.1	4.9	0.327
	4	3253.3	3118.0	135.3	95.8	4.2	0.417
	<i>Sum</i>	<i>7469.5</i>	<i>7149.0</i>	<i>320.5</i>	<i>95.7</i>	<i>4.3</i>	<i>0.956</i>
Run 3	1	128.6	122.6	6.0	95.4	4.6	0.016
	2	1090.5	1055.1	35.4	96.8	3.2	0.136
	3	2620.0	2509.3	110.8	95.8	4.2	0.324
	4	3897.1	3758.0	139.1	96.4	3.6	0.486
	<i>Sum</i>	<i>7736.2</i>	<i>7445.0</i>	<i>291.2</i>	<i>96.2</i>	<i>3.8</i>	<i>0.962</i>
Run 4	1	449.5	437.0	12.5	97.2	2.8	0.033
	2	2364.8	2288.0	76.8	96.8	3.2	0.175
	3	4293.3	4136.0	157.3	96.3	3.7	0.317
	4	5938.1	5725.0	213.1	96.4	3.6	0.439
	<i>Sum</i>	<i>13046</i>	<i>12586</i>	<i>459.7</i>	<i>96.5</i>	<i>3.5</i>	<i>0.964</i>
Run 5	1	10419	10087	331.6	96.8	3.2	0.235
	2	11025	10641	383.8	96.5	3.5	0.248
	3	11024.8	10641	383.8	96.5	3.5	0.248
	4	10419	10087	331.6	96.8	3.2	0.235

	<i>Sum</i>	42888	41457	1430.6	96.7	3.3	0.966
--	------------	-------	-------	--------	------	-----	--------------

One of the trends that should be noted from these LLDF and slab moment values is the percentage of the total moment taken by the girders and by the slab for this 50-foot simple span non-composite bridge model. The total moment taken by the slab elements ranges from 3.3% to 4.7% of the total moment taken by the bridge section. In the output listed for Run 1 in Table 6.1, the sum of the LLDF values is shown to be 0.953. The sum totals 1.0 when the slab moment percentage is added to the sum of the LLDF values for non-composite bridges.

This means the total moment taken by the girders alone ranges from 95.3% to 96.7%. This percentage of slab moment capacity is neglected using normal design procedures, but does reduce the moments in the girders. Shorter span bridges may see an even greater percentage of their total moment capacity being taken by the slab. Shorter bridges may benefit most from a finite element analysis.

Another important trend can be seen when comparing the results of Run 1 and Run 2. Each vehicle's transverse position and axle width on the bridge slab is identical, however, the total moment produced and the maximum moment location within the span differ due to the varied number of truck axles and their layout. As expected, the LLDF's for each girder in these two models are nearly identical. The exterior girders closest to the vehicle are experiencing the bulk of the applied loads in each of these analyses as expected for trucks located in the AASHTO exterior girder design lane. Section 6.4.1 compares these values with the AASHTO design LLDF values.

Comparing the results of Run 2 and Run 3 shows the difference in the LLDF's when the same truck is moved from the AASHTO design lane to an actual travel lane on the bridge slab. This was done to show the benefit of analyzing overloads in the actual transverse location they will travel, rather than forcing these loads to one extreme side of the structure (as assumed when using the AASHTO design provisions). Moving the truck (an AASHTO design vehicle in this case) towards the centerline of the structure reduces the moment on Girder 4 and slightly increases the moments in the other girders. The exterior girder LLDF is reduced from 0.49 to 0.42 in this case, with the adjacent interior girder LLDF increasing only slightly from 0.32 to 0.33. The load sharing can be seen by comparing both of the girders on the opposite side of the structure from the load position. When the trucks are placed in the design lane, very little help is offered from the two girders located on the opposite side of the structure. By simply moving the vehicle into the travel lane, the girders opposite the applied load reduce the most heavily loaded exterior girder by 14%. The benefit of simply analyzing the overloaded vehicles in their travel lanes is obvious using this example, especially when the maximum LLDF for an exterior girder can be reduced 10 to 15 percent.

Run 5 found the moment LLDF's for a Superheavy vehicle traveling along the centerline of the bridge slab. This run was made to verify the intuitive feeling that using a wide trailer for these overloads and moving the vehicle along the structure's centerline evenly spreads the load to each girder. The interior girders carry slightly more of the total moment than the outside girders. Each girder is

taking roughly one quarter of the total moment caused by this vehicle, after subtracting moment taken by the slab.

6.2. LLDF AND SLAB MOMENT RESULTS FOR EXAMPLE BRIDGE 2 (RUNS 6 THROUGH 10)

This section presents the analysis results obtained analyzing Example Bridge 2. This structure is a 195-foot, three-span continuous, non-composite stringer bridge consisting of two 60-foot exterior spans and a 75-foot interior span. See Table 1.1 and Figure 1.2 for more detailed Example Bridge 2 layout information. Table 5.1 lists the figures that diagram the vehicle locations for each run made on Example Bridge 2 (Runs 6 through 10). Vehicle location information and the analysis results are listed in Table 6.2.

Comparing the slab moment capacity percentages in these slightly longer continuous spans to the 50-foot simple span, we find similar results. The total moment taken by the slab elements in this continuous span model ranges from 3.0% to 4.0% of the total moment taken by the bridge section, which is very similar to the shorter, non-composite, simple span results.

The LLDF's from Run 7 on the three-span continuous structure are very similar to those obtained from Run 3 on the 50-foot simply supported structure. Although the span lengths differ, these bridges have the same girder spacing, slab width, and slab thickness. The girder sizes do vary, however, each girder is identical with the others in each respective span, so the relative stiffness properties of each girder with respect to the others across a section is the same in

both structures. Due to these similarities, it would be expected that the same vehicle in the same transverse position would produce similar LLDF values on each structure. Looking at the LLDF results for Run 7 and Run 3, a strong correlation is present, adding confidence to the results reported.

Both Run 9 and Run 10 analyze the same Superheavy vehicle traveling down the centerline of Example Bridge 2. The longitudinal location of this vehicle is varied between these two runs. The vehicle was positioned for maximum positive moment effect on the exterior (60-foot) span in Run 9. The vehicle was positioned for maximum negative moment at the interior support in Run 10. In these cases, the LLDF's showed the symmetry expected of a bridge loaded along its centerline, but the LLDF values varied slightly among the runs. Figures 5.23 and 5.24 show that more axles are effective in Run 10, with some axles applying different loads than the axles effective during Run 9. In each case, the interior girders see the highest percentage of the applied load, as much as 26.7% of the total moment on the bridge section.

Table 6.2: Example Bridge 2 Analysis Results (Non-Composite)

	Vehicle	Vehicle Type	Lane Used	M _{max} Line Girder (k-in)	Max. M Location		
Run 6	HS 20	Design	Design	-5640	Interior Support		
Run 7	HS 20	Design	Design	7716	25' from End		
Run 8	Veh. #87	Overload	Travel	13284	Midspan 75' Span		
Run 9	Veh. #203	Superheavy	Center	28212	26' from End		
Run 10	Veh. #203	Superheavy	Center	-41856	Interior Support		
All Moments listed in (kip-inches)							
	Girder	M _{Total}	M _{Girder}	M _{Slab}	Girder M%	Slab M%	LLDF
Run 6	1	164.8	158.0	6.8	95.9	4.1	0.028
	2	812.4	785.0	27.4	96.6	3.4	0.137
	3	1873.3	1813.0	60.3	96.8	3.2	0.316
	4	2879.1	2787.0	91.6	96.8	3.2	0.487
	<i>Sum</i>	<i>5729.5</i>	<i>5543.5</i>	<i>186.0</i>	<i>96.8</i>	<i>3.2</i>	<i>0.968</i>
Run 7	1	33.3	31.0	2.3	93.0	7.0	0.004
	2	1085.7	1051.0	34.7	96.8	3.2	0.137
	3	2681.9	2562.5	119.4	95.5	4.5	0.333
	4	3890.5	3740.5	150.0	96.1	3.9	0.486
	<i>Sum</i>	<i>7691.4</i>	<i>7385.0</i>	<i>306.4</i>	<i>96.0</i>	<i>4.0</i>	<i>0.960</i>
Run 8	1	669.5	648.0	21.5	96.8	3.2	0.049
	2	2466.7	2379.0	87.7	96.4	3.6	0.180
	3	4181.9	4019.5	162.4	96.1	3.9	0.304
	4	5901.0	5686.0	215.0	96.4	3.6	0.430
	<i>Sum</i>	<i>13219</i>	<i>12733</i>	<i>486.6</i>	<i>96.3</i>	<i>3.7</i>	<i>0.963</i>
Run 9	1	6821.0	6573.5	247.5	96.4	3.6	0.237
	2	7050.5	6753.5	297.0	95.8	4.2	0.243
	3	7050.5	6753.5	297.0	95.8	4.2	0.243
	4	8621.0	6573.5	247.5	96.4	3.6	0.237
	<i>Sum</i>	<i>27743</i>	<i>26654</i>	<i>1088.9</i>	<i>96.1</i>	<i>3.9</i>	<i>0.960</i>
Run 10	1	9358.1	9088.0	270.1	97.1	2.9	0.218
	2	11487.6	11133.5	354.1	96.9	3.1	0.267
	3	11487.6	11133.5	354.1	96.9	3.1	0.267
	4	9358.1	9088.0	270.1	97.1	2.9	0.218
	<i>Sum</i>	<i>41691</i>	<i>40443</i>	<i>1248.4</i>	<i>97.0</i>	<i>3.0</i>	<i>0.970</i>

6.3. LLDF AND SLAB MOMENT RESULTS FOR EXAMPLE BRIDGE 3 (RUNS 11 THROUGH 15)

This section presents the analysis results obtained analyzing Example Bridge 3. This structure is a 180-foot, two-span continuous composite girder bridge consisting of two 90-foot spans. This bridge was designed according to the AASHTO LRFD Specifications. See Table 1.1 and Figure 1.4 for more detailed Example Bridge 3 layout information. Table 5.1 lists the figures that diagram the vehicle locations for each run made on Example Bridge 3 (Runs 11 through 15). Some vehicle location information and all analysis results are listed in Table 6.3.

One difference that is noticed when looking at the results of runs on Example Bridge 3 is that the percentage of total moment resistance offered by the girders has dropped from the range of 95% or more in the non-composite girders to between 31% and 39% in the composite girders. This means that the percentage of total moment resistance offered by the axial load couple (generated between the slab and girders) in the two-span continuous bridge ranges from around 58% to 66%. The slab moments in this two-span continuous structure range from 2.4% to 3.4%. The axial forces generated in the slab are much more important to the total moment capacity in composite girder construction than the bending action of the slab.

This two-span continuous structure is a wider bridge than both the simply supported and the three-span continuous structures, with a girder spacing of 10 feet rather than 8 feet. This means that under loads from the same vehicles, the bridge with the larger girder spacing should exhibit higher maximum LLDF's than the bridge with smaller girder spacing. This comes from the fact that as

girder spacing increases in a bridge layout, the distance from the applied load to the adjacent girders also increases. As these distances increase, the girders closest to the load must take a greater percentage of the total load because the load-sharing members are becoming farther away. This can be seen when comparing the LLDF's in Run 12 with Run 7. In Run 12, the larger girder spacing produces an exterior girder LLDF value of 0.52 while the smaller girder spacing of Run 7 only produces an exterior girder LLDF of 0.49. Both of these analyses are for an HS20 vehicle in a design lane (see Table 6.3). The maximum interior girder LLDF in Run 12 is 0.31, while in Run 7, the corresponding value is 0.33. This shows the greater amount of load sharing in the bridge with a smaller girder spacing, while in the bridge with the larger spacing, one girder is forced to take a higher percentage of the total load.

Runs 14 and 15 are also interesting to compare in Table 6.3 because the effects of a tractor load along with the trailer load it pulls are shown in the Run 15 results. In Run 14, all of the loads on the structure are trailer loads with a wide overall spacing. The LLDF's for Run 14 are very well balanced, showing a high degree of load sharing. In Run 15, however, the tractor and trailer are present on the structure simultaneously, allowing both narrow axles and wide axles to load the bridge slab. The maximum exterior girder moment LLDF in this case is 0.18. The maximum interior girder moment LLDF is 0.31, showing how a set of narrow axles can force the interior girders to take a higher percentage of their load. Typically, when these Superheavy vehicles are analyzed, the bridge spans are not long enough to accommodate both the tractor and the trailer. When the tractor is

off the structure during the point of maximum moment effect, the interior girders take approximately 25% of the total load. This percentage can increase to about 30% when the tractor is also present on the bridge slab.

Table 6.3: Example Bridge 3 Analysis Results (Composite)

	Vehicle	Vehicle Type	Lane Used	M_{\max} Line Girder (k-in)	Max. M Location			
Run 11	HS 20	Design	Design	13320	38' from End			
Run 12	HS 20	Design	Design	-8580	Interior Support			
Run 13	Veh. #87	Overload	Travel	22620	39' from End			
Run 14	Veh. #203	Superheavy	Center	56376	40' from End			
Run 15	Veh. #203	Superheavy	Center	-82020	Interior Support			
All Moments listed in (kip-inches)								
	Girder	M_{Total}	M_{Girder}	M_{Slab}	$P*e$	$(M_T - M_S)$	$M_S\%$	LLDF
Run 11	1	401.9	152.5	10.2	239	392	2.5	0.029
	2	1782.9	568.5	56.4	1158	1727	3.2	0.129
	3	4343.8	1344.5	176.2	2823	4168	4.1	0.311
	4	6881.9	2175.5	210.3	4496	6672	3.1	0.497
	<i>Sum</i>	<i>13411</i>	<i>4241.0</i>	<i>453.1</i>	<i>8716</i>	<i>12957</i>	<i>3.4</i>	<i>0.966</i>
Run 12	1	411.4	187.5	8.0	216	403	1.9	0.046
	2	912.4	358.5	34.0	520	878	3.7	0.101
	3	2778.1	1063.5	88.3	1626	2690	3.2	0.309
	4	4604.8	1798.5	113.6	2693	4491	2.5	0.516
	<i>Sum</i>	<i>8706.7</i>	<i>3408.0</i>	<i>243.9</i>	<i>5055</i>	<i>8462</i>	<i>2.8</i>	<i>0.972</i>
Run 13	1	1876.2	605.5	68.25	1202	1808	3.6	0.078
	2	4779.1	1469.5	133.54	3176	4646	2.8	0.201
	3	7309.5	2206.5	188.7	4914	7121	2.6	0.308
	4	9161.9	2936.5	239.3	5986	8923	2.6	0.386
	<i>Sum</i>	<i>23127</i>	<i>7218.0</i>	<i>629.8</i>	<i>15278</i>	<i>22498</i>	<i>2.7</i>	<i>0.973</i>
Run 14	1	13836	4482.5	361.5	8992	13475	2.6	0.235
	2	14885	4471.0	323.7	10090	14561	2.2	0.253
	3	14885	4471.0	323.7	10090	14561	2.2	0.253
	4	13836	4482.5	361.5	8992	13475	2.6	0.235
	<i>Sum</i>	<i>57442</i>	<i>17907</i>	<i>1370.5</i>	<i>38164</i>	<i>56072</i>	<i>2.4</i>	<i>0.976</i>
Run 15	1	15168	6151.5	351.6	8665	14816	2.3	0.183
	2	25389	9605.5	613.5	15170	24776	2.4	0.305
	3	25389	9605.5	613.5	15170	24776	2.4	0.305
	4	15168	6151.5	351.6	8665	14816	2.3	0.183
	<i>Sum</i>	<i>81112</i>	<i>31514</i>	<i>1930.3</i>	<i>47670</i>	<i>79184</i>	<i>2.4</i>	<i>0.976</i>

6.4. COMPARISON OF BRUFEM RESULTS WITH AASHTO AND TxDOT LLDF VALUES

Table 6.4 lists the maximum BRUFEM moment LLDF's calculated for exterior and interior girders along with the AASHTO Design LLDF's and the TxDOT Overload LLDF's. The BRUFEM LLDF's were significantly less than the LLDF's calculated from the AASHTO design equations. For comparison in this section, the smallest LLDF using the AASHTO and TxDOT LLDF factors are compared with the corresponding BRUFEM values. The TxDOT LLDF's were calculated by applying the TxDOT Reduction Factor to the AASHTO WSD and LRFD LLDF's.

For the non-composite condition, BRUFEM produced a LLDF value of 0.49 compared with the AASHTO value of 0.57 for a design truck in a design lane (Run 3). For the same design situation on a composite girder (Run 12), BRUFEM produced an exterior girder LLDF of 0.52, compared with the AASHTO method's 0.70. The composite girders consistently achieved the most load savings due these BRUFEM analyses when compared with all of the non-composite models. These reductions in LLDF values show the amount of conservatism present in the AASHTO design values and give a ballpark estimate of the load penalty exterior girders pay during the design process and during overload permitting procedures.

When trucks are moved from design lane locations to actual travel lane locations, even greater benefits are achieved from the BRUFEM analyses. During Run 2, the BRUFEM results reduced an AASHTO LLDF of 0.57 to 0.42, which is more than a 25% reduction. The benefits of being able to analyze an overloaded

vehicle in a travel lane versus a design lane allow an exterior girder to see significantly reduced load. Even when compared with the TxDOT Overload LLDF's, BRUFEM shows a useful level of benefit. In Run 4, an overload truck in a travel lane was analyzed, with the TxDOT Overload LLDF calculated at 0.55. The BRUFEM analysis reduced this value another 20% to 0.44. Run 13 analyzed an overload truck in a travel lane, and BRUFEM reduced the LLDF from 0.68 to 0.39 (a 43% reduction from the TxDOT Overload LLDF).

In general, the exterior girders see the most benefit from these BRUFEM finite element analyses. The interior girders do see benefits from BRUFEM analyses, however, the exterior girder design LLDF values overestimate the loads truly taken by the exterior girders to a greater degree. This trend is due to the AASHTO requirement of placing a design vehicle close to the edge of the slab, even when the actual travel lane is significantly closer to the centerline of the bridge.

Table 6.4: Interior and Exterior Girder LLDF Comparison

Run	Lane Used	M Sign	AASHTO Moment LLDF			TxDOT Reduced LLDF			BRUFEM Exterior Girder LLDF	BRUFEM Interior Girder LLDF
			WSD	Ext. LRFD	Int. LRFD	WSD	Ext. LRFD	Int. LRFD		
1	Travel	Pos.	0.57	0.63	0.45		N/A		0.41	0.34
2	Travel	Pos.	0.57	0.63	0.45		N/A		0.42	0.33
3	Design	Pos.	0.57	0.63	0.45		N/A		0.49	0.32
4	Travel	Pos.	0.57	0.63	0.45	0.55	0.61	0.44	0.44	0.32
5	Center	Pos.	0.57	0.63	0.45	0.36	0.40	0.29	0.24	0.25
6	Design	Neg.	0.57	0.63	0.41		N/A		0.49	0.32
7	Design	Pos.	0.57	0.63	0.41		N/A		0.49	0.33
8	Travel	Pos.	0.57	0.63	0.38	0.55	0.61	0.39	0.43	0.30
9	Center	Pos.	0.57	0.63	0.41	0.40	0.44	0.29	0.24	0.24
10	Center	Neg.	0.57	0.63	0.41	0.40	0.44	0.29	0.22	0.27
11	Design	Pos.	0.71	0.70	0.40		N/A		0.50	0.31
12	Design	Neg.	0.71	0.70	0.42		N/A		0.52	0.31
13	Travel	Pos.	0.71	0.70	0.40	0.69	0.68	0.39	0.39	0.31
14	Center	Pos.	0.71	0.70	0.40	0.50	0.49	0.28	0.24	0.25
15	Center	Neg.	0.71	0.70	0.42	0.50	0.49	0.28	0.18	0.31

Table 6.4 lists the BRUFEM moment LLDF's calculated for interior girders along with the AASHTO Design LLDF's and the TxDOT Overload LLDF's. The BRUFEM results reduced the LLDF produced by a design truck in a design lane from 0.41 to 0.33 on the non-composite girder model of Run 7. BRUFEM also reduced the AASHTO LRFD LLDF from 0.40 to 0.31 on the composite girder model of Run 11.

The TxDOT Overload LRFD LLDF's do a good job estimating the LLDF's when an overloaded or Superheavy vehicle travels down the centerline of a bridge in these examples. To illustrate this point, in Run 14, the TxDOT Overload LLDF is 0.28 and BRUFEM calculates a value of 0.25.

In general, the AASHTO WSD empirical equations overestimate the moment carried by the interior girders. The AASHTO LRFD LLDF values, after being reduced by the TxDOT Reduction Factor, can still be reduced at least another 20% by BRUFEM when the vehicles are located in actual travel lanes. This 20% value was calculated by finding the minimum difference between the AASHTO LRFD LLDF values and the BRUFEM results. In some runs, this value is greater than 20%, however, this 20% value is a conservative estimate that greatly decreases the estimated girder moments.

From the BRUFEM results presented here, the slab moment in bridges of span lengths varying from 50 to 80 feet can be estimated to be about 3% of the total applied vehicle moment. Girders in spans of less than 50 feet could see total applied moments reduced by higher percentages of moment being taken in the deck slab. This trend is not studied extensively in this research but has been

verified through field tests recently conducted on shorter bridge spans of these types in Texas. The moment taken by the slab reduces the moment taken by the girders, and this added capacity can become significant in shorter structures. Whether slab moments are considered during overload analysis or not, the benefits of performing a finite element analysis on a critical bridge structure are substantial.

An extensive study of the effects of 138 vehicles permitted in Texas was completed during this research program to help quantify a vehicle's potential for causing structure distress. The force effects generated by these permitted vehicles were compared to the force effects generated by various AASHTO design vehicles to get a quick estimate of the permitted vehicle's overload potential.

This information alone is not enough to predict whether a certain bridge structure's components will experience distress from a permitted vehicle. This overload potential must be combined with a bridge's characteristics to quantify the stress levels in each of the bridge's critical elements. This research shows that many permitted vehicles produce moment effects on typical Texas bridges that are many times the moment effects produced by AASHTO design vehicles. This research also confirms the level of LLDF reduction that exists for any bridge previously analyzed using AASHTO-based design equations alone. Accurately estimating the LLDF values in a bridge structure can reduce the overload potential shown from line-girder analyses of permitted vehicles. Performing BRUFEM analyses improves a bridge's rating due to more accurate load assessment during permitting procedures.

6.5 USING SAP2000 OUTPUT AND BRUFEM RESULTS TO CALCULATE A BRIDGE RATING

This section describes a method for calculating a bridge rating using the programs presented in this research, BRUFEM and SAP2000. The purpose of this research is to calculate more accurate bridge ratings using advanced analysis techniques. Simply performing a line-girder analysis using SAP2000 does not give the analyst enough information to rate a bridge. The bridge rating is also a function of the transverse location of this vehicle on the bridge deck. Modeling this location accurately can drastically reduce the maximum moment values reported in critical bridge girders.

An example of the rating procedure can be demonstrated using Run 4 on the 50-foot simply supported non-composite bridge (Example Bridge 1). See Table 5.1 for the locations of the Figures that describe the longitudinal and transverse locations of the TxDOT Overload Database Vehicle #18. The maximum line-girder moment produced by this permit vehicle is 1092 kip-ft on this simple span. An AASHTO HS-20 design vehicle produces a maximum line-girder moment value of 628 kip-ft on the same structure. As defined in Equation 3.3, the maximum HS20 Moment Ratio for this vehicle on this bridge is 1.74. This relationship is also shown in Equation 6.1.

$$HS20 MR = \frac{1092 \text{ k-ft}}{628 \text{ k-ft}} = 1.74 \quad (6.1)$$

Assuming this simple span bridge was designed for an HS20 vehicle load, the analyst quickly knows that this vehicle (Vehicle Record #18) has the potential of overstressing some elements of this bridge. However, the analyst also knows that this potential for overstress may be decreased by favorably positioning the vehicle in the transverse direction. During Run 4, Vehicle Record #18 was analyzed in the bridge's travel lane. This research has shown that analyzing a vehicle in its travel lane versus its design lane significantly reduces the maximum moment effects it produces in girders. The vehicle loads are spread more evenly when analyses are performed using the travel lane, and this helps improve the bridge rating.

The moment in a critical girder can be calculated using BRUFEM's output. From Table 6.4, the maximum LLDF value reported from BRUFEM for Run 4 is 0.44 for the exterior girder. Multiplying this LLDF by the permit vehicle's maximum line-girder moment represents the moment present in the exterior girder under this vehicle's load. Equation 6.2 illustrates this calculation.

$$M_{ACTUAL} = (LLDF_{BRUFEM}) \cdot (M_{LG}) = 480 \text{ k} - \text{ft} \quad (6.2)$$

The design moment for this girder, assuming the normal AASHTO WSD design procedure for a single lane was followed, is shown in Equation 6.3. In this calculation, the AASHTO HS20 vehicle's maximum line-girder moment is multiplied by the AASHTO WSD LLDF value.

$$M_{DESIGN} = (LLDF_{AASHTO}) \cdot (HS20 M_{LG}) = 358 \text{ ft} - k \quad (6.3)$$

In order to calculate the girder's rating under the permit vehicle load, the ratio of the actual moment to the design moment must be calculated. If this value is less than 1.0, the girder is resisting less than the moment required by design. If this ratio is greater than 1.0, the girder is resisting more than the moment required by design and may experience distress under this vehicle load. Equation 6.4 illustrates this calculation.

$$Girder \text{ Rating} = \left(\frac{M_{ACTUAL}}{M_{DESIGN}} \right) = \frac{480 \text{ ft} - k}{358 \text{ ft} - k} = 1.34 \quad (6.4)$$

In this case, the permit vehicle in question produces a 34% overstress condition in the exterior girder when traveling in the striped travel lane of the bridge. This 34% overstress is quite a reduction from the HS20 Moment Ratio overstress potential of 74%. The 34% overstress value could also be reduced further by analyzing the bridge with this vehicle traveling closer to the centerline of the bridge, if this travel position is possible on the road.

Equation 6.5 illustrates how to use the permit vehicle's maximum Moment Ratio values to directly calculate a Girder Rating using the BRUFEM and AASHTO LLDF values.

$$Girder \text{ Rating} = \frac{M_{ACTUAL}}{M_{DESIGN}} = \left(\frac{LLDF_{BRUFEM}}{LLDF_{AASHTO}} \right) \cdot (Max. MR) \quad (6.5)$$

This process shows the most efficient use of both the BRUFEM LLDF values and the SAP2000 line-girder analysis results and maximum Moment Ratios. These bridge ratings can only be calculated knowing the methods used to design a structure. Bridge ratings could be calculated for many combinations of the AASHTO design vehicles and the WSD and LRFD versions of the AASHTO Design Specifications. The purpose of this section was to show the reduction of the line-girder overstress potential through BRUFEM LLDF analysis. For this simple example, the overstress percentage was reduced from 74% (the line-girder analysis) to 34%. These results show the benefits of performing the maximum Moment Ratio analyses along with the BRUFEM finite element studies.

CHAPTER 7

CONCLUSIONS AND RECOMMENDATIONS

This research was successful in showing the benefits of performing finite element analyses to better estimate the Lateral Load Distribution Factors that are critical for bridge rating. This work also shows the degree to which AASHTO design LLDF's and TxDOT Overload LLDF's can be reduced. Performing a finite element analysis can significantly improve the rating of a bridge structure by simply offering better estimates of how loads are shared by each girder. Rather than using empirical design relationships and worst-case truck position scenarios, finite element analysis offers the flexibility of analyzing the structure under the actual live loads it will likely encounter due to uncommon vehicles.

Chapter 6 shows that simply modeling loads in their true positions using a finite element analysis can reduce the maximum load capacity estimates significantly throughout the structure, especially in the exterior girders. Also, the capacity of the slab, which is ignored during design and when using the AASHTO LLDF equations, can be modeled and considered effective when completing a finite element analysis. Considering the slab as effective adds a significant percentage of load-carrying capacity to short-span bridge structures but can also add small percentages of capacity to long-span bridge structures.

Also important to this research was testing the programs SAP2000 and BRUFEM to see if they could be effective in providing an analyst the necessary

tools to complete such analyses in a timely manner. There is no question these programs can be used effectively, even though some improvements would make each better suited for these analyses. Using the AASHTO design equations or the TxDOT Overload LLDF reduction of these values is not taking advantage of the full capacity of the critical bridges in Texas, as shown in Chapter 6.

7.1. TRENDS IN LLDF COMPARISONS

The exterior girders of bridge structures are penalized when the AASHTO design LLDF's are calculated. This is due in part to code conservatism, but is also due to modeling unlikely load positions. During design, these extreme cases must be considered, but for permitting purposes, load positions can be accurately controlled to a degree that does not warrant penalizing the structure for load conditions it will not see. This research shows that analyzing a structure under actual load positions creates more load sharing among the girders, relieving the exterior girder of applied moment to a noticeable degree. The AASHTO design approaches tend to be less conservative with regard to the interior girders. Also, when overload or Superheavy vehicles travel along the centerline of the bridge, the interior girders often take the majority of the load.

This research shows the importance of the truck gage or rear axle width on the load-sharing capabilities of bridge girders. The wider the truck axle width, the better the load is distributed across the girders. Also important is the relationship between the girder spacing and truck width. When a truck is placed on a bridge structure with a wide girder spacing, the girders nearest the load are forced to take

a greater percentage of the load than if the girders were spaced more closely. Of course, increasing the truck axle width also promotes equal load sharing among the bridge girders. It was also found that when a tractor and a trailer of a wide overload vehicle are simultaneously on a bridge deck, the interior girders take the greatest percentage of the load when the vehicle is placed at the centerline of the bridge. For most common load positions, however, the exterior girder does take the highest percentage of girder moment.

It is difficult to develop general equations or rules to allow analysts an instant means of calculating LLDF's due to each bridge's unique characteristics. This research is not in-depth enough to develop these types of relationships, however, it does show where the capacity is "hidden" in these types of bridge structures. Section 6.5 shows the bridge rating procedures possible using SAP2000 and BRUFEM output.

It is recommended that analysts consider the slab's moment capacity, as shown by these results to be significant. The total slab moment capacity can be considered to be equal at each location across a section of the bridge structure, thus reducing the moments required to be taken by the each girder equally. Factors of safety should also be added to the finite element results generated by BRUFEM at the engineer's discretion. Most importantly, the permitting body should seriously consider the placement of loads in the positions that engage the most girders as possible to promote load sharing and to eliminate load "hot spots".

In order to encourage timesaving features into the finite element analysis load rating process, building a BRUFEM database of typical Texas bridge layouts would be a first step to improving the permitting procedures. BRUFEM analysis models are more difficult to create than to edit, and having a database of common bridge layouts would allow an analyst the opportunity to model a critical bridge structure by editing a bridge model from this database. Building a database of common truck layouts that classify as Overloads or Superheavy vehicles may also be useful to allow an analyst a quick approach to estimating a bridge's load response.

The procedure shown in Chapter 5 for calculating the LLDF's from BRUFEM output is also recommended rather than simply applying the numbers from BRUFEM's post-processor. Using the values from the BRUFEM "Brate.out" file increases the calculated load effects when diaphragms are present in the structure. The BRUFEM User's Manual should be read describing the calculation technique used for both composite and non-composite girder models before using the program for rating purposes.

7.2. RECOMMENDATIONS FOR USING SAP2000 AND BRUFEM FOR BRIDGE RATING

SAP2000 is well suited to performing line-girder analyses to calculate the maximum force effects created on a model due to vehicle loads. The pre-processor offers a great deal of flexibility when it comes to modeling uncommon truck layouts. Also, the interface with the user is easy to understand and allows for quick data entry of truck information. The steps for performing an analysis

are relatively easy to grasp and a tutorial example is listed in Appendix A. SAP2000 would also be the ideal finite element program to use for the LLDF calculations except it lacks the bridge model generation template BRUFEM employs. BRUFEM's pre-processor added to SAP2000's graphical user interface environment would make an ideal bridge rating program. BRUFEM's pre-processor is what makes this whole process feasible time-wise. The user does not have to be well versed in finite element modeling techniques to quickly generate a useful model that will give the desired analysis results. Some cumbersome features of BRUFEM include the lack of a high-quality graphics based post-processor, the low limit of elements and nodes available to the user, and the input files required to model uncommon trucks and varying bridge girder properties. The program does execute quickly, and with some practice, can be very useful for studying the LLDF's of many types of bridge structures.

7.3: TEXAS PERMIT TRUCK DATABASE

Chapter 2 describes the 138 Texas permit vehicles studied during this research. Tremendous variety exists among these vehicle records as shown in Table 2.1. The overload potential of these trucks is discussed, along with the line-girder analysis technique, in Chapter 3. By studying the statistics presented in Table 2.1, it is easy to see the difficulty faced by state DOT's when it comes to bridge rating. State DOT's will benefit financially by utilizing the finite element analysis technology available to them to increase the ratings of the bridges affected daily by these types of vehicle overloads. At this time, the methods

described within this report are the best tools available to develop the most accurate assessment of the damage potential caused by these permit vehicles.

In conclusion, the line-girder analysis technique, partnered with BRUFEM's finite element analysis capabilities can prove to be very powerful tools to a bridge analyst. This research uncovers the benefits of using both of these methods to get better estimates of the overload potential that exists due to overloaded vehicles and aging bridge structures. These methods can be used in an office environment to both extend the service lives of many bridges deemed inadequate for heavy loads under AASHTO provisions and provide more efficient overloaded vehicle routes across the state of Texas.

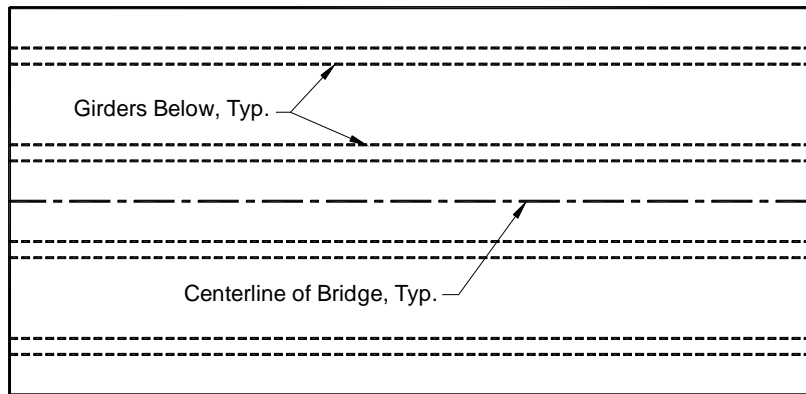
APPENDIX A

PERFORMING A LINE-GIRDER ANALYSIS USING SAP2000

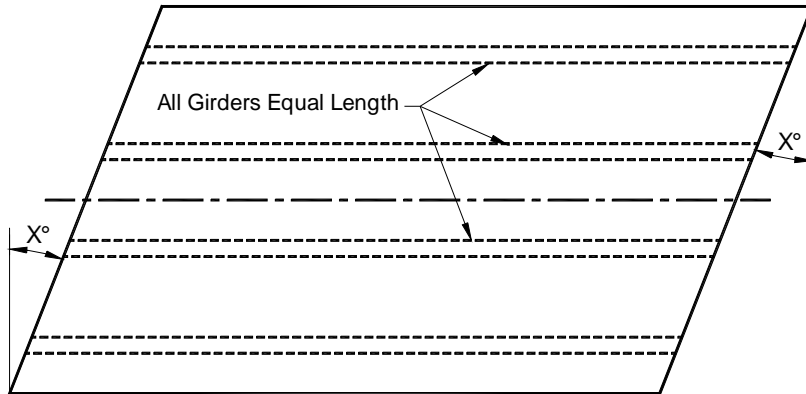
This appendix assumes the bridge analyst has never been exposed to the SAP2000 bridge analysis techniques and will give a step-by-step procedure for performing a line-girder analysis. It is assumed that the user is familiar with the use of some type of finite-element software, even if it is not SAP2000. The SAP2000 User's Guide is a helpful reference for explaining the program's layout and for gaining confidence while using the graphical user interface for pre-processing.^[6] This list serves only as a guide to line-girder analysis and assumes the user has been exposed to the basics of running the program, such as how to generate a model using the pre-processor, and how to view the model on-screen.

This example will describe the procedure of completing a line-girder analysis of a 100-foot simple span structure. Two vehicles will be analyzed, one a SAP2000 Standard Vehicle, the AASHTO HS20-44, and the other a user-defined AASHTO HS20-44. This will let the user check the results of the SAP2000 Standard Vehicle Database by comparing those results with the user-defined vehicle results. The user-defined vehicle and SAP2000 Standard Vehicle input techniques are best illustrated by completing both and comparing results. Figure A.1 illustrates three types of bridge structures that can be analyzed using line-girder techniques. This thesis deals with the right-girder bridge primarily, however, since constant skew bridges contain girders of equal

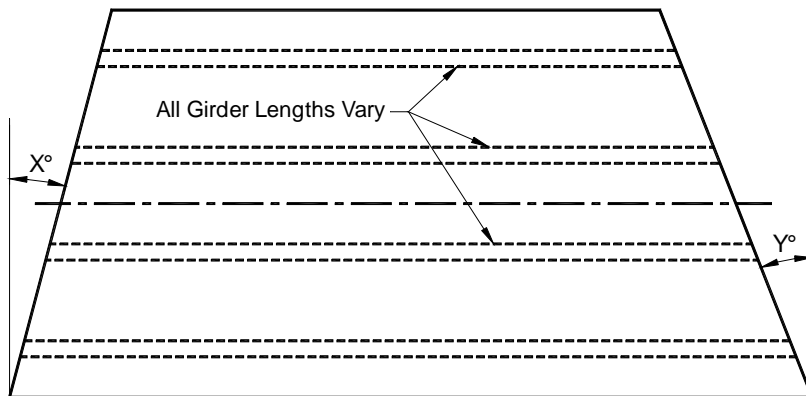
lengths, these can also be modeled using a line-girder analysis. When variable-skew bridges are encountered, it may be wise to complete line-girder analyses for both the shortest and the longest girders of the bridge, to get the force effect extremes that could occur due to a specific truck loading.



Right Girder Bridge Plan View



Constant Skew Bridge Plan View



Variable Skew Bridge Plan View

Figure A.1: Three Non-Curved Bridge Layout Classifications

The steps for inputting and analyzing a line girder structure using SAP2000 are as follows:

1. To begin the line-girder analysis using SAP2000, launch the program. Once the program has started, look in the lower right hand corner where the units are displayed. We will use units of “kip-ft” in this example. Open a new file by selecting “File...New Model from Template”. From the menu, select the Beam Template (in the upper left). Enter “1” for the number of spans, and “100” for Span Length. Also make sure the boxes next to both “Restraints” and “Gridlines” are checked. Click “OK”.
2. The line-girder should appear in the two on-screen views. The origin of the coordinate system will be located at the centerline of the span. This can be changed if desired, but it is not important in this example. All results will be listed at distances along the structure, not referenced to the global coordinate system. The default supports created by SAP2000 when using the Beam Template are one pinned joint to restrain horizontal and vertical movements, and rollers at every other joint to restrain vertical movement only. The left support in this example will be pinned by default and the right support will be the roller.

3. Use the cursor to select the frame element. Since the beam cross-section in this example is constant throughout the length of the members, it is not necessary to redefine the default cross-sectional properties. If the beam did vary in cross-sectional properties, extra nodes would have to be added at the cross-section points of variance, and section sizes defined at each location to model the relative beam section stiffnesses correctly. With the frame element still selected, click on “Assign...Frame...Output Segments”. The SAP2000 User’s Manual suggests adding output segments rather than nodes to save time during analysis. These output segments allow the user to read force and/or deflection information directly without adding new nodes to the structure. Choose 100 output segments for this example. Click “OK”.

4. Now select “Define...Moving Load Cases...Lanes”. Click on “Add New Lane”. Leave the default Lane Name as “LANE1”. This value would have to be renamed if more than one truck lane was desired on the structure. Since this is only a two-dimensional model, there is no need to add more than one lane with zero eccentricity. With “Frame 1, Eccentricity 0” in the text boxes, select “Add”. This will now appear in the gray area below. Select “OK”, twice.

5. To define the SAP2000 Standard Vehicle, select “Define...Moving Load Cases...Vehicles”. Click on “Add Standard Vehicle” in the upper right. We need to add the AASHTO HS20-44 vehicle, so find and click on the “HSn-44” designation from the pulldown menu named Vehicle Type. Input a Scale Factor of 20, designating an HS20-44. Click “OK”.

6. To define the AASHTO HS20-44 truck designation as a general vehicle, select “Add General Vehicle”. Change the vehicle name to “GENHS20”. Change the first axle load to 8. Now look down below in the table titled, Intermediate Loads. Leave the Uniform field as 0, but change the Axle value to 32. Also change both the Min. Distance and Max. Distance fields to 14. Select “Add”. This is done because the middle axle of the HS20-44 is fixed at 14 feet from the front axle. Now both the leading axle and the second axle have been input. To input the rear axle, leave the Axle value at 32. Leave the Min. Distance field at 14. Change the Max. Distance field to 30. Select “Add”. This is done to correctly model the rear floating axle position of the HS20-44 truck. The two intermediate axle’s information will be shown below. If the information is incorrect, highlight the incorrect record, change the data, and click “Modify”. If the data is correct, click “OK”, twice.

7. The next step in the input process is to define a Vehicle Class. To do this, select “Define...Moving Load Cases...Vehicle Classes”. Click on “Add Class”. Insert “STDHS20” in the Vehicle Class Name field. Select “HSn441”, with a Scale Factor equal to 1. Select “Add”. Click “OK”. Click on “Add Class”. Change the Vehicle Class Name to “GENHS20”. Under Vehicle Name, select “GENHS20”, Scale Factor equal to 1, and select “Add”. Click “OK” twice.
8. For information only: Each vehicle must be placed into a separate Vehicle Class in this example since SAP2000 generates force effect envelopes for Vehicle Classes only. SAP2000 will analyze all vehicles within each Vehicle Class and generate output for the maximum effects caused by all vehicles within the class combined. No information is given for each individual vehicle, unless each individual vehicle is defined as its own Vehicle Class. In our example, we want to examine the effects of each single vehicle, so this approach must be taken.
9. The next step in the line-girder analysis is to select “Define...Moving Load Cases...Bridge Responses”. Click on both “Reactions” and “Frame Forces”. The word “All” should be visible in the boxes to the right of each of these selections, meaning all

elements in the model are requested to have this output generated by SAP2000. When more complex models are created, the user can define element sets by name and request output only for these element sets. Make sure the “Method of Calculation” area is marked “Exact”. Select “OK”.

10. To continue, select “Define...Moving Load Cases...Moving Load Cases”. Click on “Add Load”. Change the Moving Load Case Name field to “STDHS20”. Leave the Number of Lanes equal to 1 and the Scale Factor equal to 1. Go below and click on “Add Assign”. Select the Vehicle Class as “STDHS20”. Leave the Scale Factor equal to 1. Set the Minimum Number of Loaded Lanes equal to 0, and set the Maximum Number of Loaded Lanes equal to 1. Go below and highlight “LANE1” and click “Add”. “LANE1” should now appear in the “Selected Lanes” field. Click “OK” twice.

11. To continue, select “Add Load”. Change the Moving Load Case Name field to “GENHS20”. Leave the Number of Lanes equal to 1 and the Scale Factor equal to 1. Go below and click on “Add Assign”. Select the Vehicle Class as “GENHS20”. Leave the Scale Factor equal to 1. Set the Minimum Number of Loaded Lanes equal to 0, and set the Maximum Number of Loaded Lanes equal to 1. Go

below and highlight “LANE1” and click “Add”. “LANE1” should now appear in the “Selected Lanes” field. Click “OK” three times.

12. At this point, the model has been created and it is now ready to be analyzed using SAP2000. Click on the “Run Analysis” Icon. Save the file as “EXAMPLE1.SDB”, or any other suitable name. The program will be executing its analysis once this file name has been entered. When the analysis is complete, the analysis window will prompt the user with an “OK” button. Click on “OK”. A deformed shape will show in the 3-D view. This deformed shape is due to the member self-weight. It is not important for our analysis. Select “Display...Set Output Table Mode...GENHS20 Moving Load”. Click “OK”. While pointing the cursor at the frame element, right-click the mouse. Analysis output tables will appear, showing the results at the various output segments in the units displayed in the bottom right hand corner of the screen (kip-ft). Print these results. Repeat this procedure for the “STDHS20” designation by selecting “Display...Set Output Table Mode...STDHS20 Moving Load” and continuing. Both sets of printed tables should now be available for comparison.

13. The results tables generated by SAP2000 show the File Name at the top of the tables, along with the selected units and the Moving Load

Case requested. The most important columns in these Frame Element Forces tables are the “V2” column and the “M3” column. These columns represent the maximum and minimum internal shear and moment envelope values, respectively, in our line-girder. Corresponding locations along the structure for each envelope value are also given for reference. This concludes the line-girder analysis.

14. It should be noted that the tables of output for both the “STDHS20” designation and the “GENHS20” designation should be identical. If these results tables are not identical, there has been an error during the model input stage. The maximum moment generated by the HS20 vehicle on a 100-ft simple span is 1523.8 kip-ft. The locations listed by SAP2000 corresponding to these maximum internal moments are 48 feet and 52 feet along the structure. These locations match the location of maximum moment effects shown in Figure 3.1, when determined by the rules of statics. The reason SAP2000 shows two locations where these maximums occur is due to fact that the program runs each vehicle across the structure in both directions. What is important to notice is the fact the maximum moment value is correct, as well as the location where this maximum moment occurs. The maximum shear of 65.3 kips occurs at a support, when all three of the vehicle’s axles are on the structure, and the rear 32-kip axle is directly above the support.

This position and the shear values along the structure are illustrated in Figure A.2.

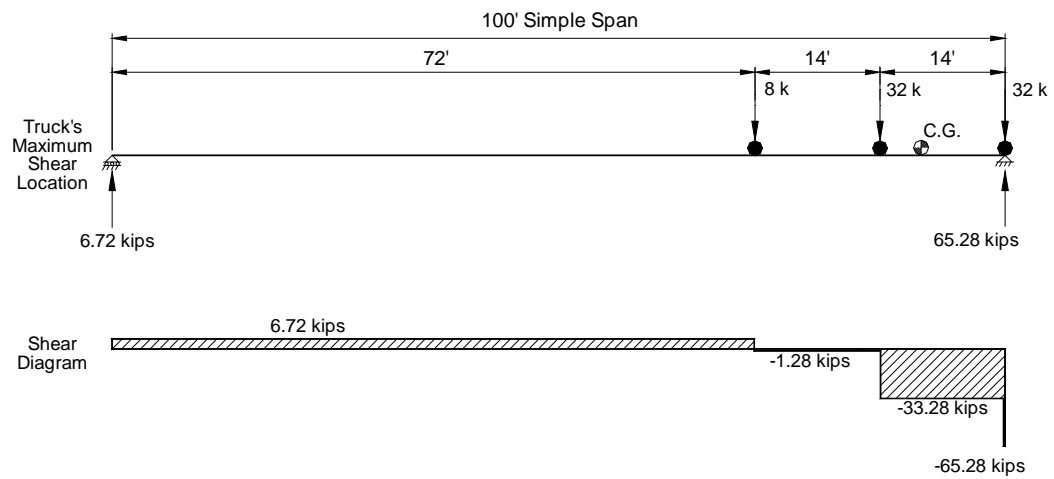


Figure A.2: Loading and Shear Diagrams for HS-20 Truck at Critical Shear Location on a 100-Foot Simple Span

APPENDIX B

BRUFEM INPUT FILES

This appendix lists the “History.pre” files for each of the 15 BRUFEM runs made for this research. The “History.pre” files are used to echo the user interactive input required while running the BRUFEMNT pre-processor. Also included are the “Bar.dat” files required to model Example Bridges 2 and 3, along with the “Veh.dat” files to model the non-standard vehicles where required.

B.1. “HISTORY.PRE” FILES FOR ALL BRUFEM RUNS

B.1.1. “History.pre” File for BRUFEM Run #1:

```
BEGIN_HISTORY_FILE
-----<PROBLEM_TITLE>-----
EX. BR. 1 - H20 IN TRAVEL LANE
-----<BRIDGE_TYPE_IBTYPE>-----
STL
-----<TYPE_OF_UNITS>-----
1
-----<VARIABLE/CONSTANT_SKEW>-----
1
-----<PRIS_NONPRIS_IXSECT>-----
1
-----<STL_BASIC_MODEL_DATA>-----
4
8
0
-----<ANALYSIS_TYPE_FULL/LIVE>-----
1
-----<COMPOSITE_MODEL_TYPE>-----
1
-----<SLAB_THICK_STRENGTH>-----
6.5
3
-----<STL_PLATE_COUNT>-----
3
-----<STL_PLATE_B_&_H>-----
11.535
0.96
-----<STL_PLATE_B_&_H>-----
0.605
```

```

31.38
-----<STL_PLATE_B_&_H>-----
11.535
0.96
-----<BASIC_SLAB_THICK>-----
6.5
-----<NUM_ELEM_BTWN_GIRD>-----
4
-----<NUM_SPANS>-----
1
-----<SPAN_LEN_&_NUM_Y_ELEMS>-----
50 50
-----<STL_DIA_TYPE>-----
2
-----<STL_DIA_CROSS_&_BTM_AREA>-----
3.05
3.05
-----<STL_DIA_TOP_&_BTM_DIST>-----
0.5
2
-----<ADDED_DIA_YESNO>-----
Y
-----<ADDED_DIA_COUNT>-----
3
-----<ADDED_DIA_DIST>-----
12.5
25
37.5
-----<EXTRA_MEMBERS_YESNO>-----
N
-----<LEFT_EDGE_WIDTH_&_COUNT>-----
3.583
3
-----<RIGHT_EDGE_WIDTH_&_COUNT>-----
3.583
3
-----<TRAVEL_CLEARANCE_L_&_R>-----
1.5
1.5
-----<VEH_LOAD_GROUP_01_YESNO>-----
Y
-----<VEH_INPUT_FILE_INTER>-----
I
-----<VEH_NUM_VEHICLES_ON_BRIDGE>-----
1
-----<VEH_STANDARD_VEHICLE_YESNO>-----
Y
-----<VEHICLE_DATA_BASE>-----
1
-----<VEH_STANDARD_VEHICLE_TYPE>-----
H20
-----<VEH_POSITION_METHOD>-----
1
-----<VEH_POSITION_FWD/REV_X_Y>-----
F 218 451
-----<LANE_LOAD_DESC_YESNO>-----
N
-----<LANE_LOAD_COUNT>-----
0
-----<MORE_LIVE_LOADS_01_YESNO>-----
N
-----<FEM_OUTPUT_QUANTITY>-----

```

```
1
-----<GRAPHICS_PLOTTING_YESNO>-----
Y
END_HISTORY_FILE
```

B.1.2. "History.pre" File for BRUFEM Run #2:

```
BEGIN_HISTORY_FILE
-----<PROBLEM_TITLE>-----
EX. BR. 1 - HS20 IN TRAVEL LANE
-----<BRIDGE_TYPE_IBTYPE>-----
STL
-----<TYPE_OF_UNITS>-----
1
-----<VARIABLE/CONSTANT_SKEW>-----
1
-----<PRIS_NONPRIS_IXSECT>-----
1
-----<STL_BASIC_MODEL_DATA>-----
4
8
0
-----<ANALYSIS_TYPE_FULL/LIVE>-----
1
-----<COMPOSITE_MODEL_TYPE>-----
1
-----<SLAB_THICK_STRENGTH>-----
6.5
3
-----<STL_PLATE_COUNT>-----
3
-----<STL_PLATE_B_&_H>-----
11.535
0.96
-----<STL_PLATE_B_&_H>-----
0.605
31.38
-----<STL_PLATE_B_&_H>-----
11.535
0.96
-----<BASIC_SLAB_THICK>-----
6.5
-----<NUM_ELEM_BTWN_GIRD>-----
4
-----<NUM_SPANS>-----
1
-----<SPAN_LEN_&_NUM_Y_ELEMS>-----
50 50
-----<STL_DIA_TYPE>-----
2
-----<STL_DIA_CROSS_&_BTM_AREA>-----
3.05
3.05
-----<STL_DIA_TOP_&_BTM_DIST>-----
0.5
2
-----<ADDED_DIA_YESNO>-----
Y
-----<ADDED_DIA_COUNT>-----
```

```

3
-----<ADDED_DIA_DIST>-----
12.5
25
37.5
-----<EXTRA_MEMBERS_YESNO>-----
N
-----<LEFT_EDGE_WIDTH_&_COUNT>-----
3.583
3
-----<RIGHT_EDGE_WIDTH_&_COUNT>-----
3.583
3
-----<TRAVEL_CLEARANCE_L_&_R>-----
1.5
1.5
-----<VEH_LOAD_GROUP_01_YESNO>-----
Y
-----<VEH_INPUT_FILE_INTER>-----
I
-----<VEH_NUM_VEHICLES_ON_BRIDGE>-----
1
-----<VEH_STANDARD_VEHICLE_YESNO>-----
Y
-----<VEHICLE_DATA_BASE>-----
1
-----<VEH_STANDARD_VEHICLE_TYPE>-----
HS20
-----<VEH_POSITION_METHOD>-----
1
-----<VEH_POSITION_FWD/REV_X_Y>-----
F 218 496
-----<LANE_LOAD_DESC_YESNO>-----
N
-----<LANE_LOAD_COUNT>-----
0
-----<MORE_LIVE_LOADS_01_YESNO>-----
N
-----<FEM_OUTPUT_QUANTITY>-----
1
-----<GRAPHICS_PLOTTING_YESNO>-----
Y
END_HISTORY_FILE

```

B.1.3. “History.pre” File for BRUFEM Run #3:

```

BEGIN_HISTORY_FILE
-----<PROBLEM_TITLE>-----
EX. BR. 1 - HS20 IN DESIGN LANE
-----<BRIDGE_TYPE_IBTYPE>-----
STL
-----<TYPE_OF_UNITS>-----
1
-----<VARIABLE/CONSTANT_SKEW>-----
1
-----<PRIS_NONPRIS_IXSECT>-----
1
-----<STL_BASIC_MODEL_DATA>-----
4

```



```

8
0
-----<ANALYSIS_TYPE_FULL/LIVE>-----
1
-----<COMPOSITE_MODEL_TYPE>-----
1
-----<SLAB_THICK_STRENGTH>-----
6.5
3
-----<STL_PLATE_COUNT>-----
3
-----<STL_PLATE_B_&_H>-----
11.535
0.96
-----<STL_PLATE_B_&_H>-----
0.605
31.38
-----<STL_PLATE_B_&_H>-----
11.535
0.96
-----<BASIC_SLAB_THICK>-----
6.5
-----<NUM_ELEM_BTWN_GIRD>-----
4
-----<NUM_SPANS>-----
1
-----<SPAN_LEN_&_NUM_Y_ELEMS>-----
50 50
-----<STL_DIA_TYPE>-----
2
-----<STL_DIA_CROSS_&_BTM_AREA>-----
3.05
3.05
-----<STL_DIA_TOP_&_BTM_DIST>-----
0.5
2
-----<ADDED_DIA_YESNO>-----
Y
-----<ADDED_DIA_COUNT>-----
3
-----<ADDED_DIA_DIST>-----
12.5
25
37.5
-----<EXTRA_MEMBERS_YESNO>-----
N
-----<LEFT_EDGE_WIDTH_&_COUNT>-----
3.583
3
-----<RIGHT_EDGE_WIDTH_&_COUNT>-----
3.583
3
-----<TRAVEL_CLEARANCE_L_&_R>-----
1.5
1.5
-----<VEH_LOAD_GROUP_01_YESNO>-----
Y
-----<VEH_INPUT_FILE_INTER>-----
I
-----<VEH_NUM_VEHICLES_ON_BRIDGE>-----
1
-----<VEH_STANDARD_VEHICLE_YESNO>-----

```

```

Y
-----<VEHICLE_DATA_BASE>-----
1
-----<VEH_STANDARD_VEHICLE_TYPE>-----
HS20
-----<VEH_POSITION_METHOD>-----
1
-----<VEH_POSITION_FWD/REV_X_Y>-----
F 244.5 496
-----<LANE_LOAD_DESC_YESNO>-----
N
-----<LANE_LOAD_COUNT>-----
0
-----<MORE_LIVE_LOADS_01_YESNO>-----
N
-----<FEM_OUTPUT_QUANTITY>-----
1
-----<GRAPHICS_PLOTTING_YESNO>-----
Y
END_HISTORY_FILE

```

B.1.4. “History.pre” File for BRUFEM Run #4:

```

BEGIN_HISTORY_FILE
-----<PROBLEM_TITLE>-----
EX. BR. 1 - VEHICLE RECORD 18 IN TRAVEL LANE
-----<BRIDGE_TYPE_IBTYPE>-----
STL
-----<TYPE_OF_UNITS>-----
1
-----<VARIABLE/CONSTANT_SKEW>-----
1
-----<PRIS_NONPRIS_IXSECT>-----
1
-----<STL_BASIC_MODEL_DATA>-----
4
8
0
-----<ANALYSIS_TYPE_FULL/LIVE>-----
1
-----<COMPOSITE_MODEL_TYPE>-----
1
-----<SLAB_THICK_STRENGTH>-----
6.5
3
-----<STL_PLATE_COUNT>-----
3
-----<STL_PLATE_B_&_H>-----
11.535
0.96
-----<STL_PLATE_B_&_H>-----
0.605
31.38
-----<STL_PLATE_B_&_H>-----
11.535
0.96
-----<BASIC_SLAB_THICK>-----
6.5
-----<NUM_ELEM_BTWN_GIRD>-----

```

```

4
-----<NUM_SPANS>-----
1
-----<SPAN_LEN_&_NUM_Y_ELEMS>-----
50 50
-----<STL_DIA_TYPE>-----
2
-----<STL_DIA_CROSS_&_BTM_AREA>-----
3.05
3.05
-----<STL_DIA_TOP_&_BTM_DIST>-----
0.5
2
-----<ADDED_DIA_YESNO>-----
Y
-----<ADDED_DIA_COUNT>-----
3
-----<ADDED_DIA_DIST>-----
12.5
25
37.5
-----<EXTRA_MEMBERS_YESNO>-----
N
-----<LEFT_EDGE_WIDTH_&_COUNT>-----
3.583
3
-----<RIGHT_EDGE_WIDTH_&_COUNT>-----
3.583
3
-----<TRAVEL_CLEARANCE_L_&_R>-----
1.5
1.5
-----<VEH_LOAD_GROUP_01_YESNO>-----
Y
-----<VEH_INPUT_FILE_INTER>-----
F
-----<VEH_POSITION_METHOD>-----
1
-----<VEH_POSITION_FWD/REV_X_Y>-----
F 222 444
-----<LANE_LOAD_DESC_YESNO>-----
N
-----<LANE_LOAD_COUNT>-----
0
-----<MORE_LIVE_LOADS_01_YESNO>-----
N
-----<FEM_OUTPUT_QUANTITY>-----
1
-----<GRAPHICS_PLOTTING_YESNO>-----
Y
END_HISTORY_FILE

```

B.1.5. “History.pre” File for BRUFEM Run #5:

```

BEGIN_HISTORY_FILE
-----<PROBLEM_TITLE>-----
EX. BR. 1 - VEHICLE RECORD 213 IN TRAVEL LANE
-----<BRIDGE_TYPE_IBTYPE>-----
STL

```

```

-----<TYPE_OF_UNITS>-----
1
-----<VARIABLE/CONSTANT_SKEW>-----
1
-----<PRIS_NONPRIS_IXSECT>-----
1
-----<STL_BASIC_MODEL_DATA>-----
4
8
0
-----<ANALYSIS_TYPE_FULL/LIVE>-----
1
-----<COMPOSITE_MODEL_TYPE>-----
1
-----<SLAB_THICK_STRENGTH>-----
6.5
3
-----<STL_PLATE_COUNT>-----
3
-----<STL_PLATE_B_&_H>-----
11.535
0.96
-----<STL_PLATE_B_&_H>-----
0.605
31.38
-----<STL_PLATE_B_&_H>-----
11.535
0.96
-----<BASIC_SLAB_THICK>-----
6.5
-----<NUM_ELEM_BTWN_GIRD>-----
4
-----<NUM_SPANS>-----
1
-----<SPAN_LEN_&_NUM_Y_ELEMS>-----
50 50
-----<STL_DIA_TYPE>-----
2
-----<STL_DIA_CROSS_&_BTM_AREA>-----
3.05
3.05
-----<STL_DIA_TOP_&_BTM_DIST>-----
0.5
2
-----<ADDED_DIA_YESNO>-----
Y
-----<ADDED_DIA_COUNT>-----
3
-----<ADDED_DIA_DIST>-----
12.5
25
37.5
-----<EXTRA_MEMBERS_YESNO>-----
N
-----<LEFT_EDGE_WIDTH_&_COUNT>-----
3.583
3
-----<RIGHT_EDGE_WIDTH_&_COUNT>-----
3.583
3
-----<TRAVEL_CLEARANCE_L_&_R>-----
1.5

```

```

1.5
-----<VEH_LOAD_GROUP_01_YESNO>-----
Y
-----<VEH_INPUT_FILE_INTER>-----
F
-----<VEH_POSITION_METHOD>-----
1
-----<VEH_POSITION_FWD/REV_X_Y>-----
F 144 505
-----<LANE_LOAD_DESC_YESNO>-----
N
-----<LANE_LOAD_COUNT>-----
0
-----<MORE_LIVE_LOADS_01_YESNO>-----
N
-----<FEM_OUTPUT_QUANTITY>-----
1
-----<GRAPHICS_PLOTTING_YESNO>-----
Y
END_HISTORY_FILE

```

B.1.6. "History.pre" File for BRUFEM Run #6:

```

BEGIN_HISTORY_FILE
-----<PROBLEM_TITLE>-----
EX. BR. 2 - HS20 IN -M LOC. DESIGN LANE
-----<BRIDGE_TYPE_IBTYPE>-----
STL
-----<TYPE_OF_UNITS>-----
1
-----<VARIABLE/CONSTANT_SKEW>-----
1
-----<PRIS_NONPRIS_IXSECT>-----
2
-----<STL_BASIC_MODEL_DATA>-----
4
8
0
-----<ANALYSIS_TYPE_FULL/LIVE>-----
1
-----<COMPOSITE_MODEL_TYPE>-----
1
-----<SLAB_THICK_STRENGTH>-----
6.5 3
-----<NUM_ELEM_BTWN_GIRD>-----
4
-----<NUM_SPANS>-----
3
-----<SPAN_LEN_&_NUM_Y_ELEMS>-----
60 45
-----<SPAN_LEN_&_NUM_Y_ELEMS>-----
75 60
-----<SPAN_LEN_&_NUM_Y_ELEMS>-----
60 45
-----<STL_DIA_TYPE>-----
2
-----<STL_DIA_CROSS_&_BTM_AREA>-----
3.05 3.05
-----<STL_DIA_TOP_&_BTM_DIST>-----

```

```

2 2
-----<ADDED_DIA_YESNO>-----
Y
-----<ADDED_DIA_COUNT>-----
7
-----<ADDED_DIA_DIST>-----
20
40
78.75
97.5
116.25
155
175
-----<STL_HINGE_YESNO>-----
N
-----<EXTRA_MEMBERS_YESNO>-----
N
-----<LEFT_EDGE_WIDTH_&_COUNT>-----
3.583 3
-----<RIGHT_EDGE_WIDTH_&_COUNT>-----
3.583 3
-----<TRAVEL_CLEARANCE_L_&_R>-----
1.5 1.5
-----<VEH_LOAD_GROUP_01_YESNO>-----
Y
-----<VEH_INPUT_FILE_INTER>-----
I
-----<VEH_NUM_VEHICLES_ON_BRIDGE>-----
1
-----<VEH_STANDARD_VEHICLE_YESNO>-----
Y
-----<VEHICLE_DATA_BASE>-----
1
-----<VEH_STANDARD_VEHICLE_TYPE>-----
HS20
-----<VEH_HS20_USE_14FT_MIN_YESNO>-----
Y
-----<VEH_POSITION_METHOD>-----
1
-----<VEH_POSITION_FWD/REV_X_Y>-----
F 244.5 1476
-----<LANE_LOAD_DESC_YESNO>-----
N
-----<LANE_LOAD_COUNT>-----
0
-----<MORE_LIVE_LOADS_01_YESNO>-----
N
-----<FEM_OUTPUT_QUANTITY>-----
1
-----<GRAPHICS_PLOTTING_YESNO>-----
Y
END_HISTORY_FILE

```

B.1.7. "History.pre" File for BRUFEM Run #7:

```

BEGIN_HISTORY_FILE
-----<PROBLEM_TITLE>-----
EX. BR. 2 - HS20 IN +M END SPAN LOC. DESIGN LANE
-----<BRIDGE_TYPE_IBTYPE>-----

```

```

STL
-----<TYPE_OF_UNITS>-----
1
-----<VARIABLE/CONSTANT_SKEW>-----
1
-----<PRIS_NONPRIS_IXSECT>-----
2
-----<STL_BASIC_MODEL_DATA>-----
4
8
0
-----<ANALYSIS_TYPE_FULL/LIVE>-----
1
-----<COMPOSITE_MODEL_TYPE>-----
1
-----<SLAB_THICK_STRENGTH>-----
6.5 3
-----<NUM_ELEM_BTWN_GIRD>-----
4
-----<NUM_SPANS>-----
3
-----<SPAN_LEN_&_NUM_Y_ELEMS>-----
60 45
-----<SPAN_LEN_&_NUM_Y_ELEMS>-----
75 60
-----<SPAN_LEN_&_NUM_Y_ELEMS>-----
60 45
-----<STL_DIA_TYPE>-----
2
-----<STL_DIA_CROSS_&_BTM_AREA>-----
3.05 3.05
-----<STL_DIA_TOP_&_BTM_DIST>-----
2 2
-----<ADDED_DIA_YESNO>-----
Y
-----<ADDED_DIA_COUNT>-----
7
-----<ADDED_DIA_DIST>-----
20
40
78.75
97.5
116.25
155
175
-----<STL_HINGE_YESNO>-----
N
-----<EXTRA_MEMBERS_YESNO>-----
N
-----<LEFT_EDGE_WIDTH_&_COUNT>-----
3.583 3
-----<RIGHT_EDGE_WIDTH_&_COUNT>-----
3.583 3
-----<TRAVEL_CLEARANCE_L_&_R>-----
1.5 1.5
-----<VEH_LOAD_GROUP_01_YESNO>-----
Y
-----<VEH_INPUT_FILE_INTER>-----
I
-----<VEH_NUM_VEHICLES_ON_BRIDGE>-----
1
-----<VEH_STANDARD_VEHICLE_YESNO>-----

```

```

Y
-----<VEHICLE_DATA_BASE>-----
1
-----<VEH_STANDARD_VEHICLE_TYPE>-----
HS20
-----<VEH_HS20_USE_14FT_MIN_YESNO>-----
Y
-----<VEH_POSITION_METHOD>-----
1
-----<VEH_POSITION_FWD/REV_X_Y>-----
F 244.5 2208
-----<LANE_LOAD_DESC_YESNO>-----
N
-----<LANE_LOAD_COUNT>-----
0
-----<MORE_LIVE_LOADS_01_YESNO>-----
N
-----<FEM_OUTPUT_QUANTITY>-----
1
-----<GRAPHICS_PLOTTING_YESNO>-----
Y
END_HISTORY_FILE

```

B.1.8. “History.pre” File for BRUFEM Run #8:

```

BEGIN_HISTORY_FILE
-----<PROBLEM_TITLE>-----
EX. BR. 2 - VEH. REC. 87 +M INT. SPAN TRAVEL LANE
-----<BRIDGE_TYPE_IBTYPE>-----
STL
-----<TYPE_OF_UNITS>-----
1
-----<VARIABLE/CONSTANT_SKEW>-----
1
-----<PRIS_NONPRIS_IXSECT>-----
2
-----<STL_BASIC_MODEL_DATA>-----
4
8
0
-----<ANALYSIS_TYPE_FULL/LIVE>-----
1
-----<COMPOSITE_MODEL_TYPE>-----
1
-----<SLAB_THICK_STRENGTH>-----
6.5 3
-----<NUM_ELEM_BTWN_GIRD>-----
4
-----<NUM_SPANS>-----
3
-----<SPAN_LEN_&_NUM_Y_ELEMS>-----
60 45
-----<SPAN_LEN_&_NUM_Y_ELEMS>-----
75 60
-----<SPAN_LEN_&_NUM_Y_ELEMS>-----
60 45
-----<STL_DIA_TYPE>-----

```



```

2
-----<STL_DIA_CROSS_&_BTM_AREA>-----
3.05 3.05
-----<STL_DIA_TOP_&_BTM_DIST>-----
2 2
-----<ADDED_DIA_YESNO>-----
Y
-----<ADDED_DIA_COUNT>-----
7
-----<ADDED_DIA_DIST>-----
20
40
78.75
97.5
116.25
155
175
-----<STL_HINGE_YESNO>-----
N
-----<EXTRA_MEMBERS_YESNO>-----
N
-----<LEFT_EDGE_WIDTH_&_COUNT>-----
3.583 3
-----<RIGHT_EDGE_WIDTH_&_COUNT>-----
3.583 3
-----<TRAVEL_CLEARANCE_L_&_R>-----
1.5 1.5
-----<VEH_LOAD_GROUP_01_YESNO>-----
Y
-----<VEH_INPUT_FILE_INTER>-----
F
-----<VEH_POSITION_METHOD>-----
1
-----<VEH_POSITION_FWD/REV_X_Y>-----
F 222 1428
-----<LANE_LOAD_DESC_YESNO>-----
N
-----<LANE_LOAD_COUNT>-----
0
-----<MORE_LIVE_LOADS_01_YESNO>-----
N
-----<FEM_OUTPUT_QUANTITY>-----
1
-----<GRAPHICS_PLOTTING_YESNO>-----
Y
END_HISTORY_FILE

```

B.1.9. "History.pre" File for BRUFEM Run #9:

```

BEGIN_HISTORY_FILE
-----<PROBLEM_TITLE>-----
EX. BR. 2 - VEH. REC. 203 IN +M END SPAN TRAVEL LANE
-----<BRIDGE_TYPE_IBTYPE>-----
STL
-----<TYPE_OF_UNITS>-----
1
-----<VARIABLE/CONSTANT_SKEW>-----

```

```

1
-----<PRIS_NONPRIS_IXSECT>-----
2
-----<STL_BASIC_MODEL_DATA>-----
4
8
0
-----<ANALYSIS_TYPE_FULL/LIVE>-----
1
-----<COMPOSITE_MODEL_TYPE>-----
1
-----<SLAB_THICK_STRENGTH>-----
6.5 3
-----<NUM_ELEM_BTWN_GIRD>-----
4
-----<NUM_SPANS>-----
3
-----<SPAN_LEN_&_NUM_Y_ELEMS>-----
60 45
-----<SPAN_LEN_&_NUM_Y_ELEMS>-----
75 60
-----<SPAN_LEN_&_NUM_Y_ELEMS>-----
60 45
-----<STL_DIA_TYPE>-----
2
-----<STL_DIA_CROSS_&_BTM_AREA>-----
3.05 3.05
-----<STL_DIA_TOP_&_BTM_DIST>-----
2 2
-----<ADDED_DIA_YESNO>-----
Y
-----<ADDED_DIA_COUNT>-----
7
-----<ADDED_DIA_DIST>-----
20
40
78.75
97.5
116.25
155
175
-----<STL_HINGE_YESNO>-----
N
-----<EXTRA_MEMBERS_YESNO>-----
N
-----<LEFT_EDGE_WIDTH_&_COUNT>-----
3.583 3
-----<RIGHT_EDGE_WIDTH_&_COUNT>-----
3.583 3
-----<TRAVEL_CLEARANCE_L_&_R>-----
1.5 1.5
-----<VEH_LOAD_GROUP_01_YESNO>-----
Y
-----<VEH_INPUT_FILE_INTER>-----
F
-----<VEH_POSITION_METHOD>-----
1
-----<VEH_POSITION_FWD/REV_X_Y>-----
F 144 2322
-----<LANE_LOAD_DESC_YESNO>-----
N
-----<LANE_LOAD_COUNT>-----

```

```

0
-----<MORE_LIVE_LOADS_01_YESNO>-----
N
-----<FEM_OUTPUT_QUANTITY>-----
1
-----<GRAPHICS_PLOTTING_YESNO>-----
Y
END_HISTORY_FILE

```

B.1.10. "History.pre" File for BRUFEM Run #10:

```

BEGIN_HISTORY_FILE
-----<PROBLEM_TITLE>-----
EX. BR. 2 - VEH. REC. 203 IN -M LOC. TRAVEL LANE
-----<BRIDGE_TYPE_IBTYPE>-----
STL
-----<TYPE_OF_UNITS>-----
1
-----<VARIABLE/CONSTANT_SKEW>-----
1
-----<PRIS_NONPRIS_IXSECT>-----
2
-----<STL_BASIC_MODEL_DATA>-----
4
8
0
-----<ANALYSIS_TYPE_FULL/LIVE>-----
1
-----<COMPOSITE_MODEL_TYPE>-----
1
-----<SLAB_THICK_STRENGTH>-----
6.5 3
-----<NUM_ELEM_BTWN_GIRD>-----
4
-----<NUM_SPANS>-----
3
-----<SPAN_LEN_ & NUM_Y_ELEMS>-----
60 45
-----<SPAN_LEN_ & NUM_Y_ELEMS>-----
75 60
-----<SPAN_LEN_ & NUM_Y_ELEMS>-----
60 45
-----<STL_DIA_TYPE>-----
2
-----<STL_DIA_CROSS_ & BTM_AREA>-----
3.05 3.05
-----<STL_DIA_TOP_ & BTM_DIST>-----
2 2
-----<ADDED_DIA_YESNO>-----
Y
-----<ADDED_DIA_COUNT>-----
7
-----<ADDED_DIA_DIST>-----
20
40
78.75
97.5

```

```

116.25
155
175
-----<STL_HINGE_YESNO>-----
N
-----<EXTRA_MEMBERS_YESNO>-----
N
-----<LEFT_EDGE_WIDTH_&_COUNT>-----
3.583 3
-----<RIGHT_EDGE_WIDTH_&_COUNT>-----
3.583 3
-----<TRAVEL_CLEARANCE_L_&_R>-----
1.5 1.5
-----<VEH_LOAD_GROUP_01_YESNO>-----
Y
-----<VEH_INPUT_FILE_INTER>-----
F
-----<VEH_POSITION_METHOD>-----
1
-----<VEH_POSITION_FWD/REV_X_Y>-----
F 144 2308
-----<LANE_LOAD_DESC_YESNO>-----
N
-----<LANE_LOAD_COUNT>-----
0
-----<MORE_LIVE_LOADS_01_YESNO>-----
N
-----<FEM_OUTPUT_QUANTITY>-----
1
-----<GRAPHICS_PLOTTING_YESNO>-----
Y
END_HISTORY_FILE

```

B.1.11. "History.pre" File for BRUFEM Run #11:

```

BEGIN_HISTORY_FILE
-----<PROBLEM_TITLE>-----
EX. BR. 3 - HS20 +M LOC. IN DESIGN LANE
-----<BRIDGE_TYPE_IBTYPE>-----
STL
-----<TYPE_OF_UNITS>-----
1
-----<VARIABLE/CONSTANT_SKEW>-----
1
-----<PRIS_NONPRIS_IXSECT>-----
2
-----<STL_BASIC_MODEL_DATA>-----
4 10 0
-----<ANALYSIS_TYPE_FULL/LIVE>-----
1
-----<COMPOSITE_MODEL_TYPE>-----
3
-----<SLAB_THICK_STRENGTH>-----
8 4
-----<NUM_ELEM_BTWN_GIRD>-----
5
-----<NUM_SPANS>-----

```

```

2
-----<SPAN_LEN_&_NUM_Y_ELEMS>-----
90 75
-----<SPAN_LEN_&_NUM_Y_ELEMS>-----
90 75
-----<STL_EFF_NEG_MOM>-----
90
-----<STL_DIA_TYPE>-----
2
-----<STL_DIA_CROSS_&_BTM_AREA>-----
4 4
-----<STL_DIA_TOP_&_BTM_DIST>-----
3 3
-----<ADDED_DIA_YESNO>-----
Y
-----<ADDED_DIA_COUNT>-----
4
-----<ADDED_DIA_DIST>-----
37
74
106
143
-----<STL_HINGE_YESNO>-----
N
-----<EXTRA_MEMBERS_YESNO>-----
N
-----<LEFT_EDGE_WIDTH_&_COUNT>-----
3.5 2
-----<RIGHT_EDGE_WIDTH_&_COUNT>-----
3.5 2
-----<TRAVEL_CLEARANCE_L_&_R>-----
1.5 1.5
-----<VEH_LOAD_GROUP_01_YESNO>-----
Y
-----<VEH_INPUT_FILE_INTER>-----
I
-----<VEH_NUM_VEHICLES_ON_BRIDGE>-----
1
-----<VEH_STANDARD_VEHICLE_YESNO>-----
Y
-----<VEHICLE_DATA_BASE>-----
1
-----<VEH_STANDARD_VEHICLE_TYPE>-----
HS20
-----<VEH_HS20_USE_14FT_MIN_YESNO>-----
Y
-----<VEH_POSITION_METHOD>-----
1
-----<VEH_POSITION_FWD/REV_X_Y>-----
F 322 1884
-----<LANE_LOAD_DESC_YESNO>-----
N
-----<LANE_LOAD_COUNT>-----
0
-----<MORE_LIVE_LOADS_01_YESNO>-----
N
-----<FEM_OUTPUT_QUANTITY>-----
1
-----<GRAPHICS_PLOTTING_YESNO>-----
Y
END_HISTORY_FILE

```

B.1.12. "History.pre" File for BRUFEM Run #12:

```
BEGIN_HISTORY_FILE
-----<PROBLEM_TITLE>-----
EX. BR. 3 - HS20 -M LOC IN DESIGN LANE
-----<BRIDGE_TYPE_IBTYPE>-----
STL
-----<TYPE_OF_UNITS>-----
1
-----<VARIABLE/CONSTANT_SKEW>-----
1
-----<PRIS_NONPRIS_IXSECT>-----
2
-----<STL_BASIC_MODEL_DATA>-----
4 10 0
-----<ANALYSIS_TYPE_FULL/LIVE>-----
1
-----<COMPOSITE_MODEL_TYPE>-----
3
-----<SLAB_THICK_STRENGTH>-----
8 4
-----<NUM_ELEM_BTWN_GIRD>-----
5
-----<NUM_SPANS>-----
2
-----<SPAN_LEN_&_NUM_Y_ELEMS>-----
90 75
-----<SPAN_LEN_&_NUM_Y_ELEMS>-----
90 75
-----<STL_EFF_NEG_MOM>-----
90
-----<STL_DIA_TYPE>-----
2
-----<STL_DIA_CROSS_&_BTM_AREA>-----
4 4
-----<STL_DIA_TOP_&_BTM_DIST>-----
3 3
-----<ADDED_DIA_YESNO>-----
Y
-----<ADDED_DIA_COUNT>-----
4
-----<ADDED_DIA_DIST>-----
37
74
106
143
-----<STL_HINGE_YESNO>-----
N
-----<EXTRA_MEMBERS_YESNO>-----
N
-----<LEFT_EDGE_WIDTH_&_COUNT>-----
3.5 2
-----<RIGHT_EDGE_WIDTH_&_COUNT>-----
3.5 2
-----<TRAVEL_CLEARANCE_L_&_R>-----
1.5 1.5
```

```

-----<VEH_LOAD_GROUP_01_YESNO>-----
Y
-----<VEH_INPUT_FILE_INTER>-----
I
-----<VEH_NUM_VEHICLES_ON_BRIDGE>-----
1
-----<VEH_STANDARD_VEHICLE_YESNO>-----
Y
-----<VEHICLE_DATA_BASE>-----
1
-----<VEH_STANDARD_VEHICLE_TYPE>-----
HS20
-----<VEH_HS20_USE_14FT_MIN_YESNO>-----
Y
-----<VEH_POSITION_METHOD>-----
1
-----<VEH_POSITION_FWD/REV_X_Y>-----
F 322 1800
-----<LANE_LOAD_DESC_YESNO>-----
N
-----<LANE_LOAD_COUNT>-----
0
-----<MORE_LIVE_LOADS_01_YESNO>-----
N
-----<FEM_OUTPUT_QUANTITY>-----
1
-----<GRAPHICS_PLOTTING_YESNO>-----
Y
END_HISTORY_FILE

```

B.1.13. "History.pre" File for BRUFEM Run #13:

```

BEGIN_HISTORY_FILE
-----<PROBLEM_TITLE>-----
EX. BR. 3 - VEH. REC 87 +M IN TRAVEL LANE
-----<BRIDGE_TYPE_IBTYPE>-----
STL
-----<TYPE_OF_UNITS>-----
1
-----<VARIABLE/CONSTANT_SKEW>-----
1
-----<PRIS_NONPRIS_IXSECT>-----
2
-----<STL_BASIC_MODEL_DATA>-----
4 10 0
-----<ANALYSIS_TYPE_FULL/LIVE>-----
1
-----<COMPOSITE_MODEL_TYPE>-----
3
-----<SLAB_THICK_STRENGTH>-----
8 4
-----<NUM_ELEM_BTWN_GIRD>-----
5
-----<NUM_SPANS>-----
2
-----<SPAN_LEN_&_NUM_Y_ELEMS>-----
90 75

```

```

-----<SPAN_LEN_&_NUM_Y_ELEMS>-----
90 75
-----<STL_EFF_NEG_MOM>-----
90
-----<STL_DIA_TYPE>-----
2
-----<STL_DIA_CROSS_&_BTM_AREA>-----
4 4
-----<STL_DIA_TOP_&_BTM_DIST>-----
3 3
-----<ADDED_DIA_YESNO>-----
Y
-----<ADDED_DIA_COUNT>-----
4
-----<ADDED_DIA_DIST>-----
37
74
106
143
-----<STL_HINGE_YESNO>-----
N
-----<EXTRA_MEMBERS_YESNO>-----
N
-----<LEFT_EDGE_WIDTH_&_COUNT>-----
3.5 2
-----<RIGHT_EDGE_WIDTH_&_COUNT>-----
3.5 2
-----<TRAVEL_CLEARANCE_L_&_R>-----
1.5 1.5
-----<VEH_LOAD_GROUP_01_YESNO>-----
Y
-----<VEH_INPUT_FILE_INTER>-----
F
-----<VEH_POSITION_METHOD>-----
1
-----<VEH_POSITION_FWD/REV_X_Y>-----
F 258 1956
-----<LANE_LOAD_DESC_YESNO>-----
N
-----<LANE_LOAD_COUNT>-----
0
-----<MORE_LIVE_LOADS_01_YESNO>-----
N
-----<FEM_OUTPUT_QUANTITY>-----
1
-----<GRAPHICS_PLOTTING_YESNO>-----
Y
END_HISTORY_FILE

```

B.1.14. "History.pre" File for BRUFEM Run #14:

```

BEGIN_HISTORY_FILE
-----<PROBLEM_TITLE>-----
EX. BR. 3 - VEH. REC. 203 +M IN TRAVEL LANE
-----<BRIDGE_TYPE_IBTYPE>-----
STL
-----<TYPE_OF_UNITS>-----

```



```

1
-----<VARIABLE/CONSTANT_SKEW>-----
1
-----<PRIS_NONPRIS_IXSECT>-----
2
-----<STL_BASIC_MODEL_DATA>-----
4 10 0
-----<ANALYSIS_TYPE_FULL/LIVE>-----
1
-----<COMPOSITE_MODEL_TYPE>-----
3
-----<SLAB_THICK_STRENGTH>-----
8 4
-----<NUM_ELEM_BTWN_GIRD>-----
5
-----<NUM_SPANS>-----
2
-----<SPAN_LEN_&_NUM_Y_ELEMS>-----
90 75
-----<SPAN_LEN_&_NUM_Y_ELEMS>-----
90 75
-----<STL_EFF_NEG_MOM>-----
90
-----<STL_DIA_TYPE>-----
2
-----<STL_DIA_CROSS_&_BTM_AREA>-----
4 4
-----<STL_DIA_TOP_&_BTM_DIST>-----
3 3
-----<ADDED_DIA_YESNO>-----
Y
-----<ADDED_DIA_COUNT>-----
4
-----<ADDED_DIA_DIST>-----
37
74
106
143
-----<STL_HINGE_YESNO>-----
N
-----<EXTRA_MEMBERS_YESNO>-----
N
-----<LEFT_EDGE_WIDTH_&_COUNT>-----
3.5 2
-----<RIGHT_EDGE_WIDTH_&_COUNT>-----
3.5 2
-----<TRAVEL_CLEARANCE_L_&_R>-----
1.5 1.5
-----<VEH_LOAD_GROUP_01_YESNO>-----
Y
-----<VEH_INPUT_FILE_INTER>-----
F
-----<VEH_POSITION_METHOD>-----
1
-----<VEH_POSITION_FWD/REV_X_Y>-----
F 180 1987
-----<LANE_LOAD_DESC_YESNO>-----
N
-----<LANE_LOAD_COUNT>-----
0
-----<MORE_LIVE_LOADS_01_YESNO>-----
N

```

```

-----<FEM_OUTPUT_QUANTITY>-----
1
-----<GRAPHICS_PLOTTING_YESNO>-----
Y
END_HISTORY_FILE

```

B.1.15. “History.pre” File for BRUFEM Run #15:

```

BEGIN_HISTORY_FILE
-----<PROBLEM_TITLE>-----
EX. BR. 3 - VEH. REC 203 -M IN TRAVEL LANE
-----<BRIDGE_TYPE_IBTYPE>-----
STL
-----<TYPE_OF_UNITS>-----
1
-----<VARIABLE/CONSTANT_SKEW>-----
1
-----<PRIS_NONPRIS_IXSECT>-----
2
-----<STL_BASIC_MODEL_DATA>-----
4 10 0
-----<ANALYSIS_TYPE_FULL/LIVE>-----
1
-----<COMPOSITE_MODEL_TYPE>-----
3
-----<SLAB_THICK_STRENGTH>-----
8 4
-----<NUM_ELEM_BTWN_GIRD>-----
5
-----<NUM_SPANS>-----
2
-----<SPAN_LEN_&_NUM_Y_ELEMS>-----
90 75
-----<SPAN_LEN_&_NUM_Y_ELEMS>-----
90 75
-----<STL_EFF_NEG_MOM>-----
90
-----<STL_DIA_TYPE>-----
2
-----<STL_DIA_CROSS_&_BTM_AREA>-----
4 4
-----<STL_DIA_TOP_&_BTM_DIST>-----
3 3
-----<ADDED_DIA_YESNO>-----
Y
-----<ADDED_DIA_COUNT>-----
4
-----<ADDED_DIA_DIST>-----
37
74
106
143
-----<STL_HINGE_YESNO>-----
N
-----<EXTRA_MEMBERS_YESNO>-----
N
-----<LEFT_EDGE_WIDTH_&_COUNT>-----

```

```

3.5 2
-----<RIGHT_EDGE_WIDTH_&_COUNT>-----
3.5 2
-----<TRAVEL_CLEARANCE_L_&_R>-----
1.5 1.5
-----<VEH_LOAD_GROUP_01_YESNO>-----
Y
-----<VEH_INPUT_FILE_INTER>-----
F
-----<VEH_POSITION_METHOD>-----
1
-----<VEH_POSITION_FWD/REV_X_Y>-----
F 180 2076
-----<LANE_LOAD_DESC_YESNO>-----
N
-----<LANE_LOAD_COUNT>-----
0
-----<MORE_LIVE_LOADS_01_YESNO>-----
N
-----<FEM_OUTPUT_QUANTITY>-----
1
-----<GRAPHICS_PLOTTING_YESNO>-----
Y
END_HISTORY_FILE

```

B.2. “BAR.DAT” FILES FOR EXAMPLE BRIDGES 2 AND 3

B.2.1. “Bar.dat” File for BRUFEM Runs 6 through 10 – Ex. Bridge 2

```

CROSS SECTIONS
: BASIC GIRDER - Bridge 2
ENGLISH
2
1 6.5 3
11.51 0.855
0.58 31.38
11.51 0.855
2 6.5 5
10 0.4375
11.51 0.855
0.58 31.38
11.51 0.855
10 0.4375
1
1
54.5 1
0 2
11 2
0 1
64 1
0 2
11 2
0 1
54.5 1
END-DATA
WEB STIFFENERS

```

```
ENGLISH
1
1 2340
END-DATA
```

B.2.2. “Bar.dat” File for BRUFEM Runs 11 through 15 – Ex. Bridge 3

```
CROSS SECTIONS
: BASIC GIRDER - Bridge 3
ENGLISH
3
1 9.25 3 :5.355
16 0.75
0.4375 36
16 0.875
2 9.25 3 :5.355
16 1
0.5 36
16 1.5
3 9.25 3 :5.355
12 0.75
0.4375 36
16 0.875
6
1
63 1
0 2
54 2
0 3
63 3
END-DATA
WEB STIFFENERS
ENGLISH
2
1 1080
1 1080
END-DATA
```

B.3. “VEH.DAT” FILES FOR ALL NON-STANDARD VEHICLES

B.3.1. “Veh.dat” File for Vehicle #18 – BRUFEM Run #4

```
VEHICLE DATA
ENGLISH
1
4
24 7 0 2
24 24 24 24
7 7 7 7
0 0 0 0
2 2 2 2
1 1 1 1
```

```
7 5 6 5
0 0 0 0
END-DATA
```

B.3.2. “Veh.dat” File for Vehicle #213 – BRUFEM Run #5

```
VEHICLE DATA
ENGLISH
1
1
61.5 4.927 3.439 4
61.5
4.927
3.439
4
7
5.25
5.25
END-DATA
```

B.3.3. “Veh.dat” File for Vehicle #87 – BRUFEM Run #8

```
VEHICLE DATA
ENGLISH
1
4
16.5 7 0 2
16.5 16.5 21.5 22.5
7 6 6 6
0 1 1 1
2 4 4 4
1 1 3 2
4 4 10 17
0 0 4 4
END-DATA
```

B.3.4. “Veh.dat” File for Vehicle #203 – BRUFEM Run #9

```
VEHICLE DATA
ENGLISH
1
1
35.61 4.333 5.25 4
35.61
4.333
5.25
4
10
5.08
5.08
END-DATA
```

B.3.5. “Veh.dat” File for Vehicle #203 – BRUFEM Run #10

```
VEHICLE DATA
ENGLISH
1
2
34.18 4.333 5.25 4
34.18 35.61
4.333 4.333
5.25 5.25
4 4
9 12
5.08 24
5.08 5.08
END-DATA
```

B.3.6. “Veh.dat” File for Vehicle #87 – BRUFEM Run #13

```
VEHICLE DATA
ENGLISH
1
4
16.5 7 0 2
16.5 16.5 21.5 22.5
7 6 6 6
0 1 1 1
2 4 4 4
1 1 3 2
4 4 10 17
0 0 4 4
END-DATA
```

B.3.7. “Veh.dat” File for Vehicle #203 – BRUFEM Run #14

```
VEHICLE DATA
ENGLISH
1
1
35.61 4.333 5.25 4
35.61
4.333
5.25
4
11
5.08
5.08
END-DATA
```

B.3.8. "Veh.dat" File for Vehicle #203 – BRUFEM Run #15

```
VEHICLE DATA
ENGLISH
1
3
39.75 8 1 4
39.75 34.18 35.61
8 4.333 0
1 5.25 5.25
4 4 4
1 12 12
4.5 14 24
0 5.08 5.08
END-DATA
```

References

- [1] American Association of State Highway and Transportation Officials (AASHTO), *AASHTO LRFD Bridge Design Specifications: Customary US Units*, 1st ed., AASHTO, Washington, D.C., 1994.
- [2] American Association of State Highway and Transportation Officials (AASHTO), *Standard Specifications for Highway Bridges*, 16th ed., AASHTO, Washington, D.C., 1996.
- [3] American Association of State Highway and Transportation Officials (AASHTO), *Manual for Condition Evaluation of Bridges*, AASHTO, Washington, D.C., 1994.
- [4] Hays, Jr., C.O., Consolazio, G.R., Hoit, M.I., and Kakhandiki, A., “Bridge Rating of Girder – Slab Bridges Using Automated Finite Element Technology”, Final Project Report, University of Florida, Gainesville, December 1994.
- [5] Hays, Jr., C.O., Consolazio, G.R., Hoit, M.I., Garcelon, J.H., and Moy, W., “Metric/SI and PC Conversion of BRUFEM and SALOD Systems”, Final Project Report, University of Florida, Gainesville, May 1995.
- [6] Computers and Structures, Inc., “SAP2000 Analysis Reference - Volume 1”, Version 6.1, 1997.
- [7] Carnahan, J.D., Grubb, M.A., and Hartmann, J.L., “Two-Span Continuous Composite I Girder – Load and Resistance Factor Design (Customary U.S. Units)”, CE397 Class Handout Design Example, University of Texas at Austin, 1998.
- [8] Letter from John Holt, P.E., Bridge Design Section, Texas Department of Transportation, Austin, June 30, 1997.
- [9] Telephone communication with Robert Crowson, Texas Department of Transportation, Austin, April 27, 1999.
- [10] Mabsout, M.E., Tarhini, K.M., Frederick, G.R., and Kobrosly, M., “Influence of Sidewalks and Railings on Wheel Load Distribution in Steel Girder Bridges”, *Journal of Bridge Engineering*, Vol. 2, Num. 3, August 1997.
- [11] Mabsout, M.E., Tarhini, K.M., Frederick, G.R., and Tayar, C., “Finite Element Analysis of Steel Grider Highway Bridges”, *Journal of Bridge Engineering*, Vol. 2, Num. 3, August 1997.